NASA TECHNICAL NOTE

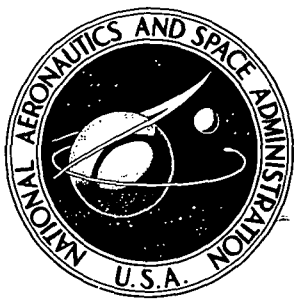

NASA TN D-7343

NASA TN D-7343

FORTRAN PROGRAM FOR CALCULATING VELOCITIES AND STREAMLINES ON THE HUB-SHROUD MID-CHANNEL FLOW SURFACE OF AN AXIAL- OR MIXED-FLOW TURBOMACHINE

I - User's Manual

by Theodore Katsanis and William D. McNally

Lewis Research Center
Cleveland, Ohio 44135

NATIONAL AERONAUTICS AND SPACE ADMINISTRATION • WASHINGTON, D. C. • JULY 1973

1. Report No. NASA TN D-7343	2. Government Accession No.	3. Recipient's Catalog No.
4. Title and Subtitle FORTRAN PROGRAM FOR CALCULATING VELOCITIES AND STREAMLINES ON THE HUB-SHROUD MID-CHANNEL FLOW SURFACE OF AN AXIAL- OR MIXED-FLOW TURBOMACHINE. I - USER'S MANUAL		5. Report Date July 1973 6. Performing Organization Code
7. Author(s) Theodore Katsanis and William D. McNally		8. Performing Organization Report No. E-7154
9. Performing Organization Name and Address Lewis Research Center National Aeronautics and Space Administration Cleveland, Ohio 44135		10. Work Unit No. 501-24 11. Contract or Grant No.
12. Sponsoring Agency Name and Address National Aeronautics and Space Administration Washington, D.C. 20546		13. Type of Report and Period Covered Technical Note 14. Sponsoring Agency Code

15. Supplementary Notes

16. Abstract

A FORTRAN-IV computer program has been developed that obtains a subsonic or shock-free transonic flow solution on the hub-shroud mid-channel flow surface of a turbomachine. The blade row may be fixed or rotating, and may be twisted and leaned. Flow may be axial or mixed, up to 45^{o} from axial. Upstream and downstream flow variables may vary from hub to shroud, and provision is made to correct for loss of stagnation pressure. The results include velocities, streamlines, and flow angles on the flow surface; and approximate blade surface velocities. Subsonic solutions are obtained by a finite-difference stream-function solution. Transonic solutions are obtained by a velocity-gradient method, using information from a finite-difference stream-function solution at a reduced mass flow.

17. Key Words (Suggested by Author(s))	18. Distribution Statement
Meridional plane; Turbomachine flow; Mid-channel flow surface; Axial flow turbomachine; Mixed-flow turbomachine; Transonic flow	Unclassified - unlimited

19. Security Classif. (of this report)	20. Security Classif. (of this page)	21. No. of Pages	22. Price*
Unclassified	Unclassified	96	$3.00

* For sale by the National Technical Information Service, Springfield, Virginia 22151

Page Intentionally Left Blank

CONTENTS

FORTRAN PROGRAM FOR CALCULATING VELOCITIES AND STREAMLINES ON THE HUB-SHROUD MID-CHANNEL FLOW SURFACE OF AN AXIAL- OR MIXED-FLOW TURBOMACHINE

I - USER'S MANUAL

by Theodore Katsanis and William D. McNally

Lewis Research Center

SUMMARY

A FORTRAN-IV computer program has been developed which obtains a subsonic or transonic, nonviscous flow solution on the hub-shroud mid-channel flow surface of a turbomachine. The flow must be essentially subsonic, but there may be locally supersonic flow. The solution is for two-dimensional, adiabatic shock-free flow. The blade row may be fixed or rotating, and may be twisted and leaned. The flow may be axial or mixed, up to approximately 45° from axial. Upstream and downstream flow conditions can vary from hub to shroud, and provision is made for an approximate correction for loss of stagnation pressure.

The basic analysis is based on the stream function and consists of the solution of the simultaneous, nonlinear, finite-difference equations of the stream function. This basic solution, however, is limited to strictly subsonic flow. When there is locally supersonic flow, a transonic solution must be obtained. The transonic solution is obtained by a combination of a finite-difference stream-function solution and a velocity-gradient solution. The finite-difference solution at a reduced mass flow provides information which is used to obtain a velocity-gradient solution at the full mass flow.

The program input consists of blade and flow-channel geometry, upstream and downstream flow conditions from hub to shroud, and mass flow. The output includes streamline coordinates, flow angles, and velocities on the mid-channel flow surface; incidence and deviation angles at the blade leading and trailing edges; and approximations to the blade surface velocities. The output may also include input information for a blade-to-blade flow analysis program.

The program is reported in two volumes, with part I as the user's manual and part II as the programmer's manual. This report, part I, contains all the information necessary to use the program as is. It explains the equations involved and the method of solution and gives a numerical example to illustrate the use of the program. Part II includes the complete program listing and a detailed program procedure.

INTRODUCTION

The design of blades for compressors and turbines ideally requires analysis methods for unsteady, rotational, three-dimensional, viscous flow through a turbomachine. Clearly, such solutions are impossible at the present time, even on the largest and fastest computers. The usual approach at present is to analyze only steady flows and to separate inviscid solutions from viscous solutions. Three-dimensional inviscid solutions are just beginning to be contemplated for coming generations of computers. So at present, inviscid analyses usually involve a combination of several two-dimensional solutions on intersecting families of stream surfaces to obtain what is called a quasi-three-dimensional solution.

Since there are several choices of two-dimensional surfaces to analyze, and many ways of combining them, there are many approaches to obtaining a quasi-three-dimensional solution. Most two-dimensional solutions are either on a blade-to-blade surface of revolution (Wu's S_1 surface, ref. 1) or on the meridional or mid-channel stream surface between two blades (Wu's S_2 surface). However, when three-dimensional effects are most important, significant information can often be obtained from a solution on a passage cross-sectional surface (normal to the flow). This is called a channel solution (see fig. 1).

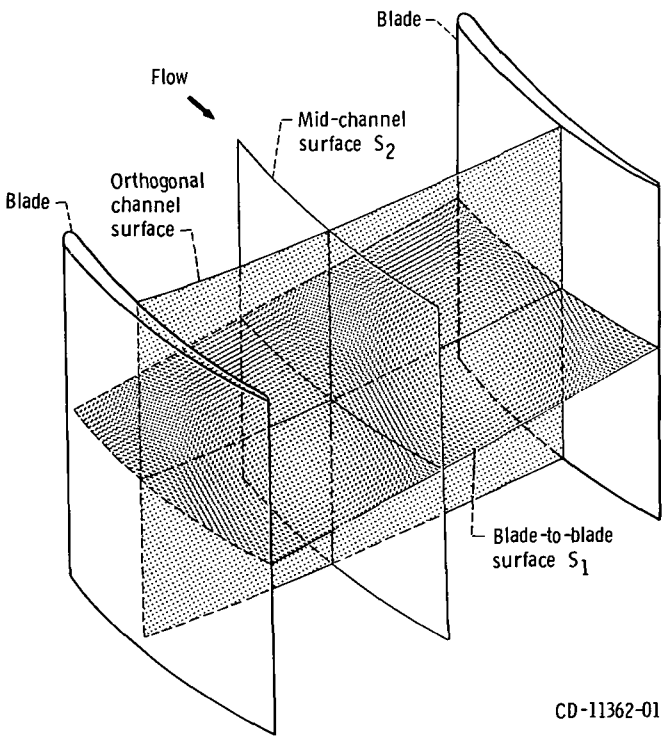

Figure 1. - Two-dimensional analysis surfaces in a turbomachine.

In this report a solution to the equations of flow on the meridional S_2 surface is carried out. This solution surface is chosen when the turbomachine under consideration has significant variation in flow properties in the hub-shroud direction. A solution on the meridional surface will show this variation. The solution can be obtained either by the quasi-orthogonal method, which solves the velocity-gradient equation from hub to shroud on the meridional flow plane (ref. 2), or by a finite-difference method, which solves a finite-difference equation for stream function on the same flow plane. The quasi-orthogonal method is efficient in many cases and can obtain solutions into the transonic regime. However, there is difficulty in obtaining a solution when aspect ratios are above 1. Difficulties are also encountered with curved passages and low-hub-tip-ratio blades. For such cases, the most promising method is the finite-difference solution, but this solution is limited to completely subsonic flows.

Two finite-difference programs for flow on the mid-channel surface of a turbomachine have been reported in the literature (refs. 3 and 4). Since both are finite-difference methods, they are necessarily limited to subsonic flow cases. Marsh's method (ref. 3), termed the matrix throughflow method, closely follows the development given by Wu in reference 1. However, the computer program was not included in reference 3, nor is it available to the general user. Davis' program is provided in reference 4 but is limited to certain families of compressor blades and flow surfaces.

The method described in this report uses both the finite-difference and the quasi-orthogonal (velocity gradient) methods, combined in a way which takes maximum advantage of both. The finite-difference method is used to obtain a subsonic-flow solution. The velocity-gradient method is then used if necessary to extend the range of solutions into the transonic regime.

A computer program, MERIDL, has been written to perform these calculations. This program is written for axial- or mixed-flow turbomachines, both compressors and turbines, to approximately 45° from axial. Upstream and downstream flow conditions can vary from hub to shround. The solution is for compressible, shock-free flow, or incompressible flow. Provision is made for an approximate correction for loss of stagnation pressure through the blade row. The blade row may be either fixed or rotating and may be twisted and leaned. The blades can have high aspect ratio and arbitrary thickness distribution.

The solution obtained by this program also provides the information necessary for a more detailed blade shape analysis on blade-to-blade surfaces (fig. 1). A useful program for this purpose is TSONIC (ref. 5). Information needed to prepare all the input for TSONIC is calculated and printed by MERIDL.

The MERIDL program has been implemented on the NASA Lewis time-sharing IBM-TSS/360-67 computer. For the numerical example of this report, storage of variables required 60 000 words for a 21×41 grid of 861 points. Variable storage could be

easily reduced by equivalencing of variables or by using a coarser mesh. Storage for the program code is 18 000 words. This storage could be reduced by overlay of code. Run times for the program range from 3 to 15 minutes on IBM 360-67 equipment, depending upon the mesh size used and the compressibility of the flow.

The MERIDL program is reported in two volumes, with part I as the user's manual and part II (ref. 6) as the programmer's manual. This report, part I, contains all the information necessary to use the program as is. It explains the method of solution, describes the input and output, gives a numerical example to illustrate the use of the program, and derives the equations used (in the appendixes). Part II includes a complete program listing, detailed program procedure, and appendixes which derive special numerical techniques used.

METHOD OF ANALYSIS

BASIC ASSUMPTIONS

It is desired to determine the flow distribution through a stationary or rotating cascade of blades on a mid-channel hub-shroud stream surface. The following simplifying assumptions are used in deriving the equations and in obtaining a solution:

(1) The flow relative to the blade is steady.

(2) The fluid is a perfect gas with constant specific heat C_p.

(3) The fluid is a nonviscous gas.

(4) There is no heat transfer.

(5) The mid-channel surface is a stream surface which has the same shape as the blade mean camber surface, except near the leading and trailing edges, where an arbitrary correction is made to match the free-stream flow.

(6) The only forces are those due to momentum and pressure gradient.

(7) The velocity varies linearly between blade surfaces.

(8) The relative stagnation pressure loss is known through the blade row.

The flow may be axial or mixed, to about 45° from axial. There may be a variation of whirl, stagnation pressure, and stagnation temperature from hub to shroud, both upstream and downstream of the blade row. The blade row may be either fixed or rotating, with leaned and twisted blades. Within the given assumptions, no terms are omitted from the equations.

SOLUTION BY COMBINATION OF METHODS

A flow analysis on the meridional flow surface can be obtained either by the velocity-gradient method or by the finite-difference method. The finite-difference method is limited to subsonic flow, whereas the velocity-gradient method is limited to relatively low-aspect-ratio blades. The most accurate solution is obtained by the finite-difference technique, so that this method is used where possible (i.e., for subsonic flow). With locally supersonic flow, the finite-difference solution is first obtained at a reduced mass flow for which the flow field is completely subsonic. The streamline curvatures and flow angles throughout the passage which are obtained from this solution provide the information necessary to obtain an approximate velocity-gradient solution at full mass flow, regardless of aspect ratio.

SUBSONIC STREAM-FUNCTION SOLUTION

The stream-function equation is a partial differential equation on a mid-channel hub-shroud stream surface (see assumption 5). This equation is in one unknown (the stream function) as a function of two variables, r and z (see fig. 2). This is equation (A1) and

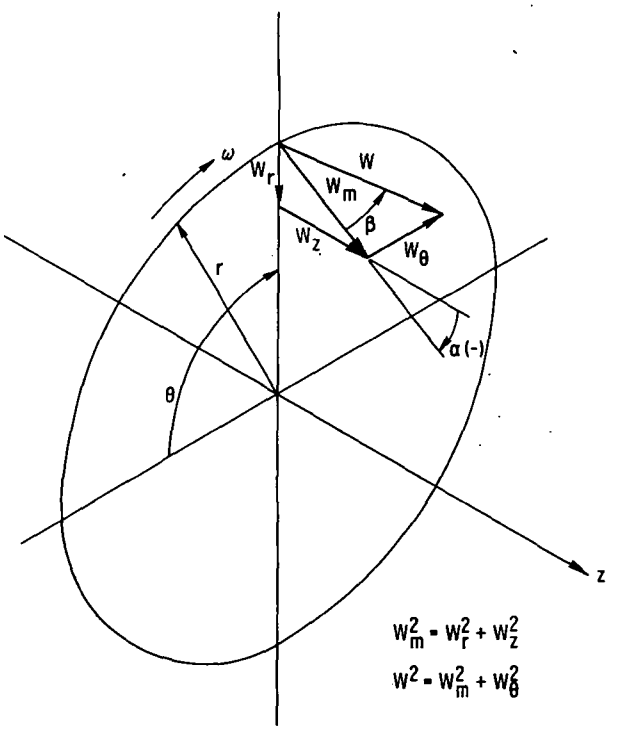

Figure 2. - Cylindrical coordinate system and velocity components.

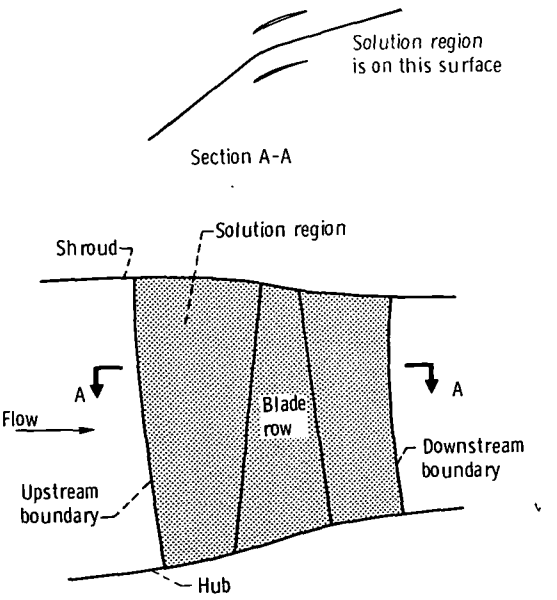

Figure 3. - Solution region.

is derived from Wu's equation (eq. (107a), ref. 1) for the stream function on what he calls an S_2 surface. Equation (A1) is nonlinear but can be solved iteratively by the finite-difference method when the flow is completely subsonic.

A finite region (as indicated in fig. 3) is considered for the solution of equation (A1). It is assumed that the upstream and downstream boundaries are sufficiently far from the blade so as to have a negligible effect on the solution. Equation (A1) is elliptic for subsonic flow. Therefore, when the flow is entirely subsonic, equation (A1) can be solved when proper boundary conditions are specified on the entire boundary of the region. These conditions are the values of the stream function on all four boundaries. The stream function has the value 0 on the hub and 1 at the shroud. The value of the stream function on the upstream and downstream boundaries can be calculated if the stagnation pressure, stagnation temperature, and whirl distribution from hub to shroud are specified upstream and downstream of the blade.

The numerical solution of equation (A1) is obtained by the finite-difference method. A grid must be used for the finite-difference equations. The type of grid that was chosen is an orthogonal mesh which is generated by the program. The method used to generate the grid follows that reported in reference 7. The space between the hub and the shroud is divided into equal increments along several radial lines. Spline curves are then fit through the resulting points to obtain the streamwise orthogonals (see fig. 4).

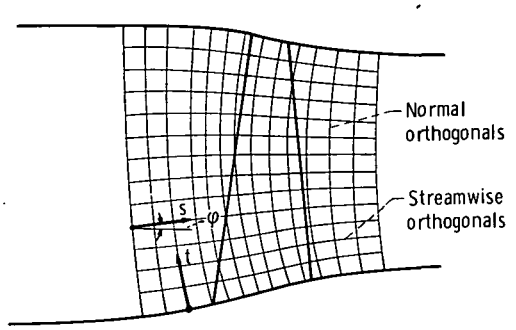

Figure 4. - Orthogonal finite-difference mesh on the solution region.

The normal orthogonals are obtained by a predictor-corrector technique. This technique is analogous to the second-order Runge-Kutta method for solving ordinary differential equations, known also as the improved Euler method or Heun's method (ref. 8). The orthogonal mesh coordinates are s and t. The s-coordinate is in the streamwise direction and the t-coordinate is normal to this, as indicated in figure 4. With the mesh determined, the finite-difference equations can be derived. The finite-difference equations on the orthogonal mesh are given in part II of this report.

The finite-difference equations are nonlinear since the original equation (A1) is

nonlinear. These equations can be solved iteratively. On the first iteration an initial density is assumed; this linearizes some of the terms. The remaining nonlinear terms are omitted for the first iteration so that the finite-difference equations are entirely linearized. These linearized equations are then solved to obtain the first approximate solution for stream function. This solution provides information used to obtain a better estimate of the density and an estimate of the other nonlinear terms. The equations are then solved again to obtain an improved solution. This process is repeated, and by iteration a final converged solution can be obtained if the flow is subsonic.

For each step of this iteration the linearized finite-difference equations must be solved. The method used to solve the equations is successive overrelaxation (ref. 9) with an optimum overrelaxation factor. Since this is also an iterative method, we have two levels of iteration. The overrelaxation is performed in the "inner iteration," and the corrections to the nonlinear terms are made in the "outer iteration."

After the stream function is obtained, the velocity distribution is obtained by numerical partial differentiation of the stream function and by using equations (A5) and (A6). The details of the numerical procedure and programming technique are described in part II.

TRANSONIC VELOCITY-GRADIENT APPROXIMATE SOLUTION

For the case where there is locally supersonic flow, equation (A1) is no longer elliptic in the entire region but is hyperbolic in the region of supersonic flow (ref. 10). This changes the boundary conditions and means that there will probably be shock losses in going from supersonic to subsonic flow. The finite-difference method cannot be used with locally supersonic flow. However, an approximate solution can be obtained by getting a reduced-flow solution with the finite-difference method and extending this to the full flow by using the velocity-gradient method. This technique is described in reference 5.

The velocity-gradient equations are equations (A7) to (A11). Equation (A7) is solved as an initial-value problem, where the velocity W is specified at the hub for any given vertical mesh line running from hub to tip. By finding several solutions for varying values of W at the hub, a solution satisfying the specified mass flow (eq. (A12)) will be found. When equation (A7) has been solved, subject to giving the correct mass flow, for every hub-shroud mesh line in the region, the entire velocity distribution at full mass flow has been obtained.

BLADE SURFACE VELOCITIES

The solution which is obtained by either the finite-difference or velocity-gradient method is for the mid-channel surface between the blades. Of greater interest are the blade surface velocities. These can be estimated since the blade loading is dependent on the rate of change of whirl. By assuming a linear variation of velocity between blade surfaces, equation (A13) can be derived for calculating the blade surface velocities.

APPLICATION OF PROGRAM

The program can be used both for analysis and as a design tool. When used for design, other programs should be used with this program. For axial compressors, reference 11 describes a program that will give blade mean-camber-line coordinates and thicknesses for an axial compressor blade. This blade design can be checked by using the MERIDL program to analyze the flow distribution in detail. Usually, changes must be made to the blade design to achieve a desirable flow distribution. These changes may involve more than just the blade shape; for example, hub and shroud profile, inlet and outlet whirl distribution, and loss distribution may have to be changed. Of course, the accuracy of the MERIDL solution depends on the accuracy of the boundary conditions used.

When a reasonable flow pattern is achieved by the MERIDL flow analysis on the mid-channel flow plane, more detailed blade surface velocities can be obtained on blade-to-blade planes by flow analyses on various blade elements from hub to shroud. A useful program for this purpose is TSONIC (ref. 5). Most of the information required to compute input for TSONIC is calculated and printed directly by MERIDL. The section Printed Output explains how to obtain and use this output from MERIDL. Further changes in blade shape or whirl distribution may be considered at this time. Reference 12 (Ch. VII) gives information on incidence and deviation for good design and for off-design conditions.

For cases when the flow is well guided in the channel but has large variations, both blade to blade and hub to shroud, the CHANEL program (ref. 13) is useful. The CHANEL program obtains a solution on a channel cross-section surface. The CHANEL program is particularly useful for calculating choking mass flow through a blade row.

DESCRIPTION OF INPUT AND OUTPUT

The principal block of input required by the program is a geometrical description of the blade row to be analyzed, given in the form of blade sections from hub to shroud.

Each blade section is described by a set of z-, r-, θ-, and normal-thickness coordinates on any general, smooth surface of revolution. There does not have to be any geometrical relation between analogous points on adjacent blade sections. Other inputs include upstream and downstream flow conditions, a geometric description of hub and shroud, appropriate gas constants, operating conditions such as mass flow and rotational speed, and a description of the finite-difference solution mesh. Requests are also given for various blocks of output data.

Output is given at any or all of three principal geometric locations: (1) on all mesh points of the orthogonal solution mesh, (2) along user-designated streamlines through the blade row, or (3) along straight lines from hub to shroud (station lines) located either inside or outside the blades or at the blade leading or trailing edges. In each of these locations, output consists mainly of z- and r-coordinates of orthogonal mesh lines or streamlines, stream function, relative velocities and velocity components, flow angles, and streamline curvature. Along streamlines and station lines which lie within the blades, estimates are also given of the blade surface velocities. Other desired output may be easily obtained by user modification of the program.

INPUT

Figure 5 shows the input variables as they are punched on the data cards. The first input data card is for a title, which serves for problem identification. Any information may be put in the 80 columns of this card.

All the numbers on the three input cards beginning with MBI, LSFR, and IMESH are integers (no decimal point) in a five-column field (see fig. 5). These must all be right-adjusted. The input variables on all other data cards are real numbers (punch decimal point) in 10-column fields.

Figure 5 indicates that several options exist for the statement of upstream and downstream flow conditions. First, the user can specify either whirl or absolute tangential velocity (LAMIN or VTHIN, and LAMOUT or VTHOUT). Whirl must be given as a function of stream function (SFIN and SFOUT). Tangential velocity is usually given as a function of radius (RADIN and RADOUT). And finally, on the downstream boundary, either absolute total pressure or absolute total pressure loss may be given (PROP or LOSOUT).

Input variables are both geometric and nongeometric. The geometric input variables are shown in figures 6 to 10. Further information concerning the input variables is given in the section Special Instructions for Preparing Input, pages 19 to 24.

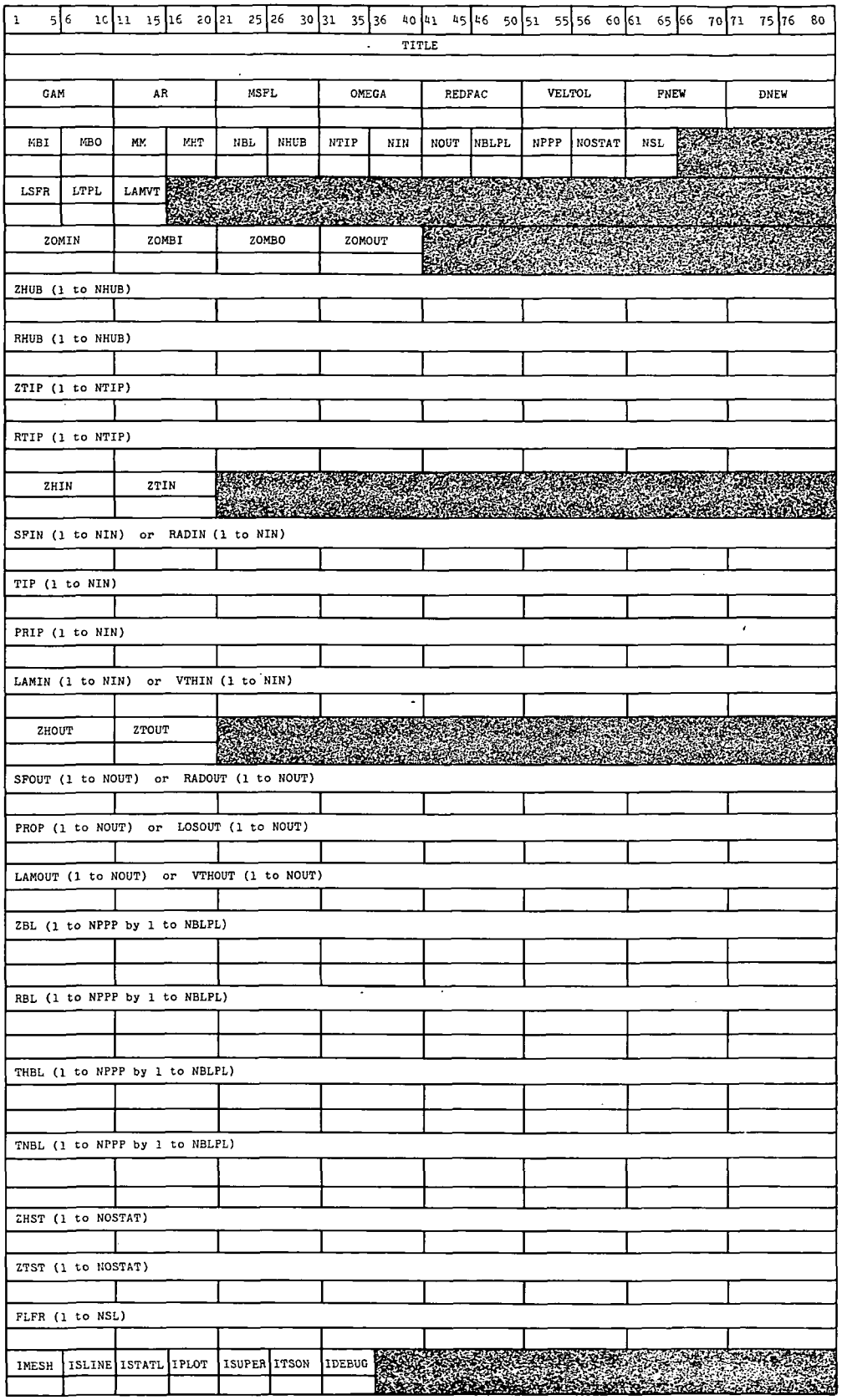

Figure 5. - Input form.

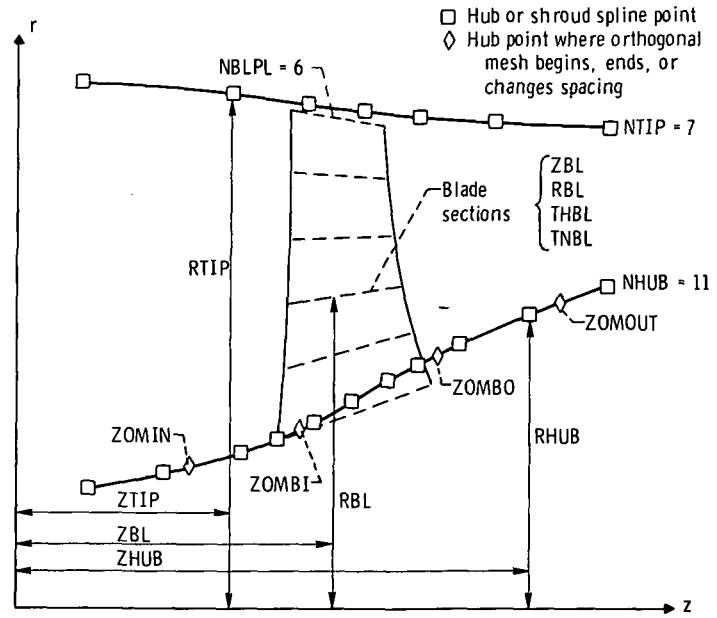

Figure 6. - Input variables - hub, shroud, and blade sections.

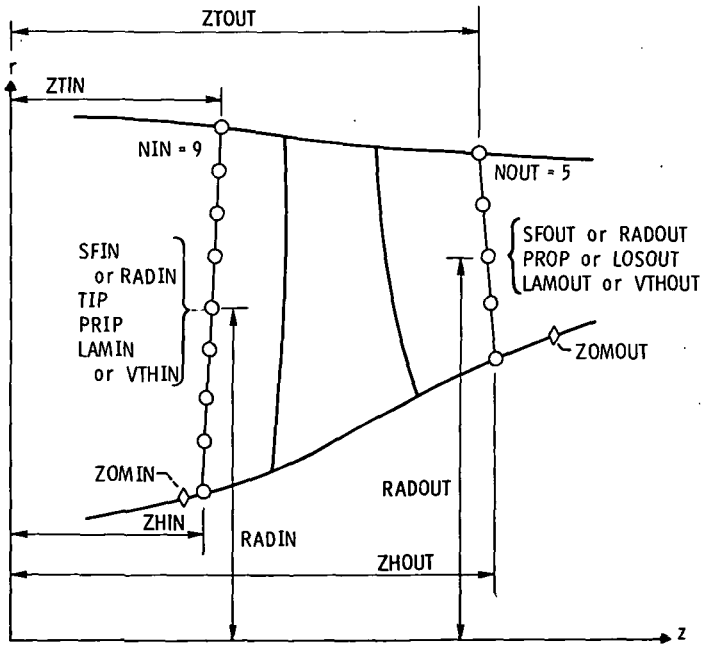

Figure 7. - Input variables - upstream and downstream flow variables.

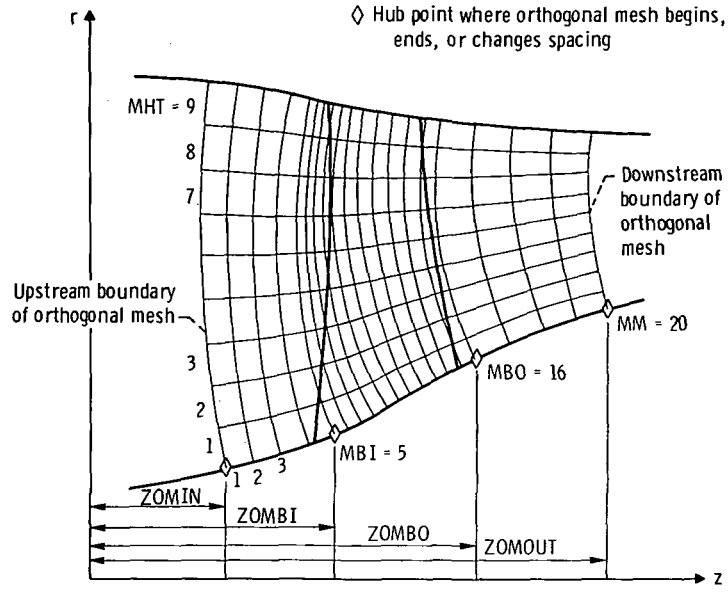

Figure 8. - Input variables - orthogonal mesh.

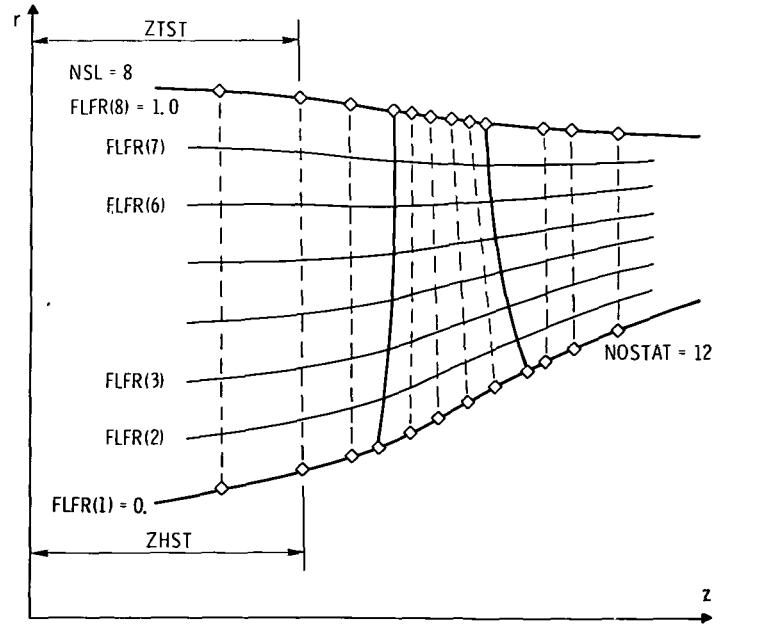

Figure 9. - Input variables - locating streamlines and station lines for output.

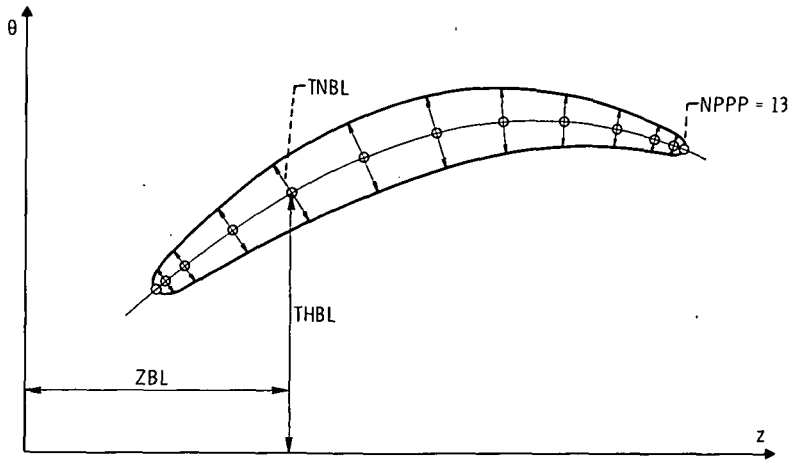

Figure 10. - Input variables - blade section. RBL must be given for each ZBL, THBL location (see fig. 6).

Input Dictionary

The input variables are described in terms of a consistent set of metric units: newtons, kilograms, meters, joules, kelvins, and seconds. The program, however, will run with input in any consistent set of units.

The input variables are the following:

GAM — Specific-heat ratio, γ

AR — Gas constant, J/(kg)(K)

MSFL — Total mass flow through entire circumferential annulus of machine, kg/sec

OMEGA — Rotational speed, ω, rad/sec. Note that ω is negative if rotation is in opposite direction of that shown in fig. 2.

REDFAC — Factor by which mass flow (MSFL) must be reduced in order to assure subsonic flow throughout flow passage. REDFAC may be left blank, in which case a value of 1.0 will be used. See section (k), p. 24.

VELTOL — Convergence tolerance on maximum velocity change in each outer iteration, over all mesh points, for reduced mass flow. VELTOL may be left blank, and a value of 0.01 will be used by the program. Whatever value is given is multiplied by the minimum of FNEW and DNEW before it is printed and subsequently used by the program. A value of 0.001 for VELTOL is a tight tolerance, 0.01 is a medium tolerance, and 0.1 is a loose tolerance.

FNEW — Damping factor on calculation of F_r from outer iteration to outer iteration. A value of 0.5 is suggested for FNEW. FNEW may be left blank, in which case the program will use a value of 0.5. See section (b), p. 20.

DNEW — Damping factor on calculation of $\partial(rV_\theta)/\partial r$ within blade row from iteration to iteration. DNEW may be left blank, and the program will use a value of 0.5. DNEW does not have to be equal to FNEW. See section (b), p. 20.

MBI — Number of vertical mesh lines from left boundary of orthogonal mesh (ZOMIN) to point of first mesh size change (ZOMBI). See fig. 8 and section (d), p. 21.

MBO — Total number of vertical mesh lines from left boundary of orthogonal mesh (ZOMIN) to point of second mesh size change (ZOMBO). See fig. 8 and section (d), p. 21.

MM — Total number of vertical mesh lines from left to right boundaries of orthogonal mesh (ZOMIN to ZOMOUT), maximum of 100. See fig. 8 and section (d), p. 21.

MHT — Total number of horizontal mesh spaces from hub to shroud of orthogonal mesh, maximum of 100. See fig. 8 and section (d), p. 21.

NBL — Number of blades in total circumference of blade row.

NHUB — Number of spline points given in ZHUB and RHUB arrays, maximum of 50. See fig. 6 and section (c), p. 20.

NTIP — Number of spline points given in ZTIP and RTIP arrays, maximum of 50. See fig. 6 and section (c), p. 20.

NIN — Number of data points given in upstream arrays of flow properties (SFIN, RADIN, TIP, PRIP, LAMIN, VTHIN), maximum of 50. See fig. 7 and section (e), p. 21.

NOUT — Number of data points given in downstream arrays of flow properties (SFOUT, RADOUT, PROP, LOSOUT, LAMOUT, VTHOUT), maximum of 50. See fig. 7 and section (e), p. 21.

NBLPL — Number of blade planes or blade sections on which data (ZBL, RBL, THBL, TNBL) are given to describe mean flow surface and blade thickness, maximum of 50. See fig. 6 and section (f), p. 22.

NPPP — Number of data points per blade section or blade plane in ZBL, RBL, THBL, and TNBL arrays, maximum of 50. See fig. 10 and section (f), p. 22.

NOSTAT Number of hub-shroud stations (located by coordinates in ZHST and ZTST) at which output is desired, maximum of 50. See fig. 9 and section (h), p. 23. NOSTAT may be left blank, in which case no input cards should be included for ZHST and ZTST arrays.

NSL Number of streamlines from hub to shroud (designated by values in FLFR) at which output is desired, maximum of 50. See fig. 9. NSL may be left blank, in which case no cards should be included for FLFR array. If NSL is left blank, the program will set it equal to 11 and print requested streamline output on 11 streamlines which vary by 10 percent of total flow (i. e., 0, 10, 20, . . ., 100 percent).

LSFR Integer (0 or 1) indicating whether upstream and downstream flow conditions are given as a function of stream function (0) or radius (1). If LAMVT = 0, LSFR must equal 0.

LTPL Integer (0 or 1) indicating whether downstream total pressure (0) or fractional loss of stagnation pressure (1) is given as input.

LAMVT Integer (0 or 1) indicating whether upstream and downstream whirl (0) or tangential velocity (1) is given as input.

ZOMIN z-Coordinate of intersection of left boundary of orthogonal mesh with hub profile, m. See figs. 6 and 8 and section (d), p. 21.

ZOMBI z-Coordinate of intersection of vertical mesh line with hub profile where first change in mesh spacing occurs (MBI), m. See figs. 6 and 8 and section (d), p. 21.

ZOMBO z-Coordinate of intersection of vertical mesh line with hub profile where second change in mesh spacing occurs (MBO), m. See figs. 6 and 8 and section (d), p. 21.

ZOMOUT z-Coordinate of intersection of right boundary of orthogonal mesh (MM) with hub profile, m. See figs. 6 and 8 and section (d), p. 21.

ZHUB Array of z-coordinates of input points defining hub or bottom boundary of flow channel, m. See fig. 6 and section (c), p. 20.

RHUB Array of r-coordinates of input points defining hub or bottom boundary of flow channel, m. See fig. 6 and section (c), p. 20.

ZTIP Array of z-coordinates of input points defining shroud or top boundary of flow channel, m. See fig. 6 and section (c), p. 20.

RTIP Array of r-coordinates of input points defining shroud or top boundary of flow channel, m. See fig. 6 and section (c), p. 20.

ZHIN — z-Coordinate of intersection with hub profile of line on which upstream flow conditions are given, m. See fig. 7 and section (e), p. 21.

ZTIN — z-Coordinate of intersection with shroud profile of line on which upstream flow conditions are given, m. See fig. 7 and section (e), p. 21.

SFIN — Array of values of stream function for input points from hub to shroud along line on which upstream flow conditions are given. See fig. 7 and section (e), p. 21.

RADIN — Array of r-coordinates of input points along line from hub to shroud on which upstream flow conditions are given, m. See fig. 7 and section (e), p. 21.

TIP — Array of absolute total temperatures T_i' at input points along line from hub to shroud on which upstream flow conditions are given, K. See fig. 7 and section (e), p. 21.

PRIP — Array of absolute total pressures p_i' at input points along line from hub to shroud on which upstream flow conditions are given, N/m^2. See fig. 7 and section (e), p. 21.

LAMIN — Array of values of absolute whirl $\left(rV_\theta\right)_i$ at input points along line from hub to shroud on which upstream flow conditions are given, m^2/sec. See fig. 7 and section (e), p. 21.

VTHIN — Array of values of absolute tangential velocity $\left(V_\theta\right)_i$ at input points along line from hub to shroud on which upstream flow conditions are given, m/sec. See fig. 7 and section (e), p. 21.

ZHOUT — z-Coordinate of intersection with hub profile of line on which downstream flow conditions are given, m. See fig. 7 and section (e), p. 21.

ZTOUT — z-Coordinate of intersection with shroud profile of line on which downstream flow conditions are given, m. See fig. 7 and section (e), p. 21.

SFOUT — Array of values of stream function for input points from hub to shroud along line on which downstream flow conditions are given. See fig. 7 and section (e), p. 21.

RADOUT — Array of r-coordinates of input points along line from hub to shroud on which downstream flow conditions are given, m. See fig. 7 and section (e), p. 21.

PROP — Array of absolute total pressures p_o' at input points along line from hub to shroud on which downstream flow conditions are given, N/m^2. See fig. 7 and section (e), p. 21.

LOSOUT Array of fraction of absolute total pressure loss $(p'_{o,\,id} - p'_o)/p'_{o,\,id}$ at input points along line from hub to shroud on which downstream flow conditions are given. See fig. 7 and section (e), p. 21.

LAMOUT Array of values of absolute whirl $\left(rV_\theta\right)_o$ at input points along line from hub to shroud on which downstream flow conditions are given, m^2/sec. See fig. 7 and section (e), p. 21.

VTHOUT Array of values of absolute tangential velocity $\left(V_\theta\right)_o$ at input points along line from hub to shroud on which downstream flow conditions are given, m/sec. See fig. 7 and section (e), p. 21.

ZBL Two-dimensional array of z-coordinates of points describing mean blade surface, m. See fig. 10 and section (f), p. 22. This surface is described by a series (from 2 to 50) of blade sections from hub to shroud. The hub section is given first, followed by successive sections up to the shroud.

RBL Two-dimensional array of r-coordinates, corresponding to ZBL, of points describing mean blade surface, m. See fig. 6 and section (f), p. 22.

THBL Two-dimensional array of θ-coordinates, corresponding to ZBL, of points describing mean blade surface, rad. See fig. 10 and section (f), p. 22. Theta is positive in direction of positive rotation (see fig. 2). The origin of θ-coordinates can be anywhere around the circumference.

TNBL Two-dimensional array of blade normal thicknesses, corresponding to ZBL, RBL coordinates, m. See fig. 10 and section (f), p. 22. TNBL is thickness on a surface of revolution and is normal to blade mean camber line. It is not the thickness at a constant value of z-coordinate from suction surface to pressure surface (see fig. 10). Thickness from either a conical blade section or a cylindrical blade section can be used for TNBL; it makes little difference. This input is used only to calculate local blade blockage and usually has a minor effect on computed results.

ZHST Array of z-coordinates of intersections of hub-shroud output station lines with hub profile, m. See fig. 9 and section (h), p. 23. No input cards should be given for ZHST and ZTST if user does not wish output on hub-shroud station lines (i. e., NOSTAT = 0).

ZTST Array of z-coordinates of intersections of hub-shroud output station lines with shroud profile, m. See fig. 9 and section (h), p. 23.

FLFR Array of values of stream function designating stream lines along which output is to be printed. See fig. 9 and section (h), p. 23. If no cards are given for FLFR array (i.e., NSL = 0), the program will automatically assign the following 11 values to FLFR: 0.0, 0.1, 0.2, ..., 0.9, 1.0.

The remaining seven integer variables, beginning with IMESH, are used to indicate what output is desired. The program reduces the input mass flow by REDFAC and solves the resulting problem iteratively with a stream-function analysis. The results of this analysis are then used with full mass flow to obtain a transonic analysis by velocity-gradient methods. Output can be obtained after each reduced mass-flow iteration and also after the final transonic solution.

For all these variables except ISUPER, the integer given indicates the multiple of outer iterations at which the user wishes the output associated with the variables to be printed or plotted. A zero in any of these indicates that the output associated with that variable is to be omitted. A 1 will print or plot the output on every iteration. A 3, for example, would give the output on every third iteration. Any nonzero integer will cause output to be given on the first and last iterations and after the transonic solution, in addition to the output called for at other iterations. A large integer will obviously give only the first iteration and the final converged iteration. Care should be used not to call for more output than is really useful. The following list gives the output associated with each of these variables:

IMESH Major output at every mesh point of the orthogonal mesh (i.e., mesh point indices and coordinates, stream-function value, relative velocity components and total relative velocity, critical velocity ratio, and flow angles). This output is usually not requested, except for debugging purposes, since output called for by ISLINE or ISTATL is preferable in most cases.

ISLINE Major output along streamlines (indicated by values in FLFR) at each point where streamlines are crossed by vertical mesh lines of the orthogonal mesh. Output includes z, r, and m streamline coordinates, relative velocity components and total relative velocity, critical velocity ratio, flow angles, and streamline curvature. Where the streamline passes within the blade region, an estimate of suction- and pressure-surface velocities is also printed.

ISTATL Major output along station lines from hub to shroud (at locations specified by ZHST and ZTST arrays and at values of stream function specified by FLFR array). Output corresponds to that given for ISLINE with the addition that FLFR stream-function values are printed.

IPLOT Plotting indicator requesting output to be plotted on microfilm. Any nonzero value in IPLOT will cause the input data and generated orthogonal mesh to be plotted. Also, at each outer iteration which is a multiple of IPLOT, streamlines will be plotted, and meridional and surface velocities will be plotted for each streamline value. These will also be plotted after the final transonic solution.

ISUPER Integer (0 or 1) indicating which solution (subsonic or supersonic) of the velocity-gradient equation is desired. If ISUPER = 0, only the subsonic solution will be printed. If ISUPER = 1, both subsonic and supersonic solutions will be printed.

ITSON Integer indicating when information is desired for use in calculating input for the TSONIC program (ref. 5). If ITSON = 0, no information will be given for TSONIC. Otherwise, information will be listed with other output. Usually, the user only wants TSONIC data after subsonic convergence is reached. Using a high value for ITSON (i.e., >20) will achieve this result.

IDEBUG Integer indicating whether additional debug output is desired. If IDEBUG = 0, no extra output is printed. If IDEBUG > 0, the coefficients of the finite-difference equations, as well as 21 arrays of debug output on the orthogonal mesh are printed. Fourteen of these arrays change and are reprinted after each outer interation of the reduced-mass-flow solution which is a multiple of IDEBUG.

Special Instructions for Preparing Input

It is unusual to have no errors in input to MERIDL the first time any new data set is run. Therefore, input should be checked thoroughly before it is submitted. Errors are commonly made for the following reasons: inconsistent units; improper sign on ω, V_θ, or whirl; input for arrays not agreeing with the input bounds for those arrays; and upstream and downstream input not being of the form specified by LSFR, LTPL, and LAMVT. Also geometrical input into the hub and shroud arrays and the blade geometry arrays should be smooth enough that the hub, shroud, and blade sections will be fit well with cubic spline curves (see section (g), p. 22). These input geometrical arrays are all plotted on microfilm by the program after spline fitting is completed; the microfilm output will indicate whether or not the input was smooth. All output should be checked, especially from a new input data set, to see if it is reasonable.

(a) Units of measurement. - The International System of Units (ref. 14) is used throughout this report. However, the program does not use any constants which depend on the system of units being used. Therefore, any consistent set of units may be used

in preparing input for the program. For example, if force, length, temperature, and time are chosen independently, mass units are obtained from Force = Mass × Acceleration. The gas constant R must then have the units of (Force × Length)/(Mass × Temperature). Density is mass per unit volume, and mass flow is mass per unit time. Output then gives velocity in the chosen units of length per unit time. Since any consistent set of units can be employed, the output is not labeled with any units.

(b) Damping factors FNEW and DNEW. - The input variables FNEW and DNEW are used as damping factors on the F_r and $\partial(rV_\theta)/\partial r$ terms of equation (A1). During each outer iteration of the subsonic or finite-difference portion of the program, new values for F_r and $\partial(rV_\theta)/\partial r$ are calculated. The calculated changes to these terms are often so large that if the full change was accepted on each iteration the solution would diverge. Using values of FNEW and DNEW less than 1.0 allows only a portion of these changes to be used. The value of FNEW or DNEW is the fraction of the predicted change in F_r or $\partial(rV_\theta)/\partial r$ to be added to the previous values of these variables. Therefore, if F_r or $\partial(rV_\theta)/\partial r$ do not converge, FNEW or DNEW should be reduced. However, this will reduce the rate of convergence so that caution should be used that FNEW and DNEW are not made too small. Because of the reduced rate of convergence, VELTOL is automatically reduced to obtain the same accuracy as when FNEW and DNEW are 1.0.

Limited experience has shown that for subsonic flows, where the gradients of flow variables are not large, converged solutions can be obtained with FNEW and DNEW equal to 1.0. For most practical flows, however, this is not the case and some damping is required. Values of FNEW and DNEW in the range of 0.5 are most commonly used, although at times values as low as 0.2 have been used. (Note that FNEW and DNEW do not have to be equal to each other.)

The user will have to gain experience with FNEW and DNEW before he can use them effectively to maximize rates of convergence. Maximum, minimum, and change values for F_r and $\partial(rV_\theta)/\partial r$ (DVTHDR) are printed with the output on each iteration. The maximum relative change in velocity at any point is also printed; it should gradually approach VELTOL for convergence. By observing these values, the user can learn the effects of changes in FNEW and DNEW for different runs of the program.

(c) Hub and shroud flow channel geometry. - The hub and shroud geometry are specified in the ZHUB, RHUB and ZTIP, RTIP arrays. Both of these curves must have the same z-origin (usually the blade leading edge at the hub). These two arrays must extend far enough upstream of the blade leading edge and far enough downstream of the blade trailing edge to cover the upstream and downstream boundaries of the orthogonal mesh, as well as the upstream and downstream input stations where streamflow data are given. If they do not extend this far, they will be linearly extrapolated and an incorrect flow channel may result. Relatively few points are needed to describe these smooth surfaces

(5 to 10 is a typical range for NHUB and NTIP) in order to have the program calculate smooth, accurate spline fits of these surfaces (see fig. 6).

If the user knows the amount of the boundary-layer blockage along the hub and shroud profiles, he should revise the hub and shroud arrays to include this blockage effect. In this situation the output will represent a more realistic flow condition.

(d) Orthogonal mesh. - The number of orthogonal mesh lines is specified by MBI, MBO, MM, and MHT; and the positioning of the mesh is specified by ZOMIN, ZOMBI, ZOMBO, and ZOMOUT. These four z-coordinates, all located on the hub, must use the same z-origin as all other geometrical input. The ZOMBI and ZOMBO locations are usually close to the leading and trailing edges of the blade at the hub, although they do not have to correspond to these locations exactly (see fig. 8). Mesh-size spacing in the horizontal direction is established by the relation between the four z-coordinates (ZOMIN, etc.) and the numbers of mesh spaces requested. For instance, MBO - MBI evenly spaced mesh spaces along the hub will be located in the distance given by ZOMBO - ZOMBI. Mesh spacing in the vertical direction is determined by locating MHT spaces in the hub-shroud distance. Usually, none of the vertical mesh lines follow the blade leading- or trailing-edge lines since the blade edges are not usually orthogonal to the hub or the shroud (see fig. 8). So some vertical mesh lines will pass in or out of the blade region as they progress from hub to shroud. A suggested number of mesh lines between ZOMBI and ZOMBO is 15 to 30 in order to cover the blade adequately, depending on blade geometry.

(e) Upstream and downstream flow conditions. - Upstream flow conditions are given in the SFIN (or RADIN), TIP, PRIP, and LAMIN (or VTHIN) arrays, which are all of length NIN. Downstream conditions are given in the SFOUT (or RADOUT), PROP (or LOSOUT), and LAMOUT (or VTHOUT) arrays, which are all of length NOUT. Upstream and downstream flow conditions are used, along with the assumption of conservation of angular momentum along streamlines, to establish boundary values on the upstream and downstream boundaries of the orthogonal mesh.

Ordinarily, the upstream and downstream flow conditions are given as a function of stream function (SFIN and SFOUT). In this case these input values apply at all points along streamlines upstream or downstream of the blade; and the ZHIN, ZTIN and ZHOUT, ZTOUT inputs are superfluous. Values of zero can be supplied for ZHIN and ZTIN and for ZHOUT and ZTOUT, or blank cards can be used in place of these variables. On the other hand, if input is given as a function of radius (RADIN and RADOUT), legitimate values must be supplied for ZHIN, ZTIN and ZHOUT, ZTOUT. In this case the upstream conditions are given on a straight line which passes through the two points given by ZHIN on the hub and ZTIN on the shroud. Downstream conditions are given on a straight line which passes through ZHOUT on the hub and ZTOUT on the shroud. These lines may lie anywhere in the regions from the blade edges upstream and downstream to the boundaries of the orthogonal mesh (see figs. 7 and 8).

The arrays of upstream and downstream input do not necessarily have to extend all the way from hub to shroud or lie on radial lines. They will be linearly extrapolated to the hub and shroud if necessary by the program, should the user only give data in a portion of the flow channel.

(f) Mean blade surface and thickness coordinates. - The blade shape is described from hub to shroud by the arrays ZBL, RBL, THBL, and TNBL, all of which are two-dimensional (see figs. 6 and 10). Each of these arrays has NBLPL blade sections or planes, with NPPP points in each of these planes. When giving data to each of these four arrays, start each new plane of data (NPPP points) at the beginning of a new card. All the ZBL data for all the planes are given, followed by all the RBL data, etc. The origin for z-coordinates for ZBL should be the same as that used for all other z-coordinate input arrays.

The input θ-coordinates in THBL are of the blade mean camber surface and not the mid-channel flow surface. The program, however, obtains a solution on the mid-channel flow surface. It obtains that flow surface by smoothly fairing the inlet and outlet flow angles onto the input blade surface at an appropriate distance back on the blades from the leading and trailing edges. This distance is a function of solidity (see appendix F).

The input blade thicknesses in TNBL are normal to the blade-section mean camber line and lie on a surface of revolution cutting through the blade (see figs. 6 and 10). So, in general, these thicknesses lie on a curved line whose ends are at different radii and are almost, but not quite, normal to the blade surfaces (see fig. 10). Because these thicknesses are used only for calculating blockage, it makes little difference whether they are obtained from a conical blade section or from a cylindrical section.

The first blade section given at the hub or the last one at the blade tip (in the ZBL, RBL, THBL, and TNBL arrays) does not necessarily have to conform to the hub or shroud profile. It can be given within the flow region, crossing the boundary, or completely outside of the boundary (see fig. 6). Extrapolation or interpolation will be used when necessary to obtain blade data where the blades meet the hub and shroud profiles.

The user should attempt to give smooth data for the z-, r-, θ-, and thickness arrays describing the blade. The program makes use of spline fits of these curves to compute gradients which are used throughout the program. The microfilm plots of the blade sections given as output will indicate whether input data for these arrays were acceptable.

(g) How to specify points for spline curves. - All the input arrays are fit with cubic spline curves for the purposes of interpolating, calculating derivatives, integrating, or any other required calculation. A cubic spline curve is a piecewise cubic polynomial which expresses mathematically the shape taken by an idealized spline passing through the given points. Reference 15 describes the method used for determining the equation of the spline curve. Using this method, smooth curves can be specified accurately with a few points, usually not more than four or five. Curves with uneven places, dips, or

highly variable curvatures require more points and are more difficult to fit properly. As a guide, enough points should be specified so that a physical spline passing through these points would accurately follow the curve. The minimum number of points to follow the curve should be used, since the closer the spline points are, the greater the effect of an inaccuracy in a coordinate.

(h) Requests for output data. - The seven variables IMESH, ISLINE, ISTATL, IPLOT, ISUPER, ITSON, and IDEBUG all request different portions of output from the program. The optional arrays ZHST, ZTST, and FLFR are also used in this regard. The user should be careful to request only the output needed. Usually, only one of the three major types of output (at the mesh points (IMESH), along streamlines (ISLINE), or along hub-shroud stations (ISTATL)) is needed, since ISLINE and ISTATL output are obtained from calculated mesh-point data by interpolation (see fig. 11). Most likely,

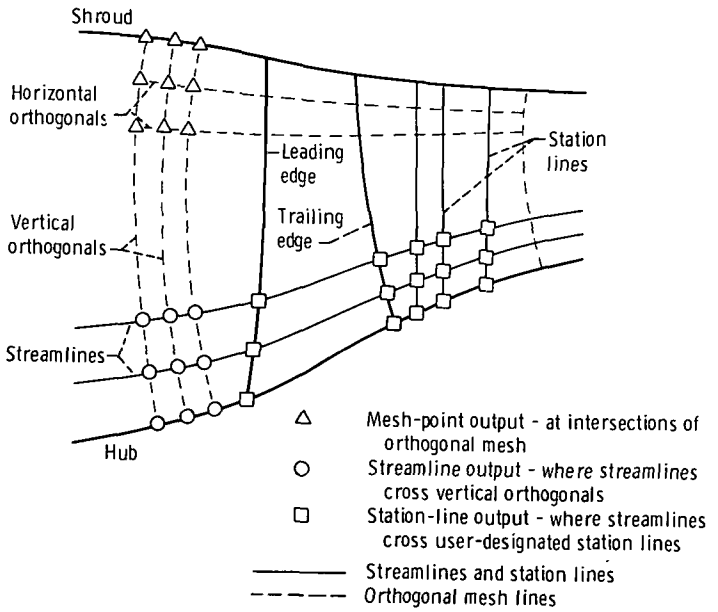

Figure 11. - Location of three major types of output.

streamline output (ISLINE) or station-line output (ISTATL) would be chosen. The frequency at which output is requested is also significant; this is controlled by the values given to IMESH, ISLINE, and ISTATL.

ZHST and ZTST are given only if ISTATL output is requested. In this case, output will be given along straight lines from hub to shroud which connect corresponding points in the ZHST and ZTST arrays. Through the values in these arrays, the user can control exactly the locations at which his output is given. These lines do not have to be radial. Typically, output is requested (through ZHST and ZTST) at several upstream and downstream locations, at the blade leading and trailing edges, and at several sta-

tions within the blade at percentages of chord from the leading to the trailing edge. To obtain output at the leading and trailing edges, the values in ZHST and ZTST should correspond (within a tolerance of 1 percent of local chord) to the intersection points of the leading and trailing edges with the hub and shroud.

FLFR need be given only if the user wishes to specify the values of streamline along which he wishes output (when ISLINE or ISTATL are used). If the user does not specify otherwise (using FLFR), the program will automatically give output at 10-percent streamlines.

(i) Incompressible flow. - Incompressible-flow cases execute as well on MERIDL as compressible-flow cases. In fact, they should converge in two or three iterations. No special input is required for an incompressible case, except that REDFAC should be set to 1.0 to avoid the transonic solution which would be redundant and less accurate.

(j) Straight infinite cascade. - The program is primarily designed for circular, stationary, or rotating blade rows; but the input can be adopted to apply to a straight infinite cascade as well. Since the radius for such a cascade would be infinite, an artificial convention must be adopted. The user should pick a large average radius for his cascade, in the neighborhood of $r = 1000$. Then, since the blade pitch P is known, an approximate number of blades to use can be calculated from $NBL = (2\pi r)/P$. This value must be rounded to an integer for use in the input. With this value of NBL and a large mean radius, all the r-coordinate arrays of input (RHUB, RTIP, RADIN, RADOUT, and RBL) can be established about the mean radius, and a value of MSFL can be calculated. Using this artificial input at large radius, the program will obtain a solution using a pitch which varies very slightly from hub to shroud and, therefore, simulates almost exactly a straight infinite cascade.

(k) Choosing a value for REDFAC. - If possible REDFAC should be 1.0. However, if there is locally supersonic flow, REDFAC must be less than 1.0, usually between 0.5 and 0.95. For the best accuracy the largest possible value of REDFAC should be used (see the section NUMERICAL EXAMPLE). When REDFAC is 1.0, the full mass flow will be used in the finite-difference solution for the stream function, and no transonic velocity-gradient calculation will be made.

OUTPUT

There are four different types of output generated by the MERIDL program:

(1) Main output - controlled by the variables IMESH, ISLINE, ISTATL, and ISUPER

(2) Debug output - controlled by IDEBUG

(3) TSONIC information - controlled by ITSON

(4) Plotted output - controlled by IPLOT

Most of this output is optional and is controlled by the final input card, as already described.

The output requested by the variables IMESH, ISLINE, and ISTATL is essentially the same for any of the three variables but is given at different locations for the convenience of the user. IMESH output is given at the orthogonal mesh points along horizontal mesh lines, as indicated in figure 11. ISLINE output is given along streamlines where the streamlines are intersected by the vertical orthogonal mesh lines (fig. 11). ISTATL output is given from hub to shroud along station lines (fig. 11) where these lines are intersected by the streamlines.

In the following sections, output is presented from the problem solved in the section NUMERICAL EXAMPLE. Since the complete output would be lengthy, only the first few lines of each section of output are reproduced here. In many instances, output labels are simply internal variable names.

The following three sections discuss the different sections of printed output, the plotted output, and all possible error messages.

Printed Output

Table I presents the printed output from the numerical example. Each section of this output has been numbered to correspond to the following description:

(1) The first output is a listing of the input data. Variable names are used as labels, and the output corresponds to the input form (fig. 5). This output is listed for every run, regardless of the values given to IMESH, etc.

(2) This output corresponds to IDEBUG. It has three principal sections, as the output indicates. The constant quantities are listed only once; while the coefficients of the matrix equation and the changing quantities are listed in between outer iterations, as called for by the value in IDEBUG. The output giving the changing quantities contains two different sets of variables. (All the IDEBUG variables are described more thoroughly in part II of this report.)

(3) This output indicates the calculated value of overrelaxation factor, ORF, to be used in the successive overrelaxation solution of the finite-difference equations. This matrix equation for the stream function u is solved iteratively (this is referred to as the "inner iteration") during each of the "outer iterations" of the reduced-mass-flow solution. This output, ORF, is given automatically on each run of the program.

(4) This output indicates the maximum value, the minimum value, and the maximum change in the values of DVTHDR ($\partial(rV_\theta)/\partial r$) and FR ($F_r$) calculated for each outer iteration of the reduced-mass-flow solution. The two quantities ($\partial(rV_\theta)/\partial r$) and F_r are critical to the convergence of the reduced-mass-flow solution, and the input variables DNEW and FNEW are used to control the percentage of the calculated changes of these

TABLE I. - SAMPLE OUTPUT

```
DATA 12 - AXIAL COMPRESSOR ROTOR - INLET WHIRL - S.I. UNITS


GENERAL INPUT DATA
    GAM              AR              MSFL            OMEGA           REDFAC          VELTOL          FNEW            CNEW
  1.400000        287.0530        42.82988       -826.5496        0.9999900    0.4999999E-02      0.5000000       0.5000000
    MBI     MBD     MM      MHT   NBL   NHUB   NTIP     NIN   NOUT   NBLPL   NPPP   NOSTAT   NSL
     11      31      41      20    17      6      6      11     11      11     15        4     11
   LSEP    LTPL   LAMVT
      1       0       1


HUB AND SHROUD INPUT DATA
    ZCMIN           ZCMBI           ZCMBO           ZCMOUT
-0.4572000E-01   0.0000000       0.1219200       0.1676400
    ZHUB ARRAY
-0.9140998E-01  -0.4063000E-01   0.1018000E-01   0.6099000E-01   0.1371900       0.2133900
    RHUB ARRAY
 0.1178660       0.1430120       0.1554480       0.1612999       0.1640739       0.1645920
    ZTIP ARRAY
-0.9140998E-01  -0.4063000E-01   0.1018000E-01   0.6099000E-01   0.1371900       0.2133900
    RTIP ARRAY
 0.3246120       0.3159860       0.3111399       0.3083659       0.3073300       0.3065680


UPSTREAM INPUT DATA
    ZHIN            ZTIN
-0.1521000E-01  -0.1521000E-01
    RADIN ARRAY
 0.1506630       0.1737660       0.1933350       0.2113180       0.2280509       0.2437789       0.2586840       0.2728570
 0.2863600       0.2992830       0.3131210
    TIP ARRAY
 288.1499        288.1499        288.1499        288.1499        288.1499        288.1499        288.1499        288.1499
 288.1499        288.1499        288.1499
    PRIP ARRAY
 101352.9        101352.9        101352.9        101352.9        101352.9        101352.9        101352.9        101352.9
 101352.9        101352.9        101352.9
    VTHIN ARRAY
-5.943600       -15.13637       -21.02814       -25.74644       -29.73323       -33.18661       -36.23462       -38.95343
-41.40402       -43.60773       -45.79619


DOWNSTREAM INPUT DATA
    ZHOUT           ZTOUT
 0.1371900       0.1371900
    RADOUT ARRAY
 0.1640739       0.1837029       0.1997350       0.2147930       0.2290270       0.2426510       0.2557270       0.2684070
 0.2806900       0.2927300       0.3073300
    PROP ARRAY
 129221.6        129221.6        129221.6        129221.6        129221.6        129221.6        129221.6        129221.6
 129221.6        129221.6        129221.6
    VTHOUT ARRAY
-168.3715       -159.1483       -153.3876       -149.5227       -146.6027       -144.3655       -142.9390       -141.9753
-141.1803       -142.2349       -146.4107
```

1

BLADE MEAN CAMBER LINE AND THICKNESS INPUT DATA

TPL ARRAY

-0.0000000	0.1128000E-02	0.6307997E-02	0.1369200E-01	0.2229900E-01	0.3327000E-01	0.4442200E-01	0.5570000E-01
0.6704497E-01	0.7839996E-01	0.8970696E-01	0.9867895E-01	0.1064500	0.1119450	0.1128179	
0.1305000E-02	0.2325000E-02	0.7351998E-02	0.1453000E-01	0.2291500E-01	0.3363700E-01	0.4457900E-01	0.5569500E-01
0.6693399E-01	0.7824898E-01	0.8958759E-01	0.9864396E-01	0.1065339	0.1121410	0.1129839	
0.2751000E-02	0.3683000E-02	0.8550998E-02	0.1551200E-01	0.2365900E-01	0.3410100E-01	0.4479400E-01	0.5569700E-01
0.6676799E-01	0.7796496E-01	0.8924496E-01	0.9829998E-01	0.1062260	0.1118820	0.1126910	
0.4230998E-02	0.5091999E-02	0.9808999E-02	0.1655900E-01	0.2446900E-01	0.3462600E-01	0.4505100E-01	0.5571000E-01
0.6656694E-01	0.7758898E-01	0.8873695E-01	0.9772295E-01	0.1056179	0.1112690	0.1120450	
0.5712997E-02	0.6514996E-02	0.1109100E-01	0.1764000E-01	0.2531900E-01	0.3519000E-01	0.4533600E-01	0.5573100E-01
0.6634396E-01	0.7714599E-01	0.8810699E-01	0.9697098E-01	0.1047810	0.1103849	0.1111290	
0.7169999E-02	0.7925998E-02	0.1237000E-01	0.1873000E-01	0.2618700E-01	0.3577600E-01	0.4564000E-01	0.5575800E-01
0.6610399E-01	0.7665598E-01	0.8738899E-01	0.9608799E-01	0.1037700	0.1092940	0.1100060	
0.8561999E-02	0.9280000E-02	0.1360300E-01	0.1978600E-01	0.2703500E-01	0.3635400E-01	0.4594400E-01	0.5578500E-01
0.6585896E-01	0.7614595E-01	0.8662599E-01	0.9513497E-01	0.1026630	0.1080820	0.1087660	
0.9888999E-02	0.1057700E-01	0.1478900E-01	0.2080900E-01	0.2786100E-01	0.3692300E-01	0.4624500E-01	0.5581200E-01
0.6560898E-01	0.7562000E-01	0.8582896E-01	0.9412795E-01	0.1014790	0.1067760	0.1074340	
0.1114200E-01	0.1180600E-01	0.1591600E-01	0.2178600E-01	0.2865400E-01	0.3747100E-01	0.4653600E-01	0.5583400E-01
0.6535596E-01	0.7508695E-01	0.8501697E-01	0.9309298E-01	0.1002520	0.1054140	0.1060480	
0.1224500E-01	0.1289000E-01	0.1690900E-01	0.2264400E-01	0.2934800E-01	0.3794700E-01	0.4678000E-01	0.5583900E-01
0.6511199E-01	0.7458895E-01	0.8426094E-01	0.9213197E-01	0.9910995E-01	0.1041450	0.1047590	
0.1320800E-01	0.1383900E-01	0.1777500E-01	0.2338700E-01	0.2994500E-01	0.3835000E-01	0.4697900E-01	0.5582500E-01
0.6487799E-01	0.7413095E-01	0.8357400E-01	0.9125996E-01	0.9807599E-01	0.1029960	0.1035950	

RRL ARRAY

0.1554829	0.1555880	0.1560680	0.1567520	0.1575500	0.1585660	0.1596000	0.1606449
0.1616960	0.1627490	0.1637959	0.1646280	0.1653480	0.1658570	0.1659380	
0.1763860	0.1764500	0.1767650	0.1772160	0.1777419	0.1784149	0.1791019	0.1798000
0.1805050	0.1812150	0.1819270	0.1824960	0.1829910	0.1833430	0.1833960	
0.1952600	0.1952960	0.1954850	0.1957549	0.1960710	0.1964750	0.1968900	0.1973130
0.1977420	0.1981760	0.1986130	0.1989640	0.1992710	0.1994900	0.1995220	
0.2126070	0.2126229	0.2127129	0.2128410	0.2129910	0.2131830	0.2133800	0.2135820
0.2137880	0.2139969	0.2142079	0.2143780	0.2145280	0.2146350	0.2146500	
0.2287440	0.2287450	0.2287560	0.2287720	0.2287900	0.2288139	0.2288380	0.2288620
0.2288880	0.2289140	0.2289400	0.2289610	0.2289790	0.2289930	0.2289940	
0.2438920	0.2438830	0.2438320	0.2437580	0.2436709	0.2435600	0.2434450	0.2433280
0.2432080	0.2430850	0.2429600	0.2428589	0.2427700	0.2427059	0.2426969	
0.2582130	0.2581960	0.2580950	0.2579510	0.2577810	0.2575630	0.2573389	0.2571090
0.2568730	0.2566320	0.2563870	0.2561880	0.2560120	0.2558849	0.2558690	
0.2718270	0.2718040	0.2716640	0.2714640	0.2712310	0.2709300	0.2706209	0.2703030
0.2699780	0.2696460	0.2693080	0.2690319	0.2687880	0.2686130	0.2685910	
0.2848260	0.2847990	0.2846299	0.2843879	0.2841060	0.2837440	0.2833700	0.2829880
0.2825969	0.2821960	0.2817880	0.2814560	0.2811610	0.2809490	0.2809229	
0.2972890	0.2972590	0.2970700	0.2968020	0.2964880	0.2960849	0.2956720	0.2952480
0.2948140	0.2943700	0.2939169	0.2935489	0.2932220	0.2929870	0.2929580	
0.3092760	0.3092450	0.3090520	0.3087760	0.3084550	0.3080420	0.3076180	0.3071840
0.3067400	0.3062860	0.3058230	0.3054460	0.3051110	0.3048699	0.3048410	

TRL ARRAY

-0.0000000	0.3439000E-02	0.1837000E-01	0.3721100E-01	0.5575800E-01	0.7440855E-01	0.8797896E-01	0.9644699E-01
0.9982097E-01	0.9814894E-01	0.9150296E-01	0.8266997E-01	0.7242697E-01	0.6369996E-01	0.6221300E-01	
-0.1322400E-01	-0.1007400E-01	0.4765999E-02	0.2391000E-01	0.4341400E-01	0.6416696E-01	0.8082598E-01	0.9333897E-01
0.1016760	0.1058310	0.1058190	0.1028300	0.9806299E-01	0.9344000E-01	0.9266800E-01	
-0.2311100E-01	-0.2017100E-01	-0.5377997E-02	0.1400900E-01	0.3423500E-01	0.5655800E-01	0.7552099E-01	0.9106100E-01
0.1031300	0.1116959	0.1167409	0.1182390	0.1177030	0.1162680	0.1160000	
-0.2977900E-01	-0.2701800E-01	-0.1235300E-01	0.7089999E-02	0.2772400E-01	0.5107300E-01	0.7164097E-01	0.8936197E-01
0.1041840	0.1160610	0.1249610	0.1259220	0.1326810	0.1337470	0.1338410	
-0.3428200E-01	-0.3167000E-01	-0.1719300E-01	0.2177000E-02	0.2300500E-01	0.4700500E-01	0.6869799E-01	0.8802098E-01
0.1049179	0.1193440	0.1312590	0.1389620	0.1443550	0.1474330	0.1477979	
-0.3726900E-01	-0.3478500E-01	-0.2053200E-01	-0.1322000E-02	0.1954200E-01	0.4394200E-01	0.6642097E-01	0.8692497E-01
0.1054070	0.1218200	0.1361240	0.1460260	0.1535520	0.1582710	0.1588430	

TABLE I. - Continued. SAMPLE OUTPUT

```
-0.3904000E-01 -0.3666200E-01 -0.2265500E-01 -0.3667000E-02  0.1712600E-01  0.4171400E-01  0.6469995E-01  0.8603698E-01
 0.1056809      0.1235920      0.1397310      0.1513450      0.1605450      0.1665620      0.1672900
-0.4000000E-01 -0.3771100E-01 -0.2396300E-01 -0.5233999E-02  0.1541200E-01  0.4005000E-01  0.6335098E-01  0.8527696E-01
 0.1057900      0.1248540      0.1424370      0.1554150      0.1659639      0.1730320      0.1738819
-0.4032700E-01 -0.3811200E-01 -0.2462800E-01 -0.6187998E-02  0.1426300E-01  0.3884700E-01  0.6231700E-01  0.8464199E-01
 0.1057900      0.1257330      0.1444400      0.1584980      0.1701240      0.1780390      0.1789860
-0.3994600E-01 -0.3779100E-01 -0.2457100E-01 -0.6430998E-02  0.1376200E-01  0.3817500E-01  0.6164400E-01  0.8414096E-01
 0.1056409      0.1261190      0.1455480      0.1603220      0.1726760      0.1811700      0.1821840
-0.3906100E-01 -0.3695300E-01 -0.2399300E-01 -0.6168999E-02  0.1373400E-01  0.3789400E-01  0.6123500E-01  0.8373499E-01
 0.1053700      0.1261200      0.1459620      0.1611680      0.1739780      0.1828400      0.1839000
    TABL  ARRAY
 0.0000000      0.2624000E-02  0.3829000E-02  0.5309999E-02  0.6706998E-02  0.8006997E-02  0.8808997E-02  0.9110000E-02
 0.8862000E-02  0.8017998E-02  0.6571997E-02  0.4974999E-02  0.3254000E-02  0.1838000E-02  0.0000000
 0.0000000      0.2395000E-02  0.3490000E-02  0.4832000E-02  0.6093998E-02  0.7260997E-02  0.7971998E-02  0.8226000E-02
 0.7985998E-02  0.7220998E-02  0.5925998E-02  0.4503999E-02  0.2976000E-02  0.1723000E-02  0.0000000
 0.0000000      0.2228000E-02  0.3234000E-02  0.4463997E-02  0.5617999E-02  0.6681997E-02  0.7323999E-02  0.7544998E-02
 0.7317998E-02  0.6614998E-02  0.5434997E-02  0.4145999E-02  0.2765000E-02  0.1632000E-02  0.0000000
 0.0000000      0.2103000E-02  0.3036000E-02  0.4177999E-02  0.5245999E-02  0.6228000E-02  0.6817997E-02  0.7015999E-02
 0.6798998E-02  0.6146997E-02  0.5057998E-02  0.3870000E-02  0.2600000E-02  0.1560000E-02  0.0000000
 0.0000000      0.2009000E-02  0.2885000E-02  0.3954999E-02  0.4956000E-02  0.5873997E-02  0.6422997E-02  0.6603997E-02
 0.6396998E-02  0.5783997E-02  0.4764996E-02  0.3656000E-02  0.2472000E-02  0.1502000E-02  0.0000000
 0.0000000      0.1939000E-02  0.2769000E-02  0.3784000E-02  0.4731998E-02  0.5600996E-02  0.6118998E-02  0.6285999E-02
 0.6086998E-02  0.5504999E-02  0.4539996E-02  0.3492000E-02  0.2373000E-02  0.1457000E-02  0.0000000
 0.0000000      0.1887000E-02  0.2683000E-02  0.3655000E-02  0.4562996E-02  0.5393997E-02  0.5888999E-02  0.6046999E-02
 0.5854998E-02  0.5295999E-02  0.4371997E-02  0.3368000E-02  0.2298000E-02  0.1422000E-02  0.0000000
 0.0000000      0.1850000E-02  0.2622000E-02  0.3563000E-02  0.4441999E-02  0.5245999E-02  0.5723000E-02  0.5874999E-02
 0.5686998E-02  0.5145997E-02  0.4249997E-02  0.3279000E-02  0.2243000E-02  0.1397000E-02  0.0000000
 0.0000000      0.1827000E-02  0.2581000E-02  0.3502000E-02  0.4361000E-02  0.5146995E-02  0.5612999E-02  0.5759999E-02
 0.5576000E-02  0.5044997E-02  0.4169997E-02  0.3220000E-02  0.2207000E-02  0.1379000E-02  0.0000000
 0.0000000      0.1814000E-02  0.2559000E-02  0.3468000E-02  0.4315998E-02  0.5089998E-02  0.5549997E-02  0.5694997E-02
 0.5512998E-02  0.4988998E-02  0.4123997E-02  0.3186000E-02  0.2186000E-02  0.1369000E-02  0.0000000
 0.0000000      0.1811000E-02  0.2552000E-02  0.3457000E-02  0.4300997E-02  0.5071998E-02  0.5530000E-02  0.5674999E-02
 0.5492996E-02  0.4972000E-02  0.4109997E-02  0.3176000E-02  0.2180000E-02  0.1366000E-02  0.0000000


 OUTPUT  STATION  LOCATION  DATA
    ZHST  ARRAY
-0.1521000E-01  0.0000000      0.1128190      0.1371900
    ZTST  ARRAY
-0.1521000E-01  0.1320700E-01  0.1035950      0.1371900


 OUTPUT  STREAMLINE  FLOW  FRACTION  DATA
    FLER  ARRAY
 0.0000000      0.9999996E-01  0.2000000      0.3000000      0.4000000      0.5000000      0.6000000      0.7000000
 0.8000000      0.9000000      1.000000


 OUTPUT  PRINT  CONTROL  DATA
   IMESH  ISLINE ISTATL IPLOT  ISUPER ITSON  IDEBUG
     10      4      4      1      1      8      1
```

1

CONSTANT QUANTITIES ON THE ORTHOGONAL MESH

I	J	SOM	TOM	BTH	DTHDT	PLOSS	CPHI	SPHI
1	1	0.000000	0.000000	0.369599	0.000000	0.000000	0.929951	0.367936
2	1	0.489445E-02	0.000000	0.369599	0.000000	0.000000	0.938356	0.345672
3	1	0.974530E-02	0.000000	0.369599	0.000000	0.000000	0.946490	0.322734
4	1	0.145569E-01	0.000000	0.369599	0.000000	0.000000	0.953719	0.300700
5	1	0.193344E-01	0.000000	0.369599	0.000000	0.000000	0.960086	0.279706
6	1	0.240824E-01	0.000000	0.369599	0.000000	0.000000	0.965646	0.259962
7	1	0.288049E-01	0.000000	0.369599	0.000000	0.000000	0.970459	0.241267
8	1	0.335057E-01	0.000000	0.369599	0.000000	0.000000	0.974588	0.224005

CALCULATED OVERRELAXATION FACTOR (ORF) = 1.797

ITERATION NO. 8 :

MAXIMUM CALCULATED VALUE OF DVTHDR = 26.037
MINIMUM CALCULATED VALUE OF DVTHDR = -216.52
MAXIMUM CALCULATED CHANGE IN DVTHDR = 28.928

COEFFICIENTS OF MATRIX EQUATION FOR STREAM FUNCTION

I	J	A(1)	A(2)	A(3)	A(4)	K
2	2	0.139942	0.135367	0.363342	0.361349	0.600462E-05
3	2	0.139258	0.134960	0.363379	0.362404	0.591905E-05
4	2	0.138511	0.134208	0.364143	0.363137	0.579377E-05
5	2	0.137923	0.133551	0.364884	0.363642	0.566183E-05
6	2	0.137501	0.133053	0.365442	0.364005	0.556708E-05
7	2	0.137225	0.132693	0.365861	0.364222	0.549692E-05
8	2	0.137078	0.132458	0.366142	0.364321	0.542330E-05

ITERATION 8. MAXIMUM RELATIVE CHANGE IN VELOCITY = 0.4765E-02

MAXIMUM CALCULATED VALUE OF ER = 40920.
MINIMUM CALCULATED VALUE OF ER = -86600.
MAXIMUM CALCULATED CHANGE IN ER = 3509.3

TABLE I. - Continued. SAMPLE OUTPUT

2

CHANGING QUANTITIES ON THE ORTHOGONAL MESH

I	J	WSURS	WSURT	VTH	RHO	RHOAV	DELRHO	DLOG
1	1	177.563	0.000000	-6.28156	1.06508	1.06508	0.000000	-18.5119
2	1	181.772	0.000000	-6.20471	1.05775	1.05775	0.000000	-18.5119
3	1	184.789	0.000000	-6.13509	1.05240	1.05240	0.000000	-18.5119
4	1	186.995	0.000000	-6.07205	1.04845	1.04845	0.000000	-18.5119
5	1	188.589	0.000000	-6.01492	1.04557	1.04557	0.000000	-18.5119
6	1	189.710	0.000000	-5.96309	1.04354	1.04354	0.000000	-18.5119
7	1	190.410	0.000000	-5.91600	1.04226	1.04226	0.000000	-18.5119
8	1	190.705	0.000000	-5.87315	1.04172	1.04172	0.000000	-18.5119

2

I	J	DTHDS	FR	DFDM	XIDM	ZETDM	CAMP	SAMP
1	1	0.000000	0.000000	-0.462905E-04	-0.297374E-04	55763.4	1.00000	0.000000
2	1	0.000000	0.000000	0.234145E-04	-0.289856E-04	57935.3	1.00000	0.000000
3	1	0.000000	0.000000	0.543992E-04	-0.516683E-04	59816.1	1.00000	0.000000
4	1	0.000000	0.000000	0.752901E-05	-0.106518E-03	61439.1	1.00000	0.000000
5	1	0.000000	0.000000	-0.394461E-04	0.339443E-05	62729.1	1.00000	0.000000
6	1	0.000000	0.000000	-0.326161E-04	0.638564E-04	63847.9	1.00000	0.000000
7	1	0.000000	0.000000	0.480329E-04	0.127880E-04	64875.0	1.00000	0.000000
8	1	0.000000	0.000000	0.215362E-04	-0.127576E-04	65701.1	1.00000	0.000000

5

*** STREAM FUNCTION, INTERIOR VELOCITIES, VELOCITY COMPONENTS, AND ANGLES ***
AT ALL MESH POINTS OF THE ORTHOGONAL MESH

****

****
* REDUCED MASSFLOW *
****
* ITERATION NO. 8 *
****

** HORIZONTAL ORTHOGONAL MESH LINE NO. 1 **

MESH-POINT COLM (I)	MESH-POINT ROW (J)	AXIAL COORD. (Z)	RADIAL COORD. (R)	STREAM FUNC. (U)	MERIC. VEL. (WM)	REL.TANG. VEL. (WTH)	REL. VEL. (W)	CRIT.VEL. RATIO (W/WCR)	MERID. ANGLE (ALPHA)	REL.FLOW ANGLE (BETA)	MESH ANGLE (PHI)
1	1	-0.45720E-01	0.14107	0.0000	177.56	110.32	209.04	0.666	21.59	31.85	21.59
2	1	-0.41148E-01	0.14282	0.0000	181.77	111.84	213.42	0.680	20.22	31.60	20.22
3	1	-0.36576E-01	0.14444	0.0000	184.79	113.25	216.73	0.690	18.83	31.50	18.83
4	1	-0.32004E-01	0.14594	0.0000	187.00	114.56	219.29	0.698	17.50	31.49	17.50
5	1	-0.27432E-01	0.14733	0.0000	188.59	115.76	221.28	0.704	16.24	31.54	16.24
6	1	-0.22860E-01	0.14861	0.0000	189.71	116.87	222.82	0.709	15.06	31.63	15.06
7	1	-0.18288E-01	0.14979	0.0000	190.41	117.89	223.95	0.712	13.96	31.76	13.96
8	1	-0.13716E-01	0.15088	0.0000	190.71	118.84	224.70	0.715	12.94	31.93	12.94

*** STREAM FUNCTION, INTERIOR VELOCITIES, VELOCITY COMPONENTS, ANGLES, AND SURFACE VELOCITIES ***
ALONG STREAMLINES
****

****
* REDUCED MASSFLOW *
****
* ITERATION NO. 8 *
****

** STREAMLINE NUMBER 1 -- STREAM FUNCTION = 0.0000 **

AXIAL COORD. (Z)	RADIAL COORD. (R)	MERID. COORD. (M)	MERID. VEL. (WM)	REL.TANG. VEL. (WTH)	REL. VEL. (W)	CRIT.VEL. RATIO (W/WCR)	MERID. ANGLE (ALPHA)	REL.FLOW ANGLE (BETA)	STREAM. CURV. (1./DIST)	SUCT.SUR. VEL. (WS)	PRES.SUR. VEL. (WP)
-0.45720E-01	0.14107	-0.47510E-01	177.56	110.32	209.04	0.666	21.59	31.85	-4.795	0.00	0.00
-0.41148E-01	0.14282	-0.42615E-01	181.77	111.84	213.42	0.680	20.22	31.60	-4.944	0.00	0.00
-0.36576E-01	0.14444	-0.37764E-01	184.79	113.25	216.73	0.690	18.83	31.50	-4.918	0.00	0.00
-0.32004E-01	0.14594	-0.32953E-01	187.00	114.56	219.29	0.698	17.50	31.49	-4.706	0.00	0.00
-0.27432E-01	0.14733	-0.28175E-01	188.59	115.76	221.28	0.704	16.24	31.54	-4.466	0.00	0.00
-0.22860E-01	0.14861	-0.23427E-01	189.71	116.87	222.82	0.709	15.06	31.63	-4.204	0.00	0.00
-0.18288E-01	0.14979	-0.18705E-01	190.41	117.89	223.95	0.712	13.96	31.76	-3.921	0.00	0.00
-0.13716E-01	0.15088	-0.14004E-01	190.71	118.84	224.70	0.715	12.94	31.93	-3.622	0.00	0.00

*** STREAM FUNCTION, INTERIOR VELOCITIES, VELOCITY COMPONENTS, ANGLES, AND SURFACE VELOCITIES ***
ALONG LINES FROM HUB TO SHROUD AT VARIOUS STATIONS THROUGH THE BLADE ROW

****
* REDUCED MASSFLOW *
****
* ITERATION NO. 8 *
****

** HUB-SHROUD STATION NO. 1 **

RADIAL COORD. (R)	AXIAL COORD. (Z)	MERID. COORD. (M)	STREAM FUNC. (U)	MERIC. VEL. (WM)	REL.TANG. VEL. (WTH)	REL. VEL. (W)	CRIT.VEL. RATIO (W/WCR)	MERID. ANGLE (ALPHA)	REL.FLOW ANGLE (BETA)	STREAM. CURV. (1./DIST)	SUCT.SUR. VEL. (WS)	PRES.SUR. VEL. (WP)
0.15054	-0.15210E-01	-0.15540E-01	0.0000	190.60	118.53	224.45	0.714	13.27	31.88	-3.718	0.00	0.00
0.17276	-0.15210E-01	-0.15433E-01	0.1000	179.30	127.61	220.07	0.699	10.37	35.44	-1.824	0.00	0.00
0.19283	-0.15210E-01	-0.15332E-01	0.2000	174.42	137.95	222.38	0.705	7.76	38.34	-1.190	0.00	0.00
0.21120	-0.15210E-01	-0.15273E-01	0.3000	171.10	148.27	226.41	0.716	5.46	40.91	-0.8264	0.00	0.00
0.22825	-0.15210E-01	-0.15233E-01	0.4000	168.72	158.32	231.37	0.730	3.39	43.18	-0.5374	0.00	0.00
0.24424	-0.15210E-01	-0.15214E-01	0.5000	166.79	168.10	236.80	0.745	1.54	45.22	-0.2957	0.00	0.00
0.25936	-0.15210E-01	-0.15210E-01	0.6000	165.37	177.60	242.67	0.762	-0.11	47.04	-0.3720E-01	0.00	0.00
0.27374	-0.15210E-01	-0.15215E-01	0.7000	164.50	186.83	248.93	0.779	-1.62	48.64	0.2552	0.00	0.00
0.28746	-0.15210E-01	-0.15228E-01	0.8000	164.07	195.80	255.46	0.798	-2.99	50.04	0.5218	0.00	0.00
0.30059	-0.15210E-01	-0.15244E-01	0.9000	164.17	204.54	262.28	0.817	-4.21	51.25	0.8216	0.00	0.00
0.31318	-0.15210E-01	-0.15262E-01	1.0000	163.99	213.05	268.86	0.835	-5.29	52.41	1.163	0.00	0.00

TABLE I. - Continued. SAMPLE OUTPUT

** HUB-SHROUD STATION NO. 2 ** ** LEADING EDGE **

RADIAL COORD. (R)	AXIAL COORD. (Z)	MERID. COORD. (M)	STREAM FUNC. (U)	MERID. VEL. (WM)	REL.TANG. VEL. (WTH)	REL. VEL. (W)	CRIT.VEL. RATIO (W/WCR)	MERID. ANGLE (ALPHA)	REL.FLOW ANGLE (BETA)	STREAM. CURV. (1./DIST)	SUCT.SUR. VEL. (WS)	PRES.SUR. VEL. (WP)
0.15370	-0.10033E-03	-0.10222E-03	0.0000	190.27	120.80	225.37	0.716	10.44	32.41	-2.648	242.05	208.70
0.17557	0.12485E-02	0.12641E-02	0.1000	191.67	130.47	231.87	0.736	8.68	34.24	-2.897	249.64	214.17
0.19508	0.27361E-02	0.27544E-02	0.2000	185.59	139.14	231.95	0.735	6.40	36.86	-1.829	247.27	216.78
0.21293	0.42596E-02	0.42739E-02	0.3000	184.21	150.28	237.74	0.751	4.37	39.21	-2.070	251.92	223.63
0.22936	0.57716E-02	0.57784E-02	0.4000	180.10	158.83	240.13	0.757	2.56	41.41	-1.089	252.11	228.27
0.24476	0.72540E-02	0.72557E-02	0.5000	180.71	168.49	247.07	0.777	1.07	43.00	-0.6539	260.10	234.14
0.25930	0.86676E-02	0.86680E-02	0.6000	180.57	178.15	253.66	0.796	-0.35	44.61	-0.7311	267.06	240.31
0.27310	0.10013E-01	0.10017E-01	0.7000	177.75	186.82	257.87	0.807	-1.69	46.43	-1.028	267.45	248.31
0.28621	0.11270E-01	0.11282E-01	0.8000	175.14	194.45	261.70	0.817	-2.65	47.99	-0.1266	267.98	255.45
0.29880	0.12371E-01	0.12395E-01	0.9000	174.97	202.73	267.79	0.834	-3.38	49.20	0.2954	273.26	262.38
0.31093	0.13336E-01	0.13373E-01	1.0000	174.45	210.87	273.67	0.851	-3.96	50.40	0.5627	278.82	268.58

** HUB-SHROUD STATION NO. 3 ** ** TRAILING EDGE **

RADIAL COORD. (R)	AXIAL COORD. (Z)	MERID. COORD. (M)	STREAM FUNC. (U)	MERID. VEL. (WM)	REL.TANG. VEL. (WTH)	REL. VEL. (W)	CRIT.VEL. RATIO (W/WCR)	MERID. ANGLE (ALPHA)	REL.FLOW ANGLE (BETA)	STREAM. CURV. (1./DIST)	SUCT.SUR. VEL. (WS)	PRES.SUR. VEL. (WP)
0.16365	0.11277	0.11321	0.0000	203.80	-33.83	206.59	0.656	1.32	-9.43	-0.5906	205.59	207.60
0.18216	0.11299	0.11320	0.1000	193.43	-10.54	193.72	0.614	0.29	-3.12	0.5161E-01	191.21	196.32
0.19912	0.11270	0.11280	0.2000	187.47	9.39	187.71	0.594	-0.18	2.87	0.2563	185.17	190.27
0.21492	0.11203	0.11206	0.3000	182.80	26.25	184.67	0.583	-0.45	8.17	0.3773	182.64	186.76
0.22982	0.11107	0.11108	0.4000	178.97	41.34	183.68	0.579	-0.63	13.01	0.4541	182.15	185.28
0.24398	0.10989	0.10990	0.5000	175.47	55.10	183.92	0.579	-0.76	17.43	0.4532	183.72	184.18
0.25753	0.10860	0.10862	0.6000	170.78	67.75	183.73	0.577	-0.87	21.64	0.3382	187.09	180.40
0.27054	0.10722	0.10726	0.7000	167.60	81.27	186.26	0.584	-0.95	25.87	0.6379	190.72	181.84
0.28312	0.10580	0.10587	0.8000	165.16	92.38	189.24	0.592	-0.99	29.22	0.6769	194.98	183.56
0.29539	0.10451	0.10460	0.9000	161.30	101.43	190.54	0.594	-0.90	32.16	0.5918	197.44	183.68
0.30753	0.10334	0.10344	1.0000	155.52	108.68	189.73	0.590	-0.51	34.95	0.3257	197.70	181.76

** HUB-SHROUD STATION NO. 4 **

RADIAL COORD. (R)	AXIAL COORD. (Z)	MERID. COORD. (M)	STREAM FUNC. (U)	MERID. VEL. (WM)	REL.TANG. VEL. (WTH)	REL. VEL. (W)	CRIT.VEL. RATIO (W/WCR)	MERID. ANGLE (ALPHA)	REL.FLOW ANGLE (BETA)	STREAM. CURV. (1./DIST)	SUCT.SUR. VEL. (WS)	PRES.SUR. VEL. (WP)
0.16407	0.13719	0.13763	0.0000	200.87	-32.76	203.53	0.646	0.76	-9.26	-0.2245	0.00	0.00
0.18234	0.13719	0.13740	0.1000	191.69	-9.55	191.92	0.608	0.54	-2.85	0.7632E-01	0.00	0.00
0.19917	0.13719	0.13728	0.2000	185.61	10.17	185.88	0.588	0.41	3.14	0.3256	0.00	0.00
0.21490	0.13719	0.13722	0.3000	180.55	27.04	182.56	0.577	0.37	8.52	0.5154	0.00	0.00
0.22976	0.13719	0.13720	0.4000	176.38	42.31	181.38	0.572	0.38	13.49	0.6643	0.00	0.00
0.24388	0.13719	0.13719	0.5000	172.87	56.22	181.78	0.572	0.42	18.02	0.7966	0.00	0.00
0.25739	0.13719	0.13721	0.6000	169.68	68.89	183.13	0.575	0.45	22.10	0.8967	0.00	0.00
0.27039	0.13719	0.13723	0.7000	166.83	80.89	185.41	0.581	0.44	25.87	0.9318	0.00	0.00
0.28293	0.13719	0.13725	0.8000	163.80	91.72	187.73	0.587	0.33	29.25	0.8486	0.00	0.00
0.29517	0.13719	0.13728	0.9000	159.17	100.49	188.24	0.587	0.08	32.27	0.5322	0.00	0.00
0.30733	0.13719	0.13729	1.0000	152.14	107.61	186.35	0.580	-0.32	35.27	-0.1172	0.00	0.00

```
*****************************************
***  INPUT DATA FOR TSONIC PROGRAM  ***
*****************************************


STREAMLINE NUMBER  1  --  STREAM FUNCTION =  0.0000

   GAM              AR              TIP             RHOIP           WTFL                                    OMEGA           ORF
 1.400000        287.0530        288.1499        1.225336        0.2519378E-01                           -826.5413       0.0000000
  RETAI           RETAO           CHORDF          STGRF
 32.40718        -9.429133       0.1134319
  REDFAC          DENTCL
0.9999900       0.9999999E-03
  MBI  MBC          MM  NBBI  NBL NBSP
                              17   41
   RII              RO1             RETI1           RETC1           SPLNC1
                                                                    21.00000
   MSP1  ARRAY
0.0000000       0.1031086E-03   0.6292768E-02   0.1246834E-01   0.1863277E-01   0.2478737E-01   0.3093314E-01   0.3707111E-01
0.4320210E-01   0.4932708E-01   0.5544674E-01   0.6156182E-01   0.6767291E-01   0.7378078E-01   0.7988596E-01   0.8598900E-01
0.9209031E-01   0.9819025E-01   0.1042892       0.1103873       0.1134319
   THSP1  ARRAY
0.9043944E-04   0.1231142E-02   0.3059510E-01   0.5012232E-01   0.6670743E-01   0.8127600E-01   0.9347647E-01   0.1036527
0.1121255       0.1180431       0.1229439       0.1247488       0.1260445       0.1236891       0.1207637       0.1145946
0.1073331       0.9746981E-01   0.8500069E-01   0.7037573E-01   0.5726729E-01
   RI2              RO2             RETI2           RETC2           SPLNO2
                                                                    21.00000
   MSP2  ARRAY
0.0000000       0.1031086E-03   0.6292768E-02   0.1246834E-01   0.1863277E-01   0.2478737E-01   0.3093314E-01   0.3707111E-01
0.4320210E-01   0.4932708E-01   0.5544674E-01   0.6156182E-01   0.6767291E-01   0.7378078E-01   0.7988596E-01   0.8598900E-01
0.9209031E-01   0.9819025E-01   0.1042892       0.1103873       0.1134319
   THSP2  ARRAY
-0.9043944E-04  -0.6299517E-03   0.4231710E-02   0.1559785E-01   0.2588356E-01   0.3526309E-01   0.4351118E-01   0.5071820E-01
0.5703574E-01   0.6193965E-01   0.6626523E-01   0.6891894E-01   0.7125890E-01   0.7173222E-01   0.7186276E-01   0.7036930E-01
0.6825590E-01   0.6496710E-01   0.6046345E-01   0.5501781E-01   0.5693282E-01
   MP  ARRAY
-0.4740649E-01  -0.4251205E-01  -0.3766119E-01  -0.3284955E-01  -0.2807207E-01  -0.2332413E-01  -0.1860162E-01  -0.1390077E-01
-0.9218272E-02  -0.4551180E-02   0.1031086E-03   0.6292768E-02   0.1246834E-01   0.1863277E-01   0.2478737E-01   0.3093314E-01
 0.3707111E-01   0.4320210E-01   0.4932708E-01   0.5544674E-01   0.6156182E-01   0.6767297E-01   0.7378083E-01   0.7988602E-01
 0.8598906E-01   0.9209037E-01   0.9819031E-01   0.1042892       0.1103874       0.1164849       0.1225820       0.1271546
 0.1317272       0.1362996       0.1408719       0.1454442       0.1500164       0.1545886       0.1591607       0.1637329
 0.1683050
   RMSP  ARRAY
 0.1410747       0.1428218       0.1444429       0.1459424       0.1473285       0.1486090       0.1497918       0.1508849
 0.1518962       0.1528335       0.1537049       0.1547776       0.1557658       0.1566818       0.1575291       0.1583098
 0.1590264       0.1596810       0.1602762       0.1608143       0.1612975       0.1617286       0.1621107       0.1624475
 0.1627425       0.1629995       0.1632218       0.1634132       0.1635773       0.1637176       0.1638378       0.1639167
 0.1639879       0.1640529       0.1641130       0.1641685       0.1642207       0.1642686       0.1643127       0.1643531
 0.1643855
   RESP  ARRAY
 0.2554916E-02   0.2482329E-02   0.2426662E-02   0.2382337E-02   0.2346428E-02   0.2316972E-02   0.2293030E-02   0.2274062E-02
 0.2259779E-02   0.2250251E-02   0.2245704E-02   0.2222087E-02   0.2174486E-02   0.2171761E-02   0.2186344E-02   0.2175471E-02
 0.2155035E-02   0.2140990E-02   0.2120544E-02   0.2100337E-02   0.2078344E-02   0.2056339E-02   0.2033191E-02   0.2010689E-02
 0.1991085E-02   0.1981462E-02   0.1963335E-02   0.1940812E-02   0.1919951E-02   0.1901856E-02   0.1891792E-02   0.1886974E-02
 0.1883565E-02   0.1881148E-02   0.1879381E-02   0.1878124E-02   0.1877240E-02   0.1876682E-02   0.1876123E-02   0.1875114E-02
 0.1872504E-02
  RLEAT  AANDK  EPSOR  STREA  SLOPE  INTVL  SURVL
    1      C      0      2      2      2      3
   MLESP  ARRAY
 0.0000000       0.1031086E-03   0.6292768E-02   0.1246834E-01   0.1863277E-01
   RTLEP1  ARRAY
 0.1389928E-04   0.1852325E-03   0.4797347E-02   0.7807340E-02   0.1045184E-01
   RTLEP2  ARRAY
-0.1389928E-04  -0.5667294E-04   0.6545738E-03   0.2429610E-02   0.4055481E-02
   MTESP  ARRAY
 0.9209031E-01   0.9819025E-01   0.1042892       0.1103873       0.1134319
   RTTEP1  ARRAY
 0.8187946E-02   0.6589215E-02   0.4559327E-02   0.2172256E-02   0.2737237E-04
   RTTEP2  ARRAY
 0.1824918E-02   0.1284075E-02   0.5496261E-03  -0.3406031E-03  -0.2736322E-04
```

8

TABLE I. - Continued. SAMPLE OUTPUT

9

*** INCIDENCE AND DEVIATION ANGLES ***

****

****
* REDUCED MASSFLOW *
****
* ITERATION NO. 8 *
****

MESH LINE	INCIDENCE		DEVIATION	
	BLOCKED	UNBLOCKED	BLOCKED	UNBLOCKED
1	8.18	8.30	8.32	8.12
2	7.86	8.34	8.51	8.39
3	7.27	8.04	8.41	8.35
4	6.78	7.72	8.13	8.10
5	6.81	6.92	8.10	8.11
6	6.17	6.59	7.73	7.77
7	5.88	6.51	7.67	7.74
8	5.44	6.20	7.35	7.44
9	5.41	5.79	7.22	7.35
10	5.16	5.32	6.94	7.10
11	4.87	5.22	6.79	6.98
12	4.66	5.13	6.48	6.71
13	4.42	4.99	6.35	6.61
14	4.23	4.85	6.26	6.38
15	4.10	4.75	6.20	6.24
16	4.21	4.59	6.02	6.12
17	4.37	4.41	5.84	6.00
18	4.35	4.46	5.72	5.93
19	4.38	4.54	5.59	5.85
20	4.31	4.50	5.75	6.05
21	4.43	4.64	5.87	6.19

*** STREAM FUNCTION, INTERIOR VELOCITIES, VELOCITY COMPONENTS, ANGLES, AND SURFACE VELOCITIES ***
ALONG STREAMLINES

****
* FULL MASSFLOW *
****
TRANSONIC SOLUTION
BY VELOCITY GRADIENT APPROXIMATE METHOD
ALL VELOCITIES SMALLER THAN CHOKING MASSFLOW SOLUTION

11

** STREAMLINE NUMBER 1 -- STREAM FUNCTION = 0.0000 **

AXIAL COORD. (Z)	RADIAL COORD. (R)	MERID. COORD. (M)	MERID. VEL. (WM)	REL.TANG. VEL. (WTH)	REL. VEL. (W)	CRIT.VEL. RATIO (W/WCR)	MERID. ANGLE (ALPHA)	REL.FLOW ANGLE (BETA)	STREAM. CURV. (1./DIST)	SUCT.SUR. VEL. (WS)	PRES.SUR. VEL. (WP)
-0.45720E-01	0.14107	-0.47510E-01	179.69	110.32	210.86	0.672	21.59	31.55	-4.795	0.00	0.00
-0.41148E-01	0.14282	-0.42615E-01	182.05	111.84	213.66	0.681	20.22	31.56	-4.944	0.00	0.00
-0.36576E-01	0.14444	-0.37764E-01	184.60	113.25	216.57	0.690	18.83	31.53	-4.918	0.00	0.00
-0.32004E-01	0.14594	-0.32953E-01	186.80	114.56	219.13	0.698	17.50	31.52	-4.705	0.00	0.00
-0.27432E-01	0.14733	-0.28175E-01	188.29	115.76	221.03	0.703	16.24	31.58	-4.466	0.00	0.00
-0.22860E-01	0.14861	-0.23427E-01	189.26	116.87	222.44	0.708	15.06	31.70	-4.204	0.00	0.00
-0.18288E-01	0.14979	-0.18705E-01	189.83	117.89	223.46	0.711	13.96	31.84	-3.921	0.00	0.00
-0.13716E-01	0.15088	-0.14004E-01	190.00	118.84	224.10	0.713	12.94	32.03	-3.622	0.00	0.00

*** STREAM FUNCTION, INTERIOR VELOCITIES, VELOCITY COMPONENTS, AND ANGLES ***
AT ALL MESH POINTS OF THE ORTHOGONAL MESH

****
* FULL MASSFLOW *
****
TRANSONIC SOLUTION
BY VELOCITY GRADIENT APPROXIMATE METHOD
ALL VELOCITIES SMALLER THAN CHOKING MASSFLOW SOLUTION

11

** HORIZONTAL ORTHOGONAL MESH LINE NO. 1 **

MESH-POINT COLM (I)	MESH-POINT ROW (J)	AXIAL COORD. (Z)	RADIAL COORD. (R)	STREAM FUNC. (U)	MERID. VEL. (WM)	REL.TANG. VEL. (WTH)	REL. VEL. (W)	CRIT.VEL. RATIO (W/WCR)	MERID. ANGLE (ALPHA)	REL.FLOW ANGLE (BETA)	MESH ANGLE (PHI)
1	1	-0.45720E-01	0.14107	0.0000	179.69	110.32	210.86	0.672	21.59	31.55	21.59
2	1	-0.41148E-01	0.14282	0.0000	182.05	111.84	213.66	0.681	20.22	31.56	20.22
3	1	-0.36576E-01	0.14444	0.0000	184.60	113.25	216.57	0.690	18.83	31.53	18.83
4	1	-0.32004E-01	0.14594	0.0000	186.80	114.56	219.13	0.698	17.50	31.52	17.50
5	1	-0.27432E-01	0.14733	0.0000	188.29	115.76	221.03	0.703	16.24	31.58	16.24
6	1	-0.22860E-01	0.14861	0.0000	189.26	116.87	222.44	0.708	15.06	31.70	15.06
7	1	-0.18288E-01	0.14979	0.0000	189.83	117.89	223.46	0.711	13.96	31.84	13.96
8	1	-0.13716E-01	0.15088	0.0000	190.00	118.84	224.11	0.713	12.94	32.03	12.94

TABLE I. - Concluded. SAMPLE OUTPUT

11

```
***  STREAM FUNCTION, INTERIOR VELOCITIES, VELOCITY COMPONENTS, ANGLES, AND SURFACE VELOCITIES  ***
         ALONG LINES FROM HUB TO SHROUD AT VARIOUS STATIONS THROUGH THE BLADE ROW
         ****************************************************************************

                              *************************
                              *    FULL    MASSFLOW   *
                         *********************************************
                         *            TRANSONIC   SOLUTION            *
                         *  BY VELOCITY GRADIENT APPROXIMATE METHOD   *
                    ************************************************************
                    *  ALL VELOCITIES SMALLER THAN CHOKING MASSFLOW SOLUTION   *
                    ************************************************************

                              ** HUB-SHROUD STATION NO.   1 **
```

RADIAL COORD. (R)	AXIAL COORD. (Z)	MERID. COORD. (M)	STREAM FUNC. (U)	MERID. VEL. (WM)	REL.TANG. VEL. (WTH)	REL. VEL. (W)	CRIT.VEL. RATIO (W/WCR)	MERID. ANGLE (ALPHA)	REL.FLOW ANGLE (BETA)	STREAM. CURV. (1./DIST)	SUCT.SUR. VEL. (WS)	PRES.SUR. VEL. (WP)
0.15054	-0.15210E-01	-0.15540E-01	0.0000	189.93	118.53	223.88	0.712	13.28	31.97	-3.718	0.00	0.00
0.17275	-0.15210E-01	-0.15433E-01	0.1000	179.40	127.59	220.15	0.699	10.37	35.42	-1.825	0.00	0.00
0.19282	-0.15210E-01	-0.15318E-01	0.2000	174.46	137.95	222.41	0.705	7.76	38.33	-1.190	0.00	0.00
0.21120	-0.15210E-01	-0.15260E-01	0.3000	171.18	148.28	226.47	0.716	5.46	40.90	-0.8263	0.00	0.00
0.22826	-0.15210E-01	-0.15224E-01	0.4000	168.72	158.34	231.38	0.730	3.39	43.18	-0.5372	0.00	0.00
0.24423	-0.15210E-01	-0.15211E-01	0.5000	166.80	168.09	236.81	0.745	1.54	45.22	-0.2958	0.00	0.00
0.25935	-0.15210E-01	-0.15211E-01	0.6000	165.35	177.59	242.65	0.762	-0.11	47.04	-0.3744E-01	0.00	0.00
0.27373	-0.15210E-01	-0.15218E-01	0.7000	164.42	186.83	248.87	0.779	-1.62	48.65	0.2550	0.00	0.00
0.28745	-0.15210E-01	-0.15231E-01	0.8000	164.01	195.80	255.41	0.797	-2.99	50.05	0.5217	0.00	0.00
0.30059	-0.15210E-01	-0.15247E-01	0.9000	164.11	204.55	262.24	0.817	-4.21	51.26	0.8216	0.00	0.00
0.31319	-0.15210E-01	-0.15262E-01	1.0000	164.74	213.05	269.32	0.836	-5.29	52.29	1.163	0.00	0.00

11

```
                    ****************************************
                    ***  INPUT DATA FOR TSONIC PROGRAM   ***
                    ****************************************

STREAMLINE NUMBER  1  --  STREAM FUNCTION =  0.0000

  GAM           AR            TIP           RHOIP         WTEL                        OMEGA        ORF
1.400000      287.0530      288.1499      1.225336      0.2519403E-01              -826.5493     0.0000000
  BETAI         BETAO         CHORDF        STGRF
32.41133      -0.5F7560     0.1134319
  REDFAC        DENTOL
1.000000      0.9999999E-03
  NBI   NBO       NM   NBBI  NBL  NRSP
                             17   41
  RI1           RO1           BETI1         BETO1         SPLNO1
                                                          21.00000
```

```
    MSP1  ARRAY
 0.0000000        0.1031086E-03   0.6292768E-02   0.1246834E-01   0.1863277E-01   0.2478737E-01   0.3093314E-01   0.3707111E-01
 0.4320210E-01    0.4932708E-01   0.5544674E-01   0.6156182E-01   0.6767291E-01   0.7378078E-01   0.7988596E-01   0.8598900E-01
 0.9209031E-01    0.9819025E-01   0.1042892       0.1103873       0.1134319
    THSP1  ARRAY
 0.9043944E-04    0.1231142E-02   0.3099510E-01   0.5012232E-01   0.6670743E-01   0.8127600E-01   0.9347647E-01   0.1036527
 0.1121255        0.1180431       0.1229439       0.1247488       0.1260445       0.1236891       0.1207637       0.1145946
 0.1073331        0.9746981E-01   0.8500069E-01   0.7037973E-01   0.5726729E-01
    PI2             RO2             PETI2           BETO2           SPLNO2
                                                                    21.00000
    MSP2  ARRAY
 0.0000000        0.1031086E-03   0.6292768E-02   0.1246834E-01   0.1863277E-01   0.2478737E-01   0.3093314E-01   0.3707111E-01
 0.4320210E-01    0.4932708E-01   0.5544674E-01   0.6156182E-01   0.6767291E-01   0.7378078E-01   0.7988596E-01   0.8598900E-01
 0.9209031E-01    0.9819025E-01   0.1042892       0.1103873       0.1134319
    THSP2  ARRAY
-0.9043944E-04   -0.6289517E-03   0.4231710E-02   0.1559785E-01   0.2588356E-01   0.3526309E-01   0.4351118E-01   0.5071820E-01
 0.5703574E-01    0.6193965E-01   0.6626523E-01   0.6891894E-01   0.7125890E-01   0.7173222E-01   0.7186276E-01   0.7036930E-01
 0.6829590E-01    0.6496710E-01   0.6046345E-01   0.5501781E-01   0.5693282E-01
    MP  ARRAY
-0.4740664E-01   -0.4251205E-01  -0.3766119E-01  -0.3284955E-01  -0.2807207E-01  -0.2332413E-01  -0.1860162E-01  -0.1390077E-01
-0.9218272E-02   -0.4551180E-02   0.1031086E-03   0.6292768E-02   0.1246834E-01   0.1863277E-01   0.2478737E-01   0.3093314E-01
 0.3707111E-01    0.4320210E-01   0.4932708E-01   0.5544674E-01   0.6156182E-01   0.6767297E-01   0.7378083E-01   0.7988602E-01
 0.8598906E-01    0.9209037E-01   0.9819031E-01   0.1042892       0.1103874       0.1164849       0.1225820       0.1271546
 0.1317272        0.1362996       0.1408719       0.1454442       0.1500164       0.1545886       0.1591607       0.1637329
 0.1683050
    PMSP  ARRAY
 0.1410747        0.1428218       0.1444429       0.1459424       0.1473285       0.1486050       0.1497918       0.1508849
 0.1518962        0.1528335       0.1537049       0.1547776       0.1557658       0.1566818       0.1575291       0.1583098
 0.1590264        0.1596810       0.1602762       0.1608143       0.1612975       0.1617286       0.1621107       0.1624475
 0.1627425        0.1629995       0.1632218       0.1634132       0.1635773       0.1637176       0.1638378       0.1639167
 0.1639879        0.1640529       0.1641130       0.1641689       0.1642207       0.1642686       0.1643127       0.1643531
 0.1643899
    PESP  ARRAY
 0.2524648E-02    0.2478558E-02   0.2429177E-02   0.2384871E-02   0.2350195E-02   0.2322448E-02   0.2300092E-02   0.2282529E-02
 0.2265550E-02    0.2266673E-02   0.2240816E-02   0.2283556E-02   0.2245503E-02   0.2220555E-02   0.2242507E-02   0.2260656E-02
 0.2245087E-02    0.2227336E-02   0.2197561E-02   0.2169558E-02   0.2142181E-02   0.2127161E-02   0.2103359E-02   0.2083102E-02
 0.2060365E-02    0.2049593E-02   0.2034399E-02   0.1999211E-02   0.2018903E-02   0.1966171E-02   0.1974716E-02   0.1966910E-02
 0.1965276E-02    0.1962765E-02   0.1961148E-02   0.1959537E-02   0.1958768E-02   0.1957742E-02   0.1959005E-02   0.1952459E-02
 0.1936068E-02
  PLOT  AANOK  EPSOR  STREN  SLORD  INTVL  SURVL
    1      C      0      2      2      2      3
    MLESP  ARRAY
 0.0000000        0.1031086E-03   0.6292768E-02   0.1246834E-01   0.1863277E-01
    PTLEP1  ARRAY
 0.1385928E-04    0.1852325E-03   0.4797347E-02   0.7807340E-02   0.1045184E-01
    PTLEP2  ARRAY
-0.1385928E-04   -0.9667294E-04   0.6549738E-03   0.2429610E-02   0.4055481E-02
    MTESP  ARRAY
 0.9209031E-01    0.9819025E-01   0.1042892       0.1103873       0.1134319
    PTTEP1  ARRAY
 0.8187546E-02    0.6589215E-02   0.4559327E-02   0.2172256E-02   0.2737237E-04
    PTTEP2  ARRAY
 0.1824918E-02    0.1284075E-02   0.5496261E-03  -0.3406031E-03  -0.2736222E-04
```

11

variables to be used in each subsequent iteration of the reduced-mass-flow solution. These maximum, minimum, and change values indicate to the user how $\partial(rV_\theta)/\partial r$ and F_r are converging and give clues as to how to change DNEW and FNEW if convergence cannot be obtained.

(5) This output corresponds to IMESH for one of the iterations of the reduced-mass-flow solution. The output is given along each horizontal mesh line at each mesh point. Typically, there are from 10 to 30 of these horizontal mesh lines, with 30 to 50 points in each. The output given at each mesh point includes the following: z- and r-coordinates of the point; stream function u; meridional velocity W_m; relative tangential velocity W_θ; relative velocity W; critical velocity ratio W/W_{cr}; meridional flow angle α; relative flow angle β; and mesh angle φ.

(6) This output corresponds to ISLINE for one of the iterations of the reduced-mass-flow solution. This output is given along each streamline, corresponding to a given stream-function value. The points along the streamline correspond to where it is intersected by the vertical mesh lines. The origin for the m-coordinate is chosen so that $m = 0$ when $z = 0$. The output given at each streamline point includes the following: z-, r-, and m-coordinates of the point; meridional velocity W_m; relative tangential velocity W_θ; relative velocity W; critical velocity ratio W/W_{cr}; meridional flow angle α; relative flow angle β; streamline curvature $1/r_c$; and within the blade-to-blade passage, the estimated suction-surface and pressure-surface velocities.

(7) This output corresponds to ISTATL for one of the iterations of the reduced-mass-flow solution. Instead of output being given along horizontal mesh lines (IMESH) or streamlines (ISLINE), it is now given in the other direction, along lines from hub to shroud. This output is given along each of the station lines specified by the input ZHST, ZTST arrays. Output is given at each point where these station lines are crossed by the streamlines (the values in the FLFR array). The output given at each point is identical to the output given for ISLINE, with the addition of the stream function u.

(8) This output corresponds to ITSON. This is a listing of the information required to prepare input for the TSONIC blade-to-blade analysis program of reference 5. This information is printed in such a way that it corresponds to the input form for TSONIC, which is shown in figure 12. (The definitions of all the input variables for TSONIC are given in the TSONIC report, ref. 5.) The TSONIC program was run for both the hub and tip blade sections of the compressor blade used in the numerical example of this report. The input numbers shown in figure 12 are those computed for use with the TSONIC run at the hub.

Much of the information printed by MERIDL has to be corrected slightly before it can be used as input for TSONIC. However, the final three arrays - MR, RMSP, and BESP - can be used as they are printed, unless the user wishes to reduce the number of points in them. The user should recall that the MERIDL program takes into account

1 5	6 10	11 15	16 20	21 25	26 30	31 35	36 40	41 50	51 60	61 70	71 80
TITLE											
STREAMLINE NUMBER 1 -- STREAM FUNCTION = 0.0000											
GAM		AR		TIP		RHOIP		WTFL		OMEGA	ORF
1.4		287.053		288.15		1.22534		0.02519		-826.55	0.
BETAI		BETAO		CHORDF		STGRF					
32.41		-9.36		.113432		.05548					
REDFAC		DENTOL									
1.0		.001									
MBI	MBO			MM	NBBI	NBL	NRSP				
10	50			60	20	17	41				
RI1		RO1		BETI1		BETO1		SPLNO1			
.001326		.000975		30.5		-24.5		10.			
MSP1 ARRAY											
0.		.012468		.024787		.037071		.049327	.061562	.073781	.085989
.098190											
THSP1 ARRAY											
0.		.046740		.077890		.10027		.11466	.12137	.12031	.11121
.09409											
RI2		RO2		BETI2		BETO2		SPLNO2			
.001326		.00975		17.5		-10.0		10.			
MSP2 ARRAY											
0.		.012468		.024787		.037071		.049327	.061562	.073781	.085989
.098190											
THSP2 ARRAY											
0.		.01222		.03188		.04734		.05856	.06554	.06835	.06699
.06158											
MR ARRAY											
RMSP ARRAY											
BESP ARRAY											
BLDAT	AANDK	ERSOR	STRFN	SLCRD	INTVL	SURVL					
2	0	0	2	2	2	3					

Figure 12. - TSONIC input form. Data shown are for numerical example at the hub. Inputs used for MR, RMSP, and BESP are the same as the data printed in item 8 of table I, p. 33.

a loss in total pressure through the blade rows. TSONIC does not do this. Therefore, to ensure compatability between the programs, the BESP array calculated by MERIDL is reduced to reflect this loss in total pressure, both through the blade row and downstream, before it is printed as input for TSONIC.

The BESP array is calculated to correspond to the given mass flow, WTFL. Any value could be used for WTFL if BESP is chosen accordingly. The value calculated by MERIDL is 1 percent of the mass flow between two blades.

Figures 13 and 14 indicate how the blade geometry information has to be corrected by the user before it can serve as input for TSONIC. First of all, the THSP1 and THSP2 arrays will usually have to be corrected to the proper origin. As figure 13 indicates, the origin for the θ-coordinates is at the center of the leading-edge radius for TSONIC but at the mean camber line in MERIDL.

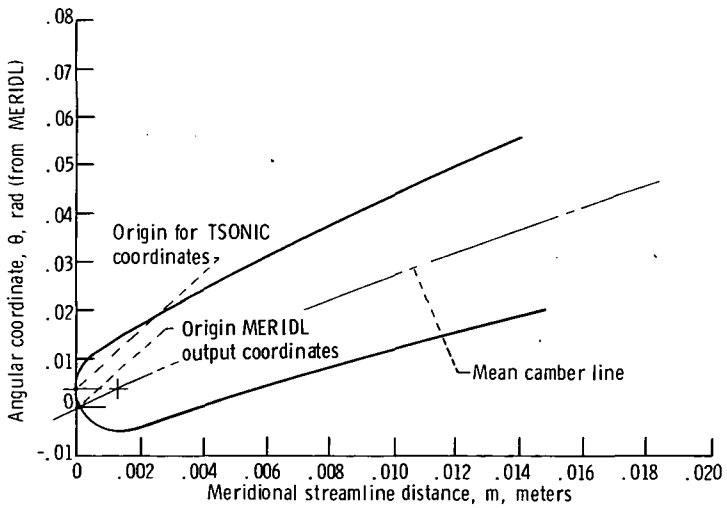

Figure 13. - Blade leading edge showing origin of coordinates for MERIDL output and for TSONIC input.

A layout (fig. 14) should be made to determine the remaining geometric input. To assist in making this layout, some additional coordinates are printed out. These additional coordinates are tangential distances ($r\theta$) from a reference plane near the leading or trailing edge, against the m-coordinate. When these are plotted at the same scale, the leading- or trailing-edge radius can be plotted and measured. This will give RI1, RI2, RO1, and RO2. Usually, RI1 is the same as RI2 and RO1 is the same as RO2.

The layout, figure 14, indicates how the leading-edge radius should be measured. In addition, the tangent angles, BETI1 and BETI2, can be measured from the layout. Finally, the layout, figure 14, should be used to obtain the correction for the THSP1 and THSP2 arrays. Figure 14 shows a tangential offset of 0.00052 meter. This is converted to radians by dividing by the local radius of 0.1537 to obtain a correction of

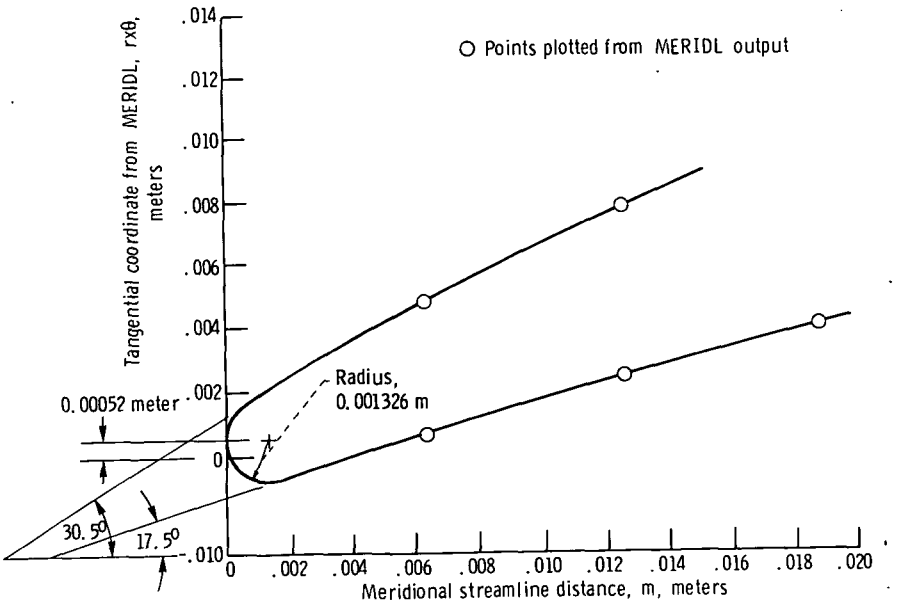

Figure 14. - Layout of blade leading edge at hub for numerical example.

0.00338 radians. Therefore, 0.00338 was subtracted from all THSP1 and THSP2 coordinates. At the trailing edge, the θ-coordinate at the center of the trailing-edge radius is calculated from a similar layout. For this case, the trailing-edge θ-coordinate is 0.05886. Then 0.00338 is subtracted to obtain 0.05548. This is the correct value to use for STGR. One further change should be made in the blade coordinates. The spacing between the MSP coordinates should be no closer than the original ZBL input for the blade shape. In this case, the ZBL coordinates were as much as 0.0011 apart along the hub. Therefore, only every other point in the MSP and THSP arrays should be used. In other cases, only every third or fourth point may be used. Also, be sure that the first spline point after the tangent point is no closer than the original ZBL input. Finally, be sure to change SPLNO1 and SPLNO2 when you do not use all the points.

After all the geometrical input is obtained, all that remains is to choose the meshpoint numbers MBI, MBO, MM, and NBBI, as described in reference 5. The user may also wish to change some of the other input variables (ORF, REDFAC, DENTOL, and BLDAT to SURVL, for instance) since MERIDL only prints suggested values.

The input used for the numerical example at the hub is shown in figure 12, except for the MR, RMSP, and BESP arrays. These three arrays were not changed from the output printed by MERIDL.

When running the TSONIC program, minor changes to the blade geometry and tangent angles are often required to obtain a smooth blade surface and a desirable velocity

distribution. Changes of this type normally would not require the MERIDL program to be rerun.

(9) This output consists of blocked and unblocked incidence and deviation angles at the blade leading and trailing edges where each of the horizontal mesh lines intersects the blade. The blocked incidence or deviation is based on the velocity diagram within the blade (subscript bf in fig. 15), whereas the unblocked is based on the free-stream (fs) velocity diagrams. This output is printed after each iteration in which output is given for either IMESH, ISLINE, or ISTATL. These angles are defined as shown in figure 15. For the blocked angles, the flow direction is corrected for blockage before the incidence and deviation are calculated.

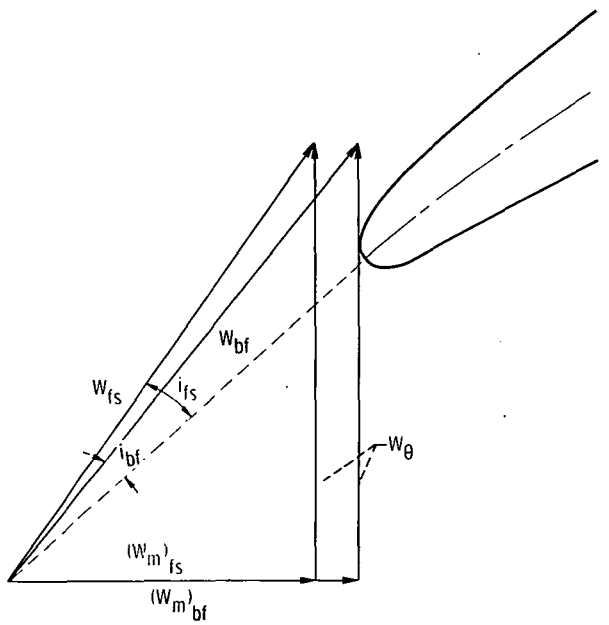

Figure 15. - Definition of incidence angles.

(10) This output indicates the maximum relative change in relative velocity W at any point on the orthogonal mesh during an iteration of the reduced-mass-flow solution. When this value becomes less than the input value of VELTOL, the reduced-mass-flow solution is considered converged.

(11) This output is analogous to outputs (5), (6), (7), and (8) for the variables IMESH, ISLINE, ISTATL, and ITSON but is given after the transonic velocity-gradient solution. Two solutions can be obtained by the velocity-gradient method, the larger or "supersonic" and the smaller or "subsonic." The input variable ISUPER controls which of these is obtained. The solution listed here is the smaller (i.e., the "subsonic" solution). If REDFAC = 1.0, no velocity-gradient solution will be obtained or printed.

Plotted Output

Since the printed output from a MERIDL run can be quite large, microfilm plots are made to enable the user to quickly check the quality of both his input and output data. The coding which generates these plots uses NASA Lewis in-house plot routines and would have to be recoded for operation on another facility. The principal sections of input data plotted are the upstream and downstream distributions of flow properties; the input blade sections; and the hub, shroud, and blade leading- and trailing-edge geometry. The amount of plotting of output data is controlled by the variable IPLOT. The plotted output data begin with the generated orthogonal mesh. Then for each outer iteration of the solution (indicated by IPLOT) and for the transonic solutions, streamlines are plotted, as well as mid-channel flow plane and blade surface velocities along each streamline from hub to shroud. The user should carefully check the plots of his input data to ensure that the program's spline fits of this data are smooth.

Selected examples of some of the microfilm plots generated by the numerical example are presented in figure 16. The description of these plots follows:

(1) Figures 16(a) to (e) present the input upstream and downstream flow conditions. These quantities $\left(T_i'; p_i'; \lambda \text{ or } \left(V_\theta\right)_i; p_o' \text{ or total pressure loss; } \left(rV_\theta\right)_o \text{ or } \left(V_\theta\right)_{\zeta}\right)$ are all plotted against either stream function or radius, whichever was used as input.

(2) Figures 16(f) and (g) indicate hub and shroud blade sections plotted from input data supplied by the user. All blade sections given as input are plotted.

(3) Figure 16(h) shows the hub and shroud channel geometry and the blade leading and trailing edges.

(4) Figure 16(i) shows the generated orthogonal mesh.

(5) Figure 16(j) shows the streamline pattern for the final iteration of the reduced-mass-flow solution.

(6) Figures 16(k) and (ℓ) show meridional velocities and blade surface velocities for the hub and shroud blade sections for the same iteration. A similar plot is made along each of the streamlines from hub to shroud.

Streamline and velocity plots similar to figures 16(j), (k), and (ℓ) are repeated after each iteration of the finite-difference stream-function solution and also after the velocity-gradient solution.

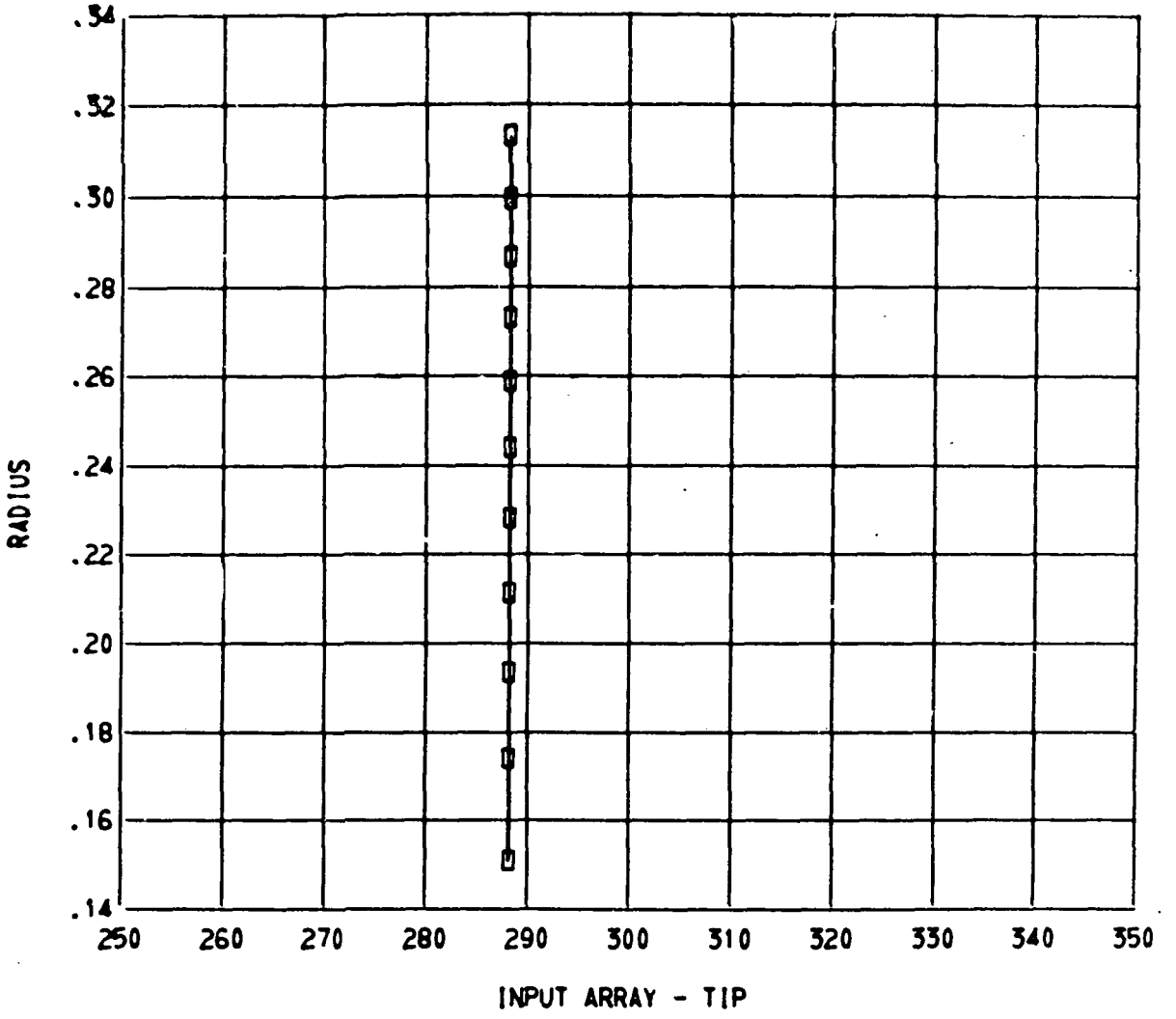

(a) Inlet absolute total temperature.

Figure 16. - Microfilm plots of input and output.

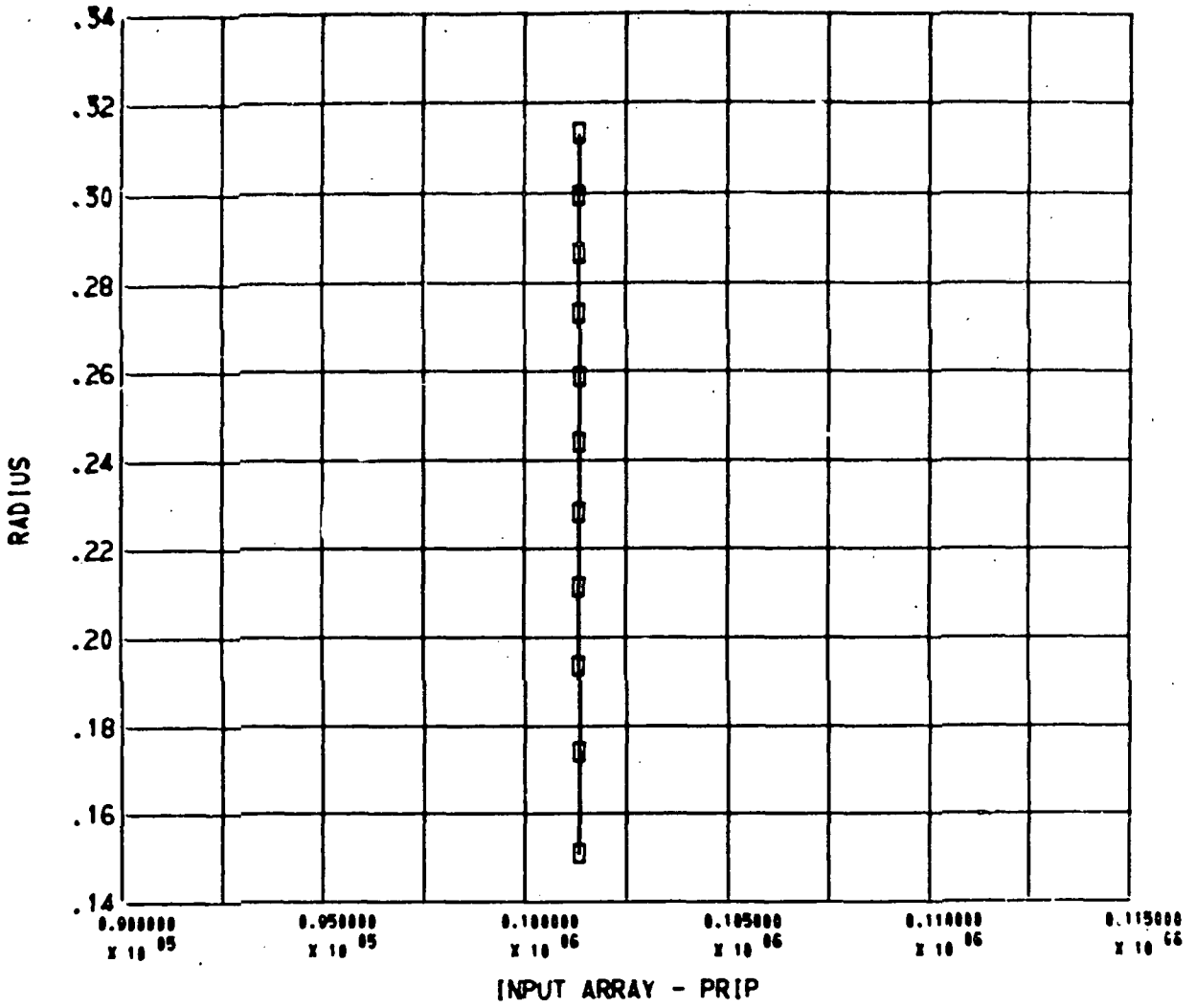

(b) Inlet absolute total pressure.

Figure 16. - Continued.

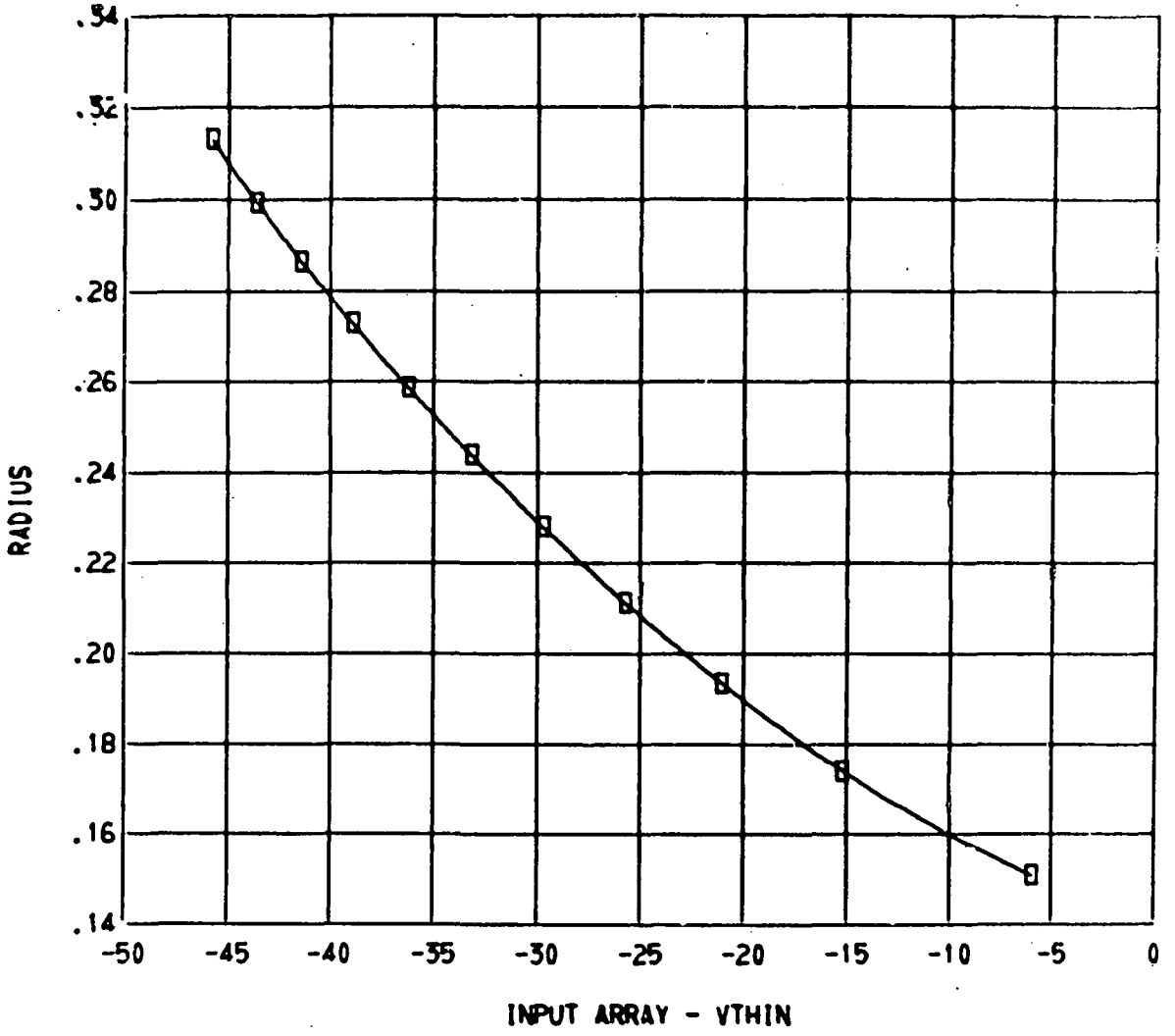

(c) Inlet absolute tangential velocity.

Figure 16. - Continued.

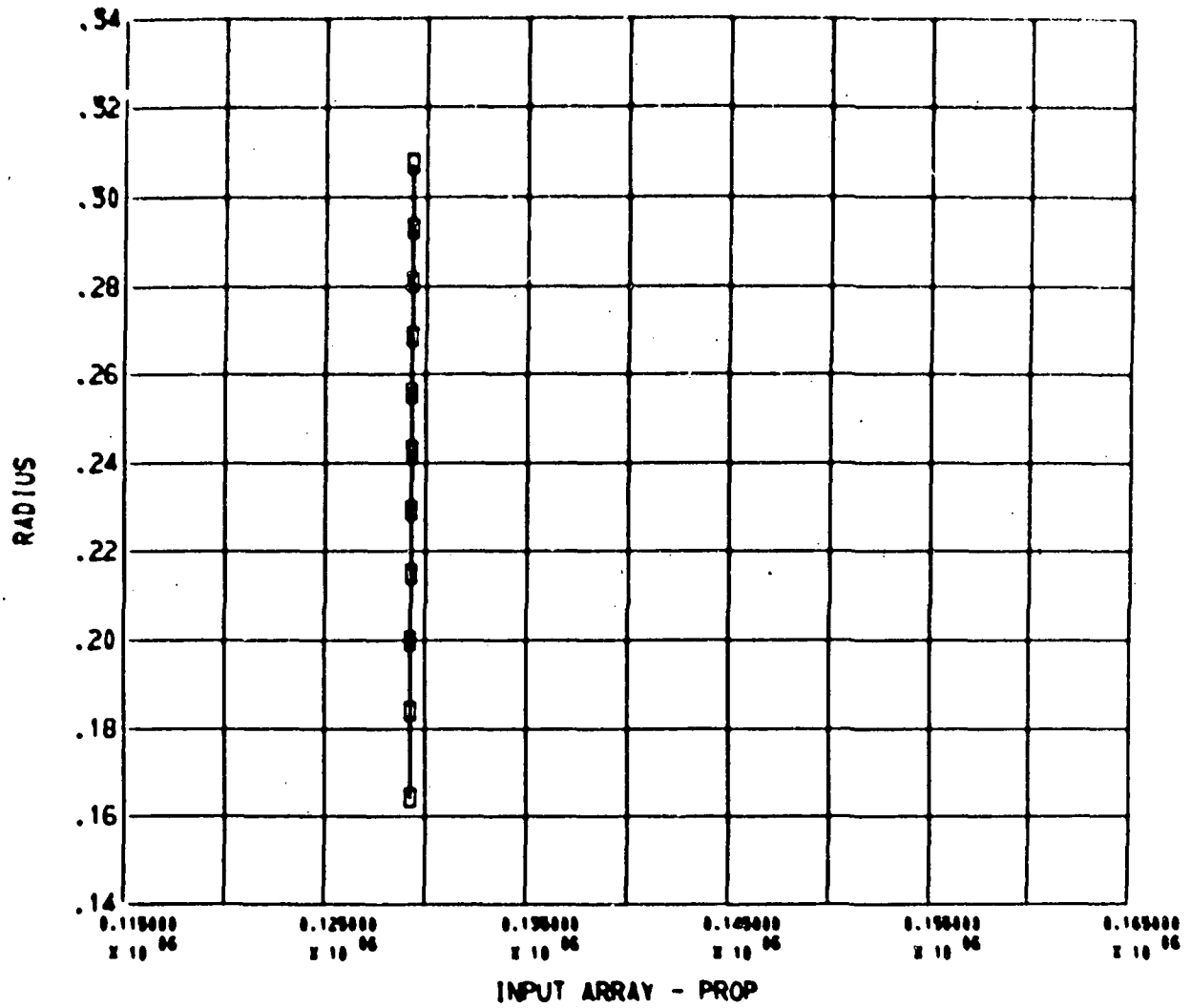

(d) Outlet absolute total pressure.

Figure 16. - Continued.

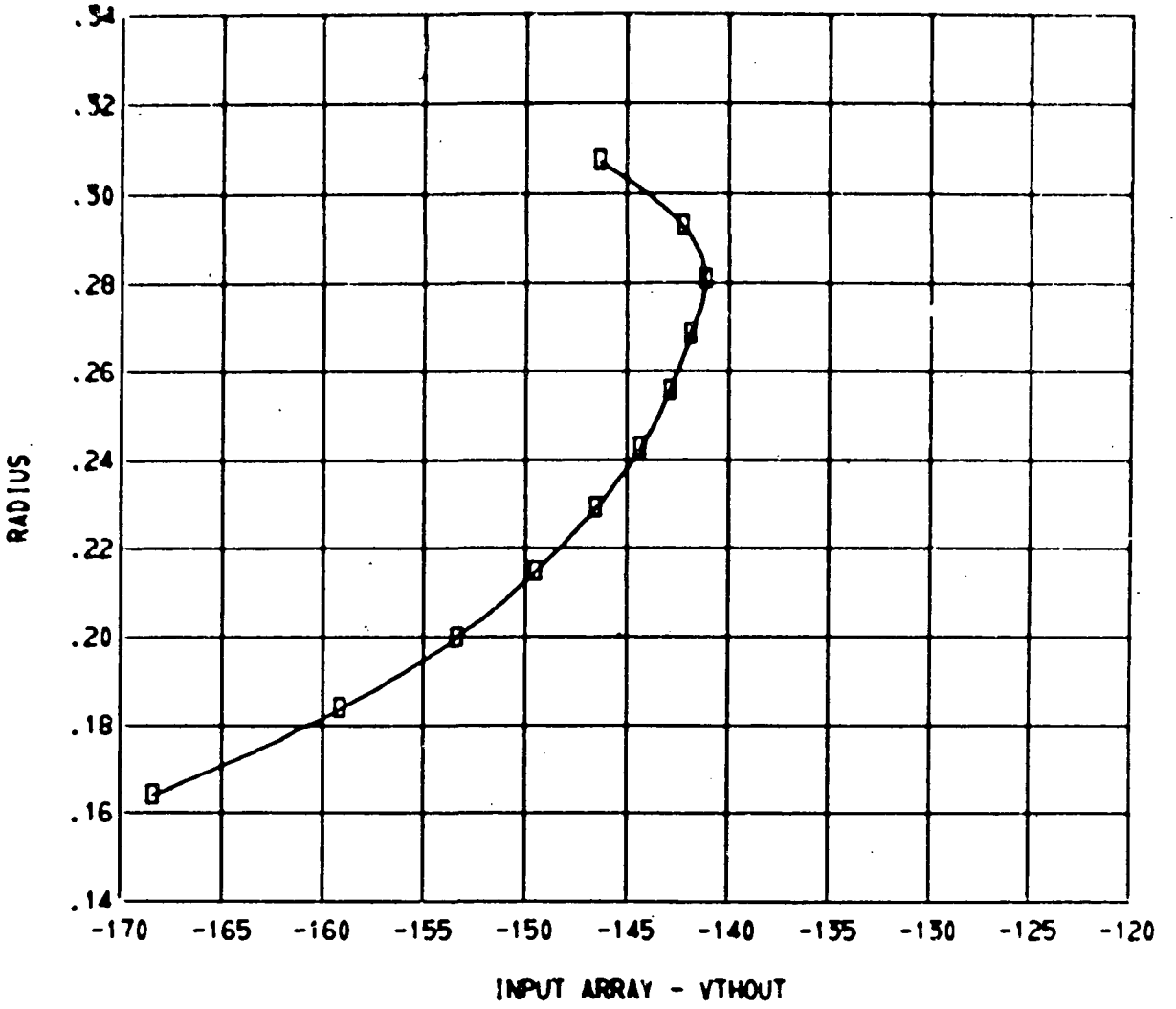

(e) Outlet absolute tangential velocity.

Figure 16. - Continued.

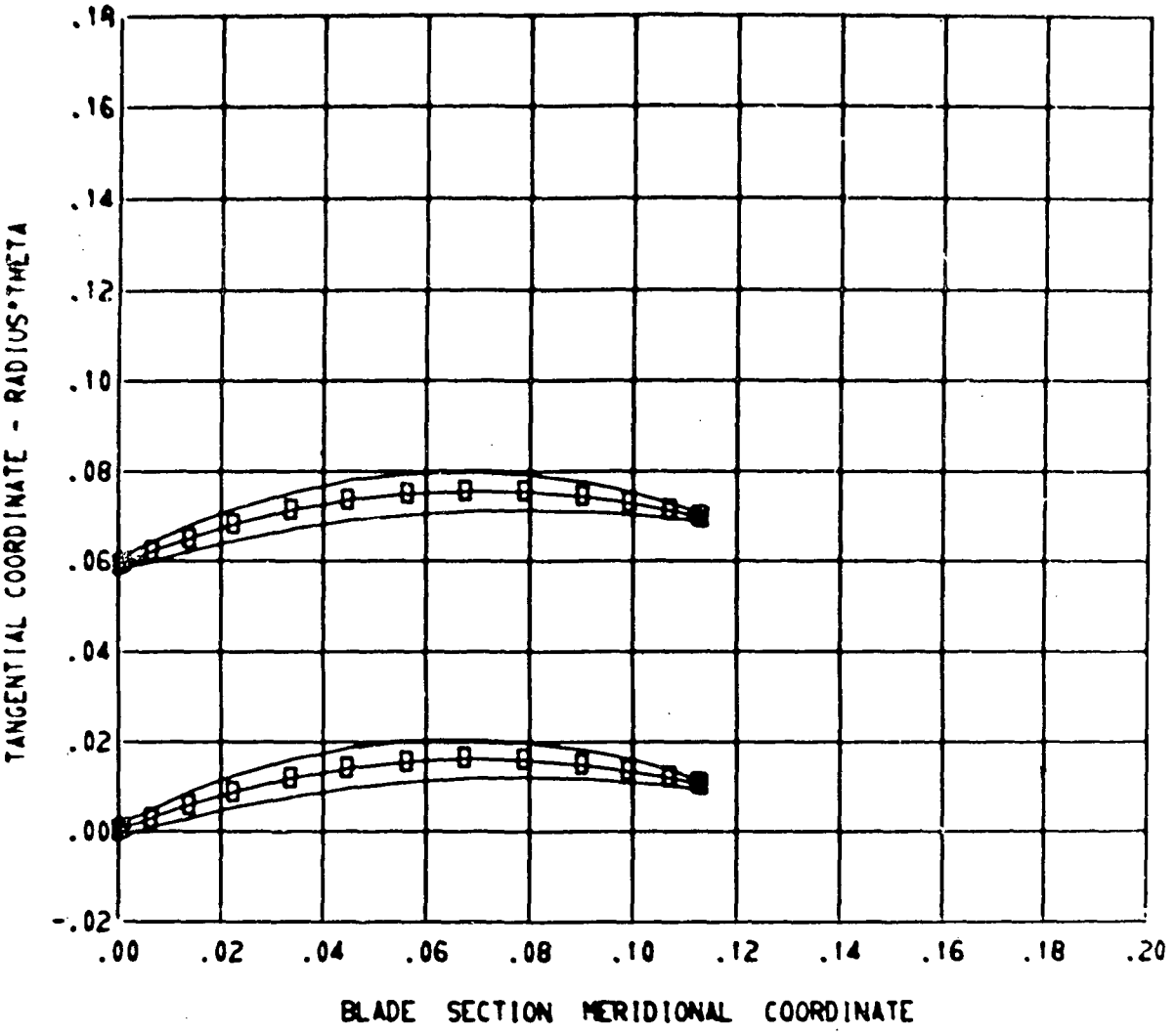

(f) Input blade sections from ZBL, RBL, THBL, and TNBL. Blade section 1.

Figure 16. - Continued.

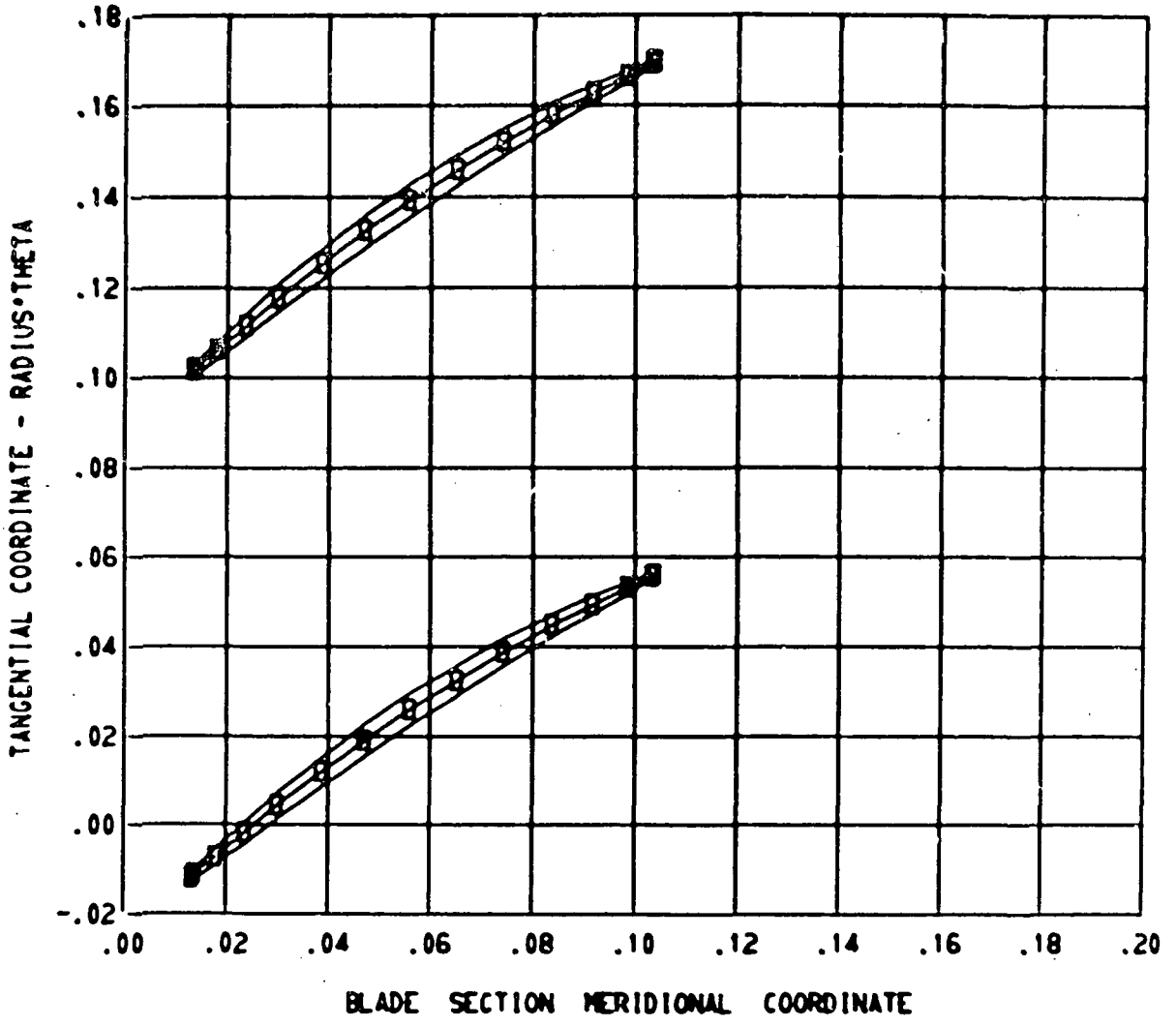

(g) Input blade sections from ZBL, RBL, THBL, and TNBL. Blade section 11.

Figure 16. - Continued.

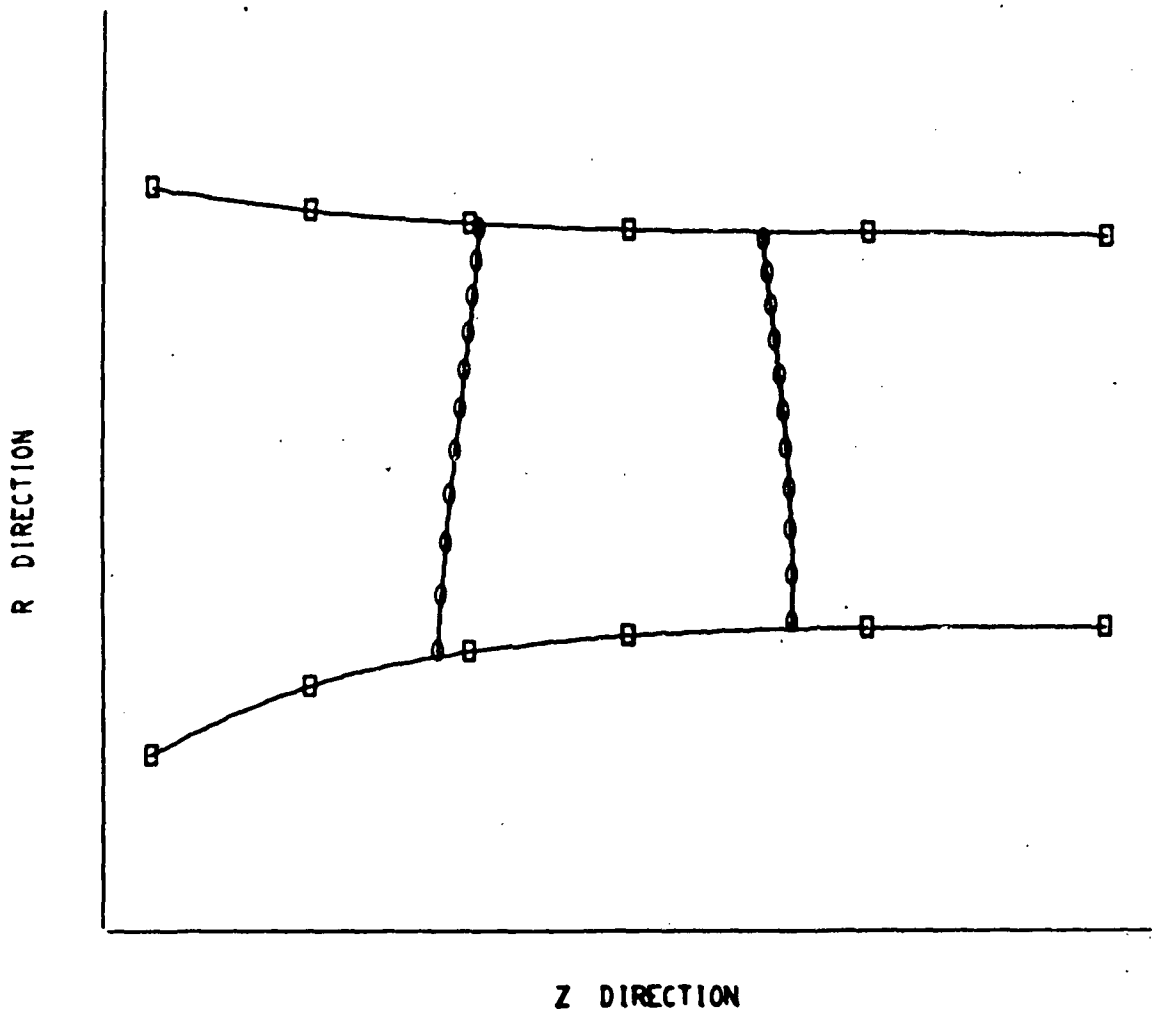

(h) Hub, shroud, and blade boundaries in meridional plane.

Figure 16. - Continued.

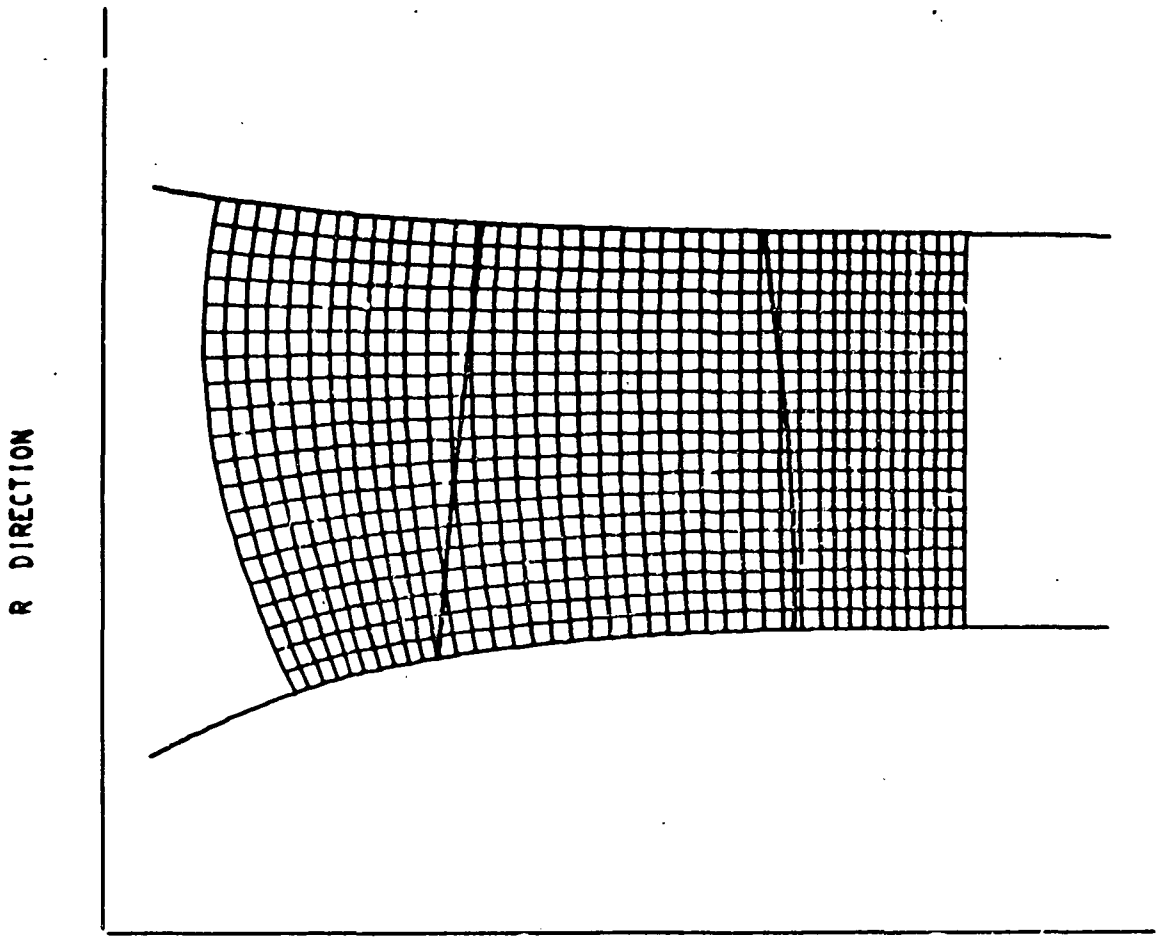

(i) Orthogonal mesh in meridional plane.

Figure 16. - Continued.

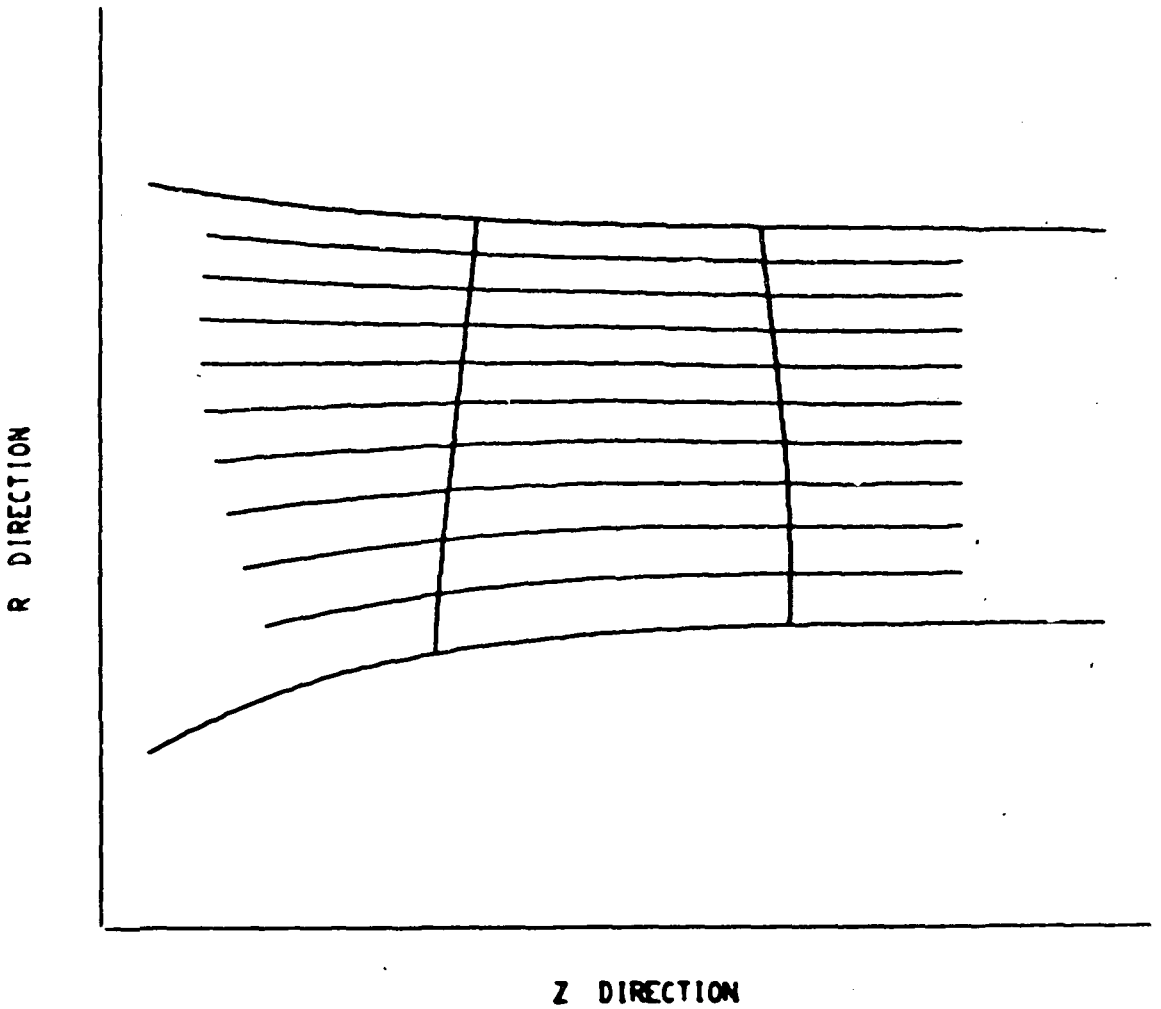

(j) Streamline plot in meridional plane.

Figure 16. - Continued.

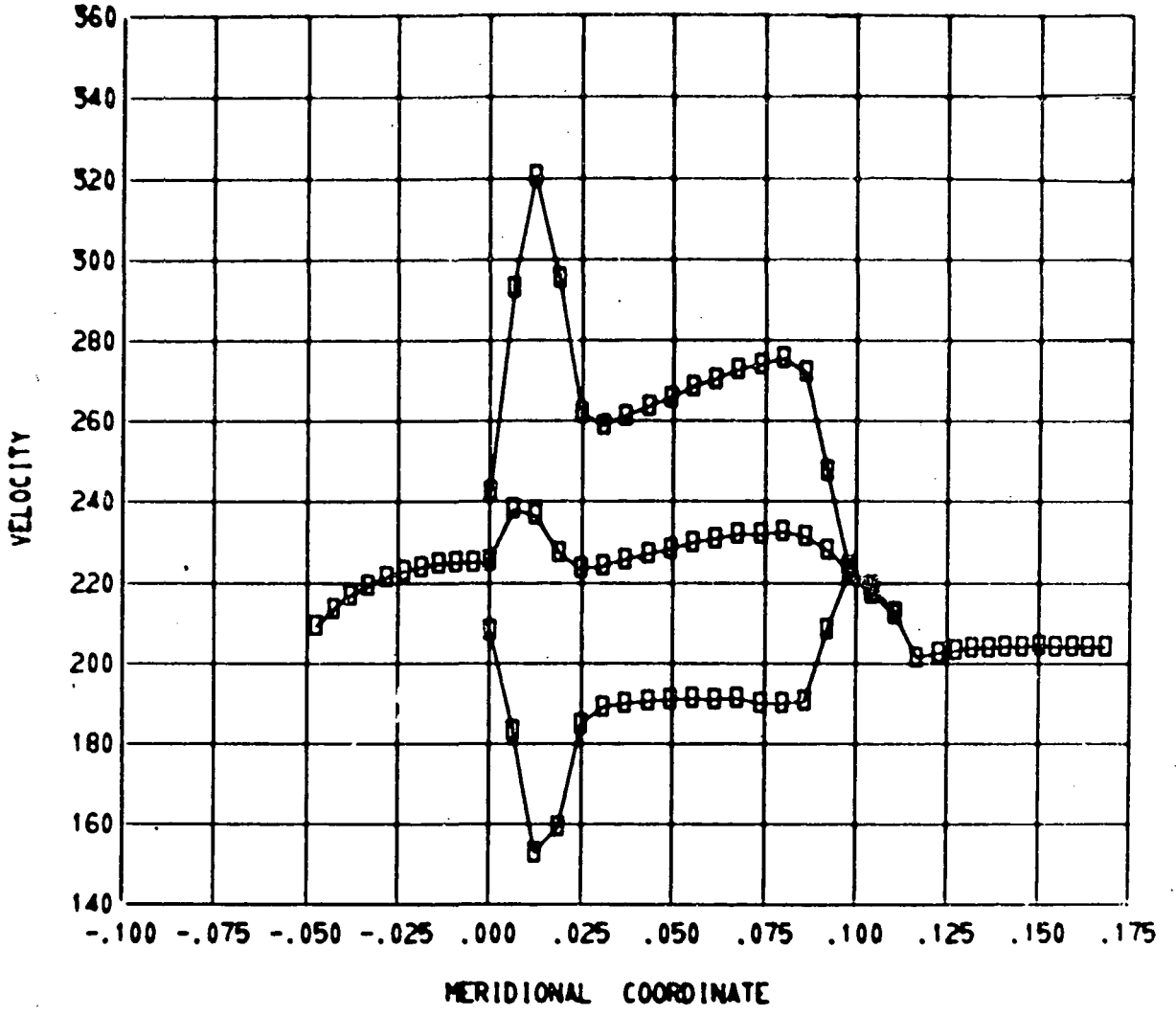

(k) Meridional and surface relative velocities. Streamline 1; normalized stream function, 0.

Figure 16. - Continued.

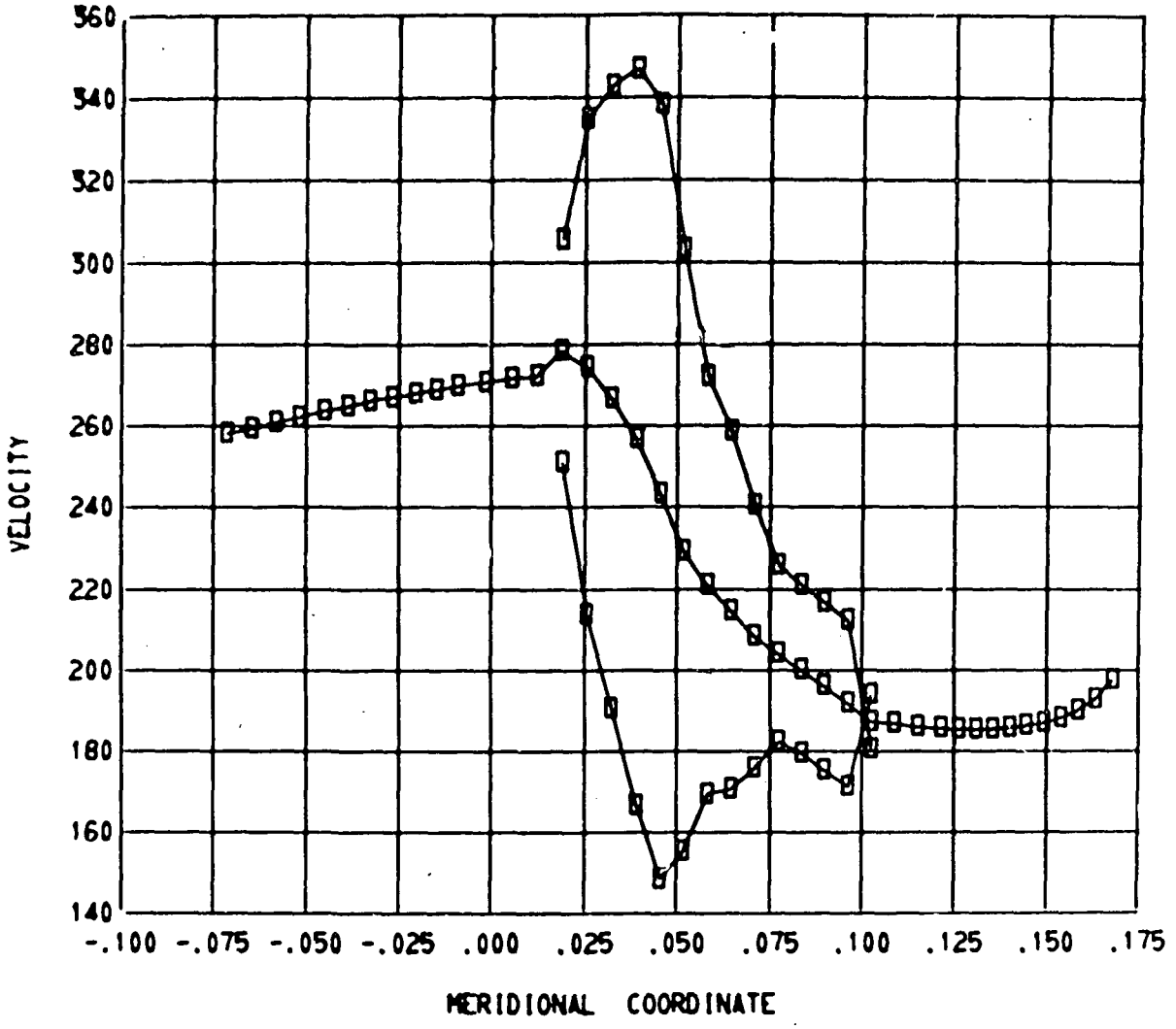

(ℓ) Meridional and surface relative velocities. Streamline 11; normalized stream function, 1.0000.

Figure 16. - Concluded.

Error Messages

A number of error messages have been incorporated into the program. These error messages are listed here. Suggestions for finding and correcting the cause of the error are given.

MM, MHT, NHUB, NTIP, NIN, NOUT, NBLPL, NPPP, NOSTAT, NSL, LSFR, LTPL, OR LAMVT IS TOO LARGE OR TOO SMALL

The input dictionary gives the maximum and minimum value for all these input variables.

LININT CANNOT FIND INTERPOLATED VALUE

This message should occur only with erroneous geometry input.

PASSAGE IS CHOKED AT THE INLET (OUTLET) WITH A MASS FLOW OF X.XXXX

This message is printed if the choking mass flow at the upstream (downstream) boundary of the mesh region is less than the input mass flow (MSFL). Usually, the mass flow must be reduced, or there is an error in the input upstream (downstream) flow conditions. Also check hub and shroud coordinates at boundary.

INLET (OUTLET) BOUNDARY CONDITIONS CANNOT BE OBTAINED

This message is printed if the upstream (downstream) boundary conditions cannot be satisfied after 100 iterations. This may be caused by a severe variation of some upstream (downstream) flow condition. Carefully check all input.

PROGRAM STOPPED IN NEWRHO DUE TO EXCESSIVE STREAM FUNCTION GRADIENT

This is usually caused by having supersonic flow in some region of the reduced-mass-flow solution. Try a smaller value for REDFAC.

UPSTREAM WHIRL OR TANGENTIAL VELOCITY IS TOO LARGE

This message is printed if the upstream whirl gives a tangential velocity so large as to result in a negative relative stagnation temperature. The upstream whirl or tangential velocity given as input should be corrected.

A VELOCITY GRADIENT SOLUTION CANNOT BE OBTAINED FOR VERTICAL ORTHOGONAL MESH LINE I = XX

ANY SUBSEQUENT OUTPUT FOR THAT MESH LINE MAY BE IN ERROR

If there is a problem in obtaining the approximate transonic solution for any particular mesh line, the attempt will be halted after 100 iterations, and this message will be printed. The problem may be caused by complex geometry or large gradients in upstream or downstream flow conditions. Sometimes a finer mesh will help.

MSFL EXCEEDS CHOKING MASS FLOW FOR VERTICAL ORTHOGONAL MESH LINE I = XX

CHOKING MASS FLOW = X.XXXX

This message is printed if the choking mass flow calculated by subroutine TVELCY is less than the input mass flow (MSFL). The following message will be printed after all vertical lines have been checked.

CHOKING MASS FLOW IS LESS THAN THE INPUT MASS FLOW
INPUT MASS FLOW = X.XXXX
MINIMUM CHOKING MASS FLOW = X.XXXX

A SOLUTION CAN BE OBTAINED ONLY IF INPUT MASS FLOW IS LESS THAN THIS MINIMUM CHOKING MASS FLOW

If the previous message was printed for any vertical mesh line, then this message will be printed at the end to give the minimum choking mass flow, which is the choking mass flow for the blade row.

INRSCT HAS FAILED TO CONVERGE IN 20 ITERATIONS
TOLERANCE = X.XXXX
DISTANCE BETWEEN LAST TWO INTERSECTION POINTS = X.XXXX

Subroutine INRSCT finds the intersection coordinates of mesh lines and streamlines with the blade leading or trailing edge by an iterative method. If the tolerance cannot be met after 20 iterations, the message is printed. If the distance between the last two intersection points is only slightly larger than the tolerance, a satisfactory solution will be obtained, with some loss of accuracy. If the distance is excessive, there is probably some error in the geometry input.

ROOT HAS FAILED TO LOCATE A ROOT IN THE INTERVAL (A, B) IN 20 ITERATIONS

ROOT ARGUMENTS -- A = X.XXXX B = X.XXXX
Y = X.XXXX TOLERY = X.XXXX

X	FX	DFX	INF
X.XXXX	X.XXXX	X.XXXX	X

Subroutine ROOT is called by subroutine MESHO to find the intersection between straight lines and spline curves in the process of generating the orthogonal mesh. If this message is printed, it is probably because the tolerance could not be met, although the problem may be caused by erroneous geometry input.

NUMERICAL EXAMPLE

An example of an axial-flow compressor rotor is used to illustrate the use of the program and to show the type of results which can be obtained. Flow is analyzed on the mid-channel flow surface of an axial-flow rotor designed with the computer program of reference 11. The design pressure ratio is 1.275, the inlet hub-tip radius ratio, 0.5; the aspect ratio, 1.5; the tip solidity, 1.0; and the tip relative Mach number at the inlet, 0.9. Although tip relative Mach number is near sonic, there are no locally supersonic regions on the meridional flow surface.

The input for this example is shown in table II. The number of mesh points used was 861: 41 in the axial direction, and 21 in the radial direction. The printed output presented earlier is from this example.

TABLE II. - INPUT FOR AXIAL-FLOW COMPRESSOR ROTOR

DATA 12 - AXIAL COMPRESSOR ROTOR - INLET WHIRL - S.I. UNITS

GENERAL INPUT DATA

GAM	AR	MSFL	OMEGA	REDFAC	VELTOL	FNEW	DNEW
1.4CCCCC	287.C530	42.82988	-826.5496	0.9999900	0.4999999E-02	0.5000000	0.5000000

MBI	MBU	MM	MHT	NBL	NHUB	NTIP	NIN	NOUT	NBLPL	NPPP	NOSTAT	NSL
11	31	41	20	17	6	6	11	11	11	15	4	11

LSFP	LTPL	LAMVT
1	0	1

HUB AND SHROUD INPUT DATA

ZCMIN	ZCMBI	ZOMBO	ZCMOUT			
-C.4572CCCE-C1	C.CCCC000	C.1219200	0.1676400			

ZHUB ARRAY

-C.9140998E-01	-0.4063000E-01	0.1018000E-01	0.6099000E-01	0.1371900	0.2133900	

RHUB ARRAY

C.1178660	C.143C12C	C.155448C	0.1612999	0.1640739	0.1645920	

ZTIP ARRAY

-C.914C998E-C1	-C.4C63CCCE-C1	C.1018000E-01	0.6099000E-01	0.1371900	0.2133900	

RTIP ARRAY

C.3246120	0.3159860	0.3111399	0.3083659	0.3073300	0.3065680	

UPSTREAM INPUT DATA

ZHIN	ZTIN
-C.1521000E-01	-0.1521000E-01

RADIN ARRAY

C.15C6630	0.1737660	C.1933350	0.2113180	0.2280509	0.2437789	0.2586840	0.2728570
0.2863600	0.2992830	C.3131210					

TIP ARRAY

288.1499	288.1499	288.1499	288.1499	288.1499	288.1499	288.1499	288.1499
288.1499	288.1499	288.1499					

PRIP ARRAY

101352.9	101352.9	101352.9	101352.9	101352.9	101352.9	101352.9	101352.9
101352.9	101352.9	101352.9					

VTHIN ARRAY

-5.943600	-15.13637	-21.02814	-25.74644	-29.73323	-33.18661	-36.23462	-38.95343
-41.40402	-43.60773	-45.79619					

DOWNSTREAM INPUT DATA

ZHOUT	ZTOUT
C.1371900	0.1371900

RADOUT ARRAY

C.1640739	0.1837029	C.1997350	0.2147930	0.2290270	0.2426510	0.2557270	0.2684070
0.2806900	0.2927300	C.3073300					

PROP ARRAY

129221.6	129221.6	129221.6	129221.6	129221.6	129221.6	129221.6	129221.6
129221.6	129221.6	129221.6					

VTHOUT ARRAY

-168.3715	-159.1483	-153.3876	-149.5227	-146.6027	-144.3655	-142.9390	-141.8753
-141.1803	-142.2349	-146.4107					

TABLE II. - Concluded. INPUT FOR AXIAL-FLOW COMPRESSOR ROTOR

PLACE MEAN CAMBER LINE AND THICKNESS INPUT DATA

ZBL ARRAY

-C.CCCCCCC	0.1128CC0E-C2	C.6307997E-02	0.1369200E-01	0.2229900E-01	0.3327000E-01	0.4442200E-01	0.5570000E-01
C.6704497E-01	0.7839996E-01	C.8970696E-01	0.9867895E-01	0.1064500	0.1119450	0.1128179	
C.13C5CCCE-C2	0.2325000E-02	0.7351998E-02	0.1453000E-01	0.2291500E-01	0.3363700E-01	0.4457900E-01	0.5569500E-01
C.6653399E-C1	C.7824898E-C1	C.8958799E-01	0.9864396E-01	0.1065339	0.1121410	0.1129839	
0.2751000E-02	0.3683000E-02	C.8550998E-02	0.1551200E-01	C.2365900E-01	0.3410100E-01	0.4479400E-01	0.5569700E-01
C.6676799E-C1	0.7796496E-01	0.8924496E-01	0.9829998E-01	0.1062260	0.1118820	0.1126910	
C.4230998E-02	0.5091999E-02	C.9808999E-02	0.1655900E-01	0.2446900E-01	0.3462600E-01	0.4505100E-01	0.5571000E-01
C.6656694E-01	0.7758898E-01	C.8873695E-01	0.9772295E-01	0.1056179	0.1112690	0.1120450	
C.5712997E-C2	0.6514996E-02	C.1109100E-01	0.1764000E-01	0.2531900E-01	0.3519000E-01	0.4533600E-01	0.5573100E-01
C.6634396E-01	0.7714599E-C1	C.8810699E-01	0.9697098E-01	0.1047810	0.1103849	0.1111290	
C.7169999E-02	0.7925998E-02	0.1237000E-01	0.1873000E-01	0.2618700E-01	0.3577600E-01	0.4564000E-01	0.5575800E-01
C.661C399E-01	0.7665598E-01	C.8738899E-01	0.9608799E-01	0.1037700	0.1092940	0.1100060	
C.8561999E-02	C.928C000E-02	C.13603C0E-01	0.1578600E-01	0.2703500E-01	0.3635400E-01	0.4594400E-01	0.5578500E-01
C.6565896E-01	0.7614595E-01	0.8662599E-01	0.9513497E-01	0.1026630	0.1080820	0.1087660	
C.9888999E-C2	C.1057700E-C1	0.1478900E-01	0.2080900E-01	0.2786100E-01	0.3692300E-01	0.4624500E-01	0.5581200E-01
C.6560898E-01	0.7562000E-01	C.8582896E-01	0.9412795E-01	0.1014790	0.1067760	0.1074340	
0.11142CCE-C1	0.1180600E-01	0.1591600E-01	0.2178600E-01	0.2865400E-01	0.3747100E-01	0.4653600E-01	0.5583400E-01
C.6535596E-01	C.7508695E-C1	C.8501697E-01	0.9309298E-01	0.1002520	0.1054140	0.1060480	
0.1224500E-01	0.1289000E-01	C.16909CCE-01	0.2264400E-01	0.2934800E-01	0.3794700E-01	0.4678000E-01	0.5583900E-01
C.6511199E-01	C.7458855E-C1	C.8426094E-01	0.9213197E-01	0.9910995E-01	0.1041450	0.1047590	
0.1320800E-01	0.1383900E-C1	C.17775C0E-01	0.2338700E-01	0.2994500E-01	0.3835000E-01	0.4697900E-01	0.5582500E-01
0.6487799E-01	0.7413095E-01	0.8357400E-01	0.9125996E-01	0.9807599E-01	0.1029960	0.1035950	

RBL ARRAY

0.1554829	0.155588C	C.1560EEC	0.1567520	0.1575500	0.1585660	0.1596000	0.1606449
0.1616960	0.1627490	0.1637959	0.1646280	0.1653480	0.1658570	0.1659380	
C.176386C	C.1764500	C.1767650	0.1772160	0.1777419	0.1784149	0.1791019	0.1798000
C.1805050	0.1812150	C.1819270	0.1824960	0.1829910	0.1833430	0.1833960	
C.195260C	0.1952960	0.1954850	0.1957549	0.1960710	0.1964750	0.1968900	0.1973130
C.197742C	0.198176C	0.198613C	0.1989640	0.1992710	0.1994900	0.1995220	
0.2126070	0.2126229	C.2127129	0.2128410	0.2129910	0.2131830	0.2133800	0.2135820
0.213788C	0.2139969	0.2142079	0.2143780	0.2145280	0.2146350	0.2146500	
C.2287440	0.2287450	C.228756C	0.2287720	0.2287900	0.2288139	0.2288380	0.2288620
0.2288880	0.2289140	C.2289400	0.2289610	0.2289790	0.2289930	0.2289940	
0.243852C	0.243883C	0.2438320	0.2437580	0.2436709	0.2435600	0.2434450	0.2433280
0.2432080	0.2430850	C.242960C	0.2428589	0.2427700	0.2427059	0.2426969	
C.2582130	0.2581960	0.2580950	0.2579510	0.2577810	0.2575630	0.2573389	0.2571090
C.256873C	C.2566320	0.2563870	0.2561880	0.2560120	0.2558849	0.2558690	
C.2718270	0.2718040	C.2716640	0.2714640	0.2712310	0.2709300	0.2706209	0.2703030
C.269578C	0.2696460	0.2693080	0.2690319	0.2687880	0.2686130	0.2685910	
C.284826C	C.284759C	0.2846299	0.2843879	0.2841060	0.2837440	0.2833700	0.2829880
0.2825969	0.2821960	C.2817880	0.2814560	0.2811610	0.2809490	0.2809229	
C.297289C	0.2972590	0.2970700	0.2968020	0.2964880	0.2960849	0.2956720	0.2952480
C.294814C	0.2943700	C.2939169	0.2935489	0.2932220	0.2929870	0.2929580	
0.3092760	0.3092450	C.309052C	0.3087760	0.3084550	0.3080420	0.3076180	0.3071840
C.3C674CC	0.3062860	C.3058230	0.3054460	0.3051110	0.3048699	0.3048410	

THBL ARRAY

-C.C000000	0.3439000E-02	C.1837CCCE-01	0.3721100E-01	0.5575800E-01	0.7440895E-01	0.8797896E-01	0.9644699E-01
C.9982C97E-C1	C.9814894E-01	0.9150296E-01	0.8266997E-01	0.7242697E-01	0.6369996E-01	0.6221300E-01	
-C.1322400E-01	-0.10C74C0E-C1	C.4765999E-02	0.2391000E-01	0.4341400E-01	0.6416696E-01	0.8082598E-01	0.9333897E-01
0.1016760	0.1058310	0.1058190	0.1028300	0.9806299E-01	0.9344000E-01	0.9266800E-01	
-C.23111C0E-C1	-C.2C171C0E-C1	-C.5377997E-02	0.1400900E-01	0.3423500E-01	0.5655800E-01	0.7552099E-01	0.9106100E-01
C.1031300	C.1116959	C.1167409	0.1182390	0.1177030	0.1162680	0.1160000	
-C.29779C0E-01	-0.2701800E-01	-0.1235300E-01	0.7089999E-02	0.2772400E-01	0.5107300E-01	0.7164097E-01	0.8936197E-01
C.1041840	C.1160610	C.1249610	0.1299220	0.1326810	0.1337470	0.1338410	
-0.3428200E-01	-0.3167000E-01	-C.17193C0E-01	0.2177C00E-02	C.23C0000E-01	0.4700500E-01	0.6869799E-01	0.8802098E-01
C.1049179	0.1193440	0.1312590	0.1389620	0.1443550	0.1474330	0.1477979	
-0.3726900E-01	-0.3478500E-01	-C.2053200E-01	-0.1322000E-02	0.1954200E-01	0.4394200E-01	0.6642097E-01	0.8692497E-01
C.1054070	0.1218200	C.136124C	0.1460260	0.1535520	0.1582710	0.1588430	

```
-C.3SC4CCCE-C1  -C.3666200E-01  -C.2265500E-01  -0.3667000E-02  0.1712600E-01  0.4171400E-01  0.6469995E-01  0.8603698E-01
 C.1056805      C.1235920       C.1397310       0.1513450       0.1605450      0.1665620      0.1672900
-C.40C0000E-01  -0.37711C0E-01  -0.2396300E-01  -0.5233999E-02  0.1541200E-01  0.4005000E-01  0.6335098E-01  0.8527696E-01
 C.1C575CC      0.1248540       0.1424370       0.1554150       0.1659639      0.1730320      0.1738819
-C.40327C0E-01  -C.381120CE-01  -0.24628C0E-01  -0.6182998E-02  0.1426300E-01  0.3884700E-01  0.6231700E-01  0.8464199E-01
 C.1C575CC      0.1257330       0.1444400       0.1584980       0.1701240      0.1780390      0.1789860
-C.39546CCE-C1  -C.377910CE-01  -C.2457100E-01  -0.6430998E-02  0.1376200E-01  0.3817500E-01  0.6164400E-01  0.8414096E-01
 C.1056409      0.1261190       C.145548C       0.1603220       0.1726760      0.1811700      0.1821840
-C.39C61C0E-01  -0.3695300E-01  -0.2399300E-01  -0.6168999E-02  0.1373400E-01  0.3789400E-01  0.6123500E-01  0.8373499E-01
 C.1C537C0      0.1261200       C.1459620       0.1611680       0.1739780      0.1828400      0.1839000
    TABL  ARRAY
 C.CCCCCCC      0.26240C0E-02   C.3829000E-02   0.5309999E-02   0.6706998E-02  0.8006997E-02  0.8808997E-02  0.9110000E-02
 C.8862000E-02  0.8017998E-02   C.6571997E-02   0.4974999E-02   0.3254000E-02  0.1838000E-02  0.0000000
 C.00C0000      0.2395000E-02   0.3490000E-02   0.4832000E-02   0.6093598E-02  0.7260997E-02  0.7971998E-02  0.8226000E-02
 C.7565998E-C2  C.722C998E-C2   C.5925998E-02   0.4503999E-02   0.2976000E-02  0.1723000E-02  0.0000000
 C.C0C0000      0.2228C00E-C2   C.3234000E-02   0.4463997E-02   0.5617999E-02  0.6681997E-02  0.7323999E-02  0.7544998E-02
 C.7317998E-C2  0.6614998E-02   0.5434997E-02   0.4145995E-02   0.2765000E-02  0.1632000E-02  0.0000000
 C.C0C0000      0.21C3000E-02   C.3036000E-02   0.4177999E-02   0.5245999E-02  0.6228000E-02  0.6817997E-02  0.7015999E-02
 0.6798998E-02  0.6146997E-02   C.5057998E-02   0.3870000E-02   0.2600000E-02  0.1560000E-02  0.0000000
 C.CCCCCCC      0.2009000E-02   0.2885000E-02   0.3554999E-02   0.4956000E-02  0.5873997E-02  0.6422997E-02  0.6603997E-02
 C.6356598E-C2  0.5783997E-C2   C.4764996E-02   C.3656000E-02   0.2472000E-02  0.1502000E-02  0.0000000
 C.00C0000      0.1939000E-02   C.2769000E-02   0.3784000E-02   0.4731998E-02  0.5600996E-02  0.6118998E-02  0.6285999E-02
 C.6C86598E-02  0.5504999E-02   0.4539996E-02   0.3492000E-02   0.2373000E-02  0.1457000E-02  0.0000000
 C.C0C0000      0.1887000E-02   C.2683000E-02   0.3655000E-02   0.4562996E-02  0.5393997E-02  0.5888999E-02  0.6046999E-02
 0.5854998E-02  0.5295999E-02   C.4371997E-02   0.3368000E-02   0.2298000E-02  0.1422000E-02  0.0000000
 C.CCCCCCC      0.185000CE-C2   0.2622000E-02   0.3563000E-02   0.4441999E-02  0.5245999E-02  0.5723000E-02  0.5874999E-02
 0.5686998E-02  0.5145997E-02   C.4249997E-02   0.3279000E-02   0.2243000E-02  0.1397000E-02  0.0000000
 C.0000000      0.1827000E-02   0.2581000E-02   0.3502000E-02   0.4361000E-02  0.5146999E-02  0.5612999E-02  0.5759999E-02
 C.5576CCCE-C2  C.5044997E-02   C.4169997E-02   0.3220000E-02   0.2207000E-02  0.1379000E-02  0.0000000
 C.0CC0000      0.1814000E-02   0.2559000E-02   0.3468000E-02   0.4315998E-02  0.5089998E-02  0.5549997E-02  0.5694997E-02
 C.5512998E-02  0.4988998E-02   0.4123997E-02   0.3186000E-02   0.2186000E-02  0.1369000E-02  0.0000000
 C.CCCCCCC      0.1811C00E-02   C.2552000E-02   0.3457000E-02   0.4300997E-02  0.5071998E-02  0.5530000E-02  0.5674999E-02
 0.5492996E-02  0.4972000E-02   C.4109997E-02   C.3176000E-02   0.2180000E-02  0.1366000E-02  0.0000000


 CUTPUT  STATION  LOCATION  DATA
    ZHST  ARRAY
-C.1521000E-01  0.CCCCC00      C.1128150       0.1371900
    ZTST  ARRAY
-C.1521CCCE-01  C.1320700E-C1  C.1035950       0.1371900


 CUTPUT  STREAMLINE  FLOW, FRACTION  DATA
    FLFR  ARRAY
 C.0000000      0.9999996E-01   0.2000000       0.3000000       0.4000000      0.5000000      0.6000000      0.7000000
 C.8CCCOCC      C.9CCC000       1.000000


 OUTPUT  PRINT  CONTROL  DATA
   IMESH  ISLINE ISTATL  IPLOT  ISUPER ITSON  IDEBUG
     10      4      4      1      1      8      8
```

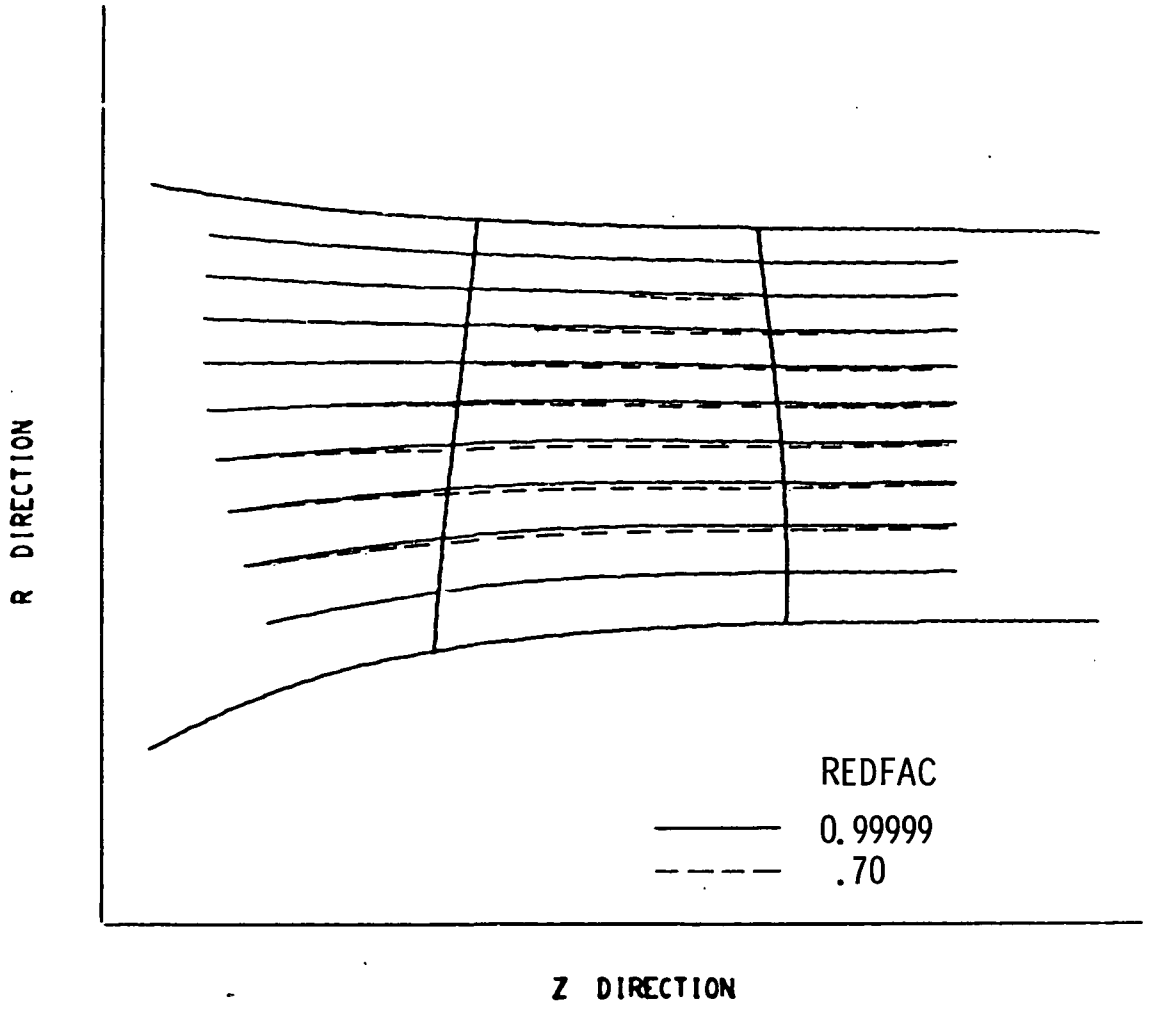

Figure 17. - Effect of change of reduction factor on streamline location.

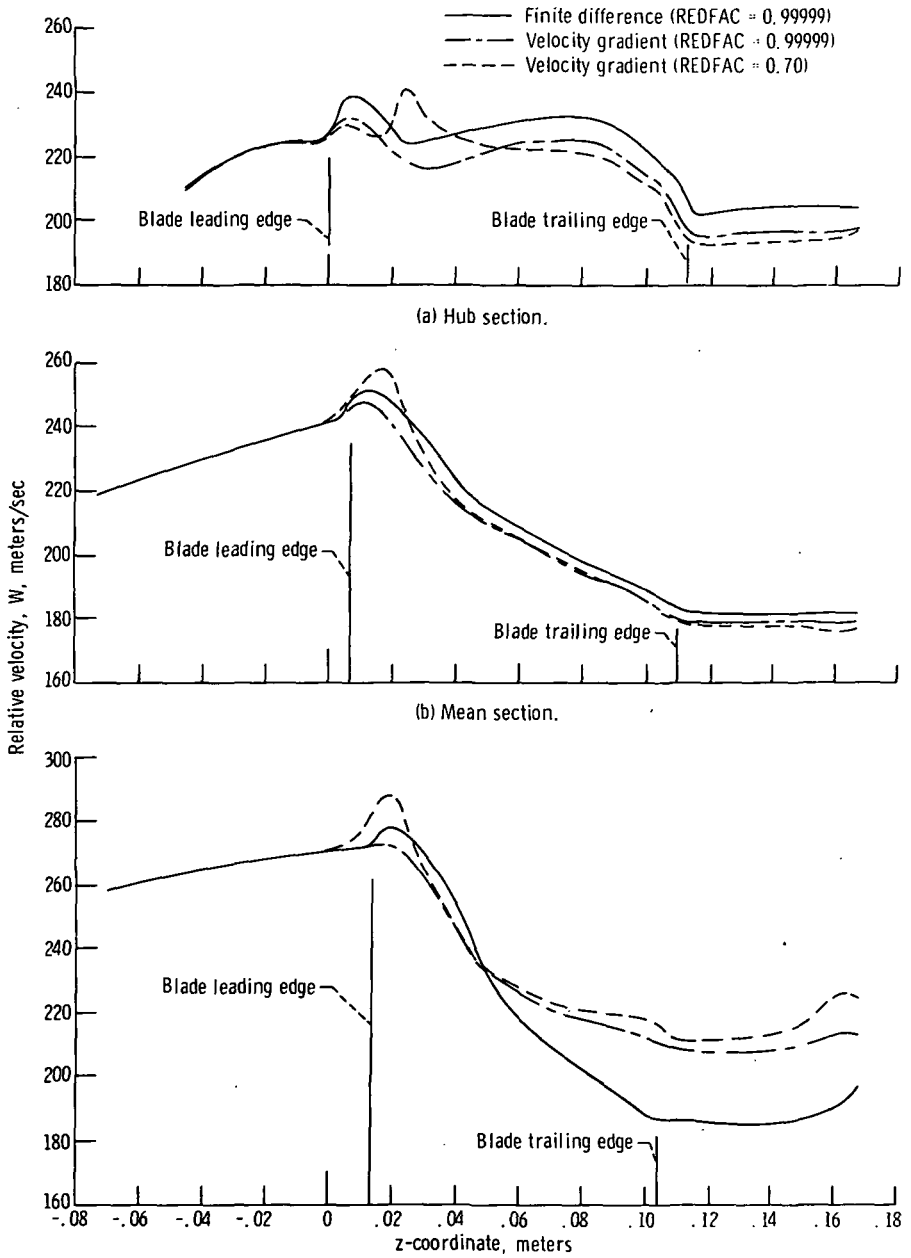

Figure 18. - Mid-channel velocities for axial-flow compressor example.

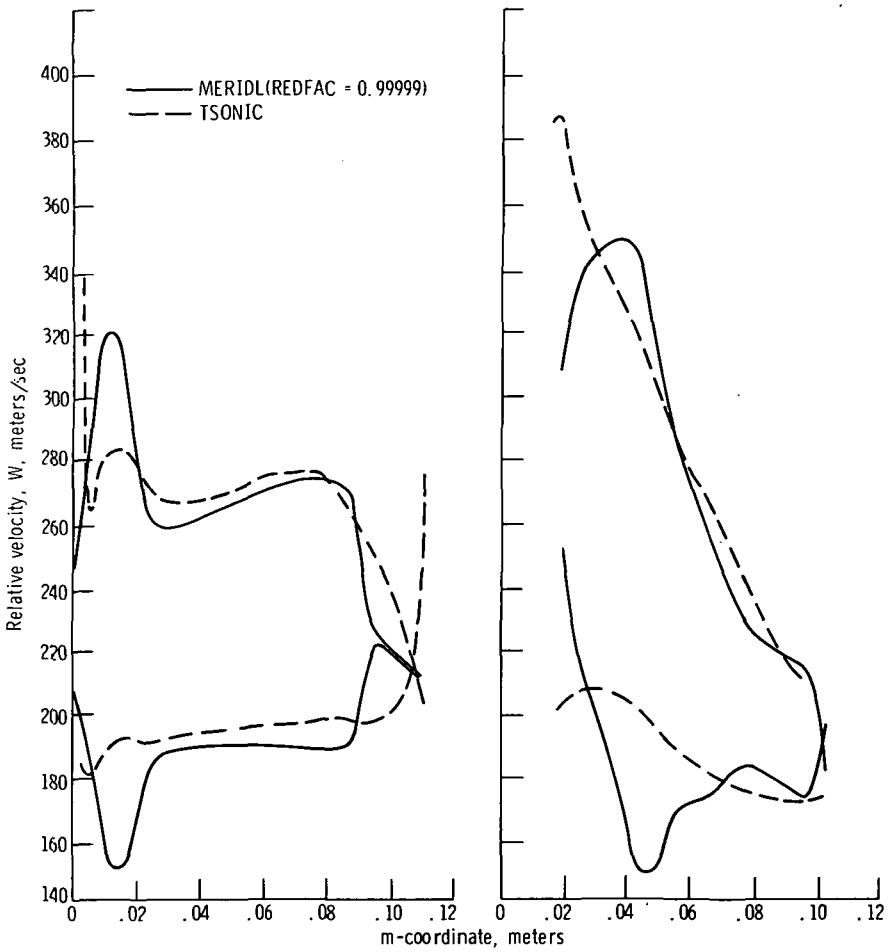

(a) Hub section.

(b) Tip section.

Figure 19. - Blade surface velocities for axial-flow compressor example.

This rotor was run twice, with values of reduction factor (REDFAC) equal to 0.99999 and 0.70. This was done in order to test the effect of reduction factor and also the accuracy of the velocity-gradient method in comparison with the finite-difference method. Since both cases have REDFAC < 1.0, both the subsonic (finite difference) and the transonic (velocity gradient) solutions will be obtained in each of them. (If REDFAC = 1.0, only the finite-difference solution is obtained.)

The first case (REDFAC = 0.99999) permits a comparison to be made between the approximate velocity-gradient method (used to obtain transonic solutions) and the more exact finite-difference stream-function solution (used for subsonic solutions) Since the reduction factor is 0.99999 (<1.0), both solutions will be obtained, but the answers should be very close if the methods compare well.

The second case (REDFAC = 0.70) permits a comparison of reduction-factor effect. Since the finite-difference solution is now obtained at only 70 percent of the mass flow and rotational speed (see appendix E), the results for the full-mass-flow velocity-gradient solution will be less accurate than when a higher reduction factor was used.

Figure 17 shows the streamline plots for the final finite-difference iteration for both the REDFAC = 0.99999 and REDFAC = 0.70 solutions. The differences in streamline location are small, but program printout of streamline curvatures shows that these curvatures differ significantly. This illustrates the point that as high a value of REDFAC should be used as possible.

This fact is further illustrated in figure 18, which shows mid-channel flow surface velocities for both reduction factors and both types of solution, the finite difference and the velocity gradient. On all parts of this figure, the solid line represents velocities from the final finite-difference iteration of the REDFAC = 0.99999 solution. This solution is mathematically most accurate.

Figure 19 shows a comparison of blade surface velocities estimated from the MERIDL program (see appendix G) and calculated from the TSONIC program (ref. 5). The TSONIC velocities are more accurate for the design blade shape.

Lewis Research Center,
National Aeronautics and Space Administration,
Cleveland, Ohio, October 16, 1972,
501-24.

APPENDIX A

GOVERNING EQUATIONS

The coordinate system is shown in figure 2. Since θ is a function of r and z on a meridional stream surface, θ can be eliminated so that the two independent variables are r and z.

For the subsonic solution, the stream function is used. The stream function u used herein is related to the stream function ψ defined in reference 1 by $\psi = uw$. With this substitution in equation (107a) of reference 1, we obtain in appendix B the basic differential equation which must be satisfied by the stream function under the given assumptions:

$$\frac{\partial^2 u}{\partial z^2} + \frac{\partial^2 u}{\partial r^2} - \frac{1}{r}\frac{\partial u}{\partial r} - \left(\frac{1}{B}\nabla B + \frac{1}{\rho}\nabla\rho\right) \cdot \nabla u + \frac{rB\rho}{wW_z}\left[\frac{W_\theta}{r}\frac{\partial(rV_\theta)}{\partial r} + \xi W^2 + \zeta + F_r\right] = 0 \tag{A1}$$

where

$$\xi = \frac{1}{2C_p}\left(\frac{R}{p''}\frac{\partial p''}{\partial r} - \frac{1}{T''}\frac{\partial I}{\partial r} - \frac{\omega^2 r}{T''}\right) \tag{A2}$$

$$\zeta = \omega^2 r - \frac{RT''}{p''}\frac{\partial p''}{\partial r} \tag{A3}$$

$$F_r = \frac{\partial\theta}{\partial r}\frac{1}{\rho}\frac{\partial p}{\partial\theta} \tag{A4}$$

Equations (A1) to (A4) are derived from Wu's equation in appendix B. Note that all the partials in equations (A1) to (A4) are on the stream surface except for $\partial p/\partial\theta$ in equation (A4), which is at constant z and r.

The derivatives of the stream function satisfy the equations

$$\frac{\partial u}{\partial z} = -\frac{rB\rho W_r}{w} \tag{A5}$$

$$\frac{\partial u}{\partial r} = \frac{rB\rho W_z}{w} \tag{A6}$$

For the final transonic solution the velocity-gradient method is used. The streamline curvatures and flow angles needed for the velocity-gradient equation are obtained first from a reduced-flow subsonic-stream-function solution.

The velocity-gradient equation is

$$dW = \left(aW + b + \frac{c}{W} + d\cos\beta\right)dt + \frac{e}{W} + Wf \tag{A7}$$

The coefficients, a, b, c, and d, are given by different experessions in the blade region, in the upstream region, and in the downstream region. These coefficients are given as follows:

Blade-region coefficients:

$$\left.\begin{aligned} a &= \frac{\cos^2\beta\cos(\alpha-\varphi)}{r_c} - \frac{\sin^2\beta\cos\varphi}{r} + \sin\alpha\sin\beta\cos\beta\frac{\partial\theta}{\partial t} \\ b &= \cos\beta\frac{dW_m}{dm}\sin(\alpha-\varphi) - 2\omega\sin\beta\cos\varphi + r\cos\beta\left(\frac{dW_\theta}{dm} + 2\omega\sin\alpha\right)\frac{\partial\theta}{\partial t} \\ c &= 0 \\ d &= 0 \end{aligned}\right\} \tag{A8}$$

Upstream-region coefficients:

$$\left.\begin{aligned} a &= \frac{\cos(\alpha-\varphi)}{r_c} \\ b &= 0 \\ c &= -\left(\frac{\lambda-\omega r^2}{r^2}\right)\left[\frac{\lambda-\omega r^2}{r_c}\cos(\alpha-\varphi) + \frac{\lambda+\omega r^2}{r}\cos\varphi\right] \\ d &= \frac{dW_m}{dm}\sin(\alpha-\varphi) \end{aligned}\right\} \tag{A9}$$

Downstream-region coefficients:

$$\left.\begin{aligned} a &= \frac{\cos(\alpha - \varphi)}{r_c} \\ b &= 0 \\ c &= -\left(\frac{\left(rV_\theta\right)_o - \omega r^2}{r^2}\right)\left[\frac{\left(rV_\theta\right)_o - \omega r^2}{r_c}\cos(\alpha - \varphi) + \frac{\left(rV_\theta\right)_o + \omega r^2}{r}\cos\varphi\right] \\ d &= \frac{dW_m}{dm}\sin(\alpha - \varphi) \end{aligned}\right\} \quad \text{(A10)}$$

Finally, in all three regions, we have

$$\left.\begin{aligned} e &= C_p T_i' - \omega\, d\lambda + C_p dT'' - \frac{RT''}{p''}dp'' \\ f &= \frac{R\,dp''}{2C_p p''} - \frac{dT''}{2T''} \end{aligned}\right\} \quad \text{(A11)}$$

Equations (A7) to (A11) are derived in appendix C. Equation (A7) is solved as an initial-value problem, where the initial value of W is specified at the hub for any given t-line running from hub to tip. By finding several solutions for varying values of W at the hub, a solution satisfying continuity will be found; that is, the solution will satisfy

$$\int_{r_h}^{r_t} \rho W\, r B \cos(\alpha - \varphi)\cos\beta\, dr = w \quad \text{(A12)}$$

When equation (A7) has been solved, subject to satisfying equation (A12), for every hub-to-tip mesh line in the region, the entire velocity distribution is obtained.

The solution obtained by either the finite-difference or velocity-gradient method is for the mid-channel surface between the blades. Of greater interest are the blade surface velocities. These can be estimated since the blade loading depends on the rate of change of whirl. By assuming a linear variation of velocity between blade surfaces,

velocities can be calculated. In appendix G the following equation for calculating blade surface velocities is derived:

$$\left.\begin{aligned} W_l &= W_{mid} - \frac{B}{2} \cos\beta \frac{d(rV_\theta)}{dm} \\ W_{tr} &= W_{mid} + \frac{B}{2} \cos\beta \frac{d(rV_\theta)}{dm} \end{aligned}\right\} \qquad \text{(A13)}$$

APPENDIX B

DERIVATION OF STREAM-FUNCTION EQUATION

Wu derives the following equation (eq. (107a), ref. 1) for the stream function on a meridional stream surface:

$$\frac{\partial^2\psi}{\partial z^2} + \frac{\partial^2\psi}{\partial r^2} - \frac{1}{r}\frac{\partial\psi}{\partial r} - \left(\frac{1}{B}\nabla B + \frac{1}{\rho}\nabla\rho\right)\nabla\psi + \frac{(rB\rho)^2}{\partial\psi/\partial r}\left[\frac{W_\theta}{r}\frac{\partial(rV_\theta)}{\partial r} - \frac{\partial I}{\partial r} + T\frac{\partial s}{\partial r} + F_r\right] = 0 \tag{B1}$$

The partial derivatives here all refer to the rate of change on the meridional stream surface. Wu used a bold partial derivative sign to indicate this, but it is not necessary here since we consider the equation only on the stream surface. The quantity B is proportional to the blade-to-blade stream surface thickness. Since the variation in local stream sheet thickness is not known, the overall blade-to-blade spacing is used. The quantity B is a function or z and r, so that we can use

$$B(z, r) = \theta_{tr}(z, r) - \theta_l(z, r) \tag{B2}$$

where θ_{tr} and θ_l are the θ-coordinates of the trailing and leading blade surfaces.

Equation (B1) is a nonlinear partial differential equation. The solution can be obtained by solving a linearized form and then making corrections to the nonlinear terms to improve the solution. After several iterations, the true solution to the nonlinear equation is obtained. The equation can be put in a linear form by expressing $\partial\psi/\partial r$ in the denominator in terms of W_z and using velocities and densities from the previous iteration. For the first iteration, the nonlinear terms are omitted.

First, the stream function will be normalized to be 0 at the hub and 1 at the tip. This is done by letting

$$\psi = uw \tag{B3}$$

where u is the normalized stream function. Then

$$\frac{\partial u}{\partial z} = -\frac{rB\rho W_r}{w} \tag{B4}$$

$$\frac{\partial u}{\partial r} = \frac{rB\rho W_z}{w} \tag{B5}$$

By using equations (B3) and (B5), equation (B1) can be written

$$\frac{\partial^2 u}{\partial z^2} + \frac{\partial^2 u}{\partial r^2} - \frac{1}{r}\frac{\partial u}{\partial r} - \left(\frac{1}{B}\nabla B + \frac{1}{\rho}\nabla\rho\right) \cdot \nabla u + \frac{rB\rho}{wW_z}\left[\frac{W_\theta}{r}\frac{\partial(rV_\theta)}{\partial r} - \frac{\partial I}{\partial r} + T\frac{\partial s}{\partial r} + F_r\right] = 0 \tag{B6}$$

Rothalpy I is defined by

$$I = C_p T_i' - \omega\lambda \tag{B7}$$

The entropy change ds can be calculated from

$$ds = C_p \frac{dT}{T} - \frac{R\,dp}{p}$$

Since the entropy of a particle at actual flow velocity is the same as the entropy of the particle at stagnation conditions (either absolute or relative), we can also use

$$ds = C_p \frac{dT''}{T''} - \frac{R\,dp''}{p''} \tag{B8}$$

This takes less calculation than using static values.

Equation (97) of reference 1 gives F_r (the radial component of the vector $\vec{F}$) as

$$F_r = -\frac{1}{n_\theta r}\frac{1}{\rho}\frac{\partial p}{\partial\theta}\,n_r \tag{B9}$$

Note that $\partial p/\partial\theta$ is at constant r and z, and not on the stream surface as the other partials are. The unit normal vector n to the stream surface is normal to any curve on the stream surface, so that

$$n_r\,dr + n_\theta\,r\,d\theta + n_z\,dz = 0 \tag{B10}$$

In particular, at constant z, we have

$$\frac{n_r}{n_\theta} = -r\left(\frac{\partial\theta}{\partial r}\right) \tag{B11}$$

where $r(\partial\theta/\partial r)$ is the tangent of the blade lean angle at constant z. Using equation (B11) in equation (B9), we get

$$F_r = \frac{\partial\theta}{\partial r}\frac{1}{\rho}\frac{\partial p}{\partial\theta} \tag{B12}$$

The static temperature T is calculated from the velocity W by

$$T = T_i' - \frac{W^2 + 2\omega\lambda - (\omega r)^2}{2C_p} \tag{B13}$$

When W is zero, equation (B13) gives the relative stagnation temperature, T''.

Equations (A1) to (A4) are obtained from equations (B6), (B7), (B8), (B12), and (B13).

STREAM-FUNCTION EQUATION IN s- AND t-COORDINATES

The solution of equation (A1) is obtained by using finite-difference methods on an orthogonal mesh. The orthogonal mesh coordinates are s in the throughflow direction and t in the hub-to-tip direction. The derivatives of the stream function in the s and t directions are related to the velocity components by

$$\left.\begin{aligned} \frac{\partial u}{\partial s} &= -\frac{rB\rho}{w} W_t \\ \frac{\partial u}{\partial t} &= \frac{rB\rho}{w} W_s \end{aligned}\right\} \tag{B14}$$

Since s and t coordinates are used in solving equation (A1), the partials must be expressed as partials with respect to s and t. This is done by using the chain rule:

$$\frac{\partial}{\partial r} = \frac{\partial}{\partial s}\frac{\partial s}{\partial r} + \frac{\partial}{\partial t}\frac{\partial t}{\partial r}$$

$$= \sin\varphi\,\frac{\partial}{\partial s} + \cos\varphi\,\frac{\partial}{\partial t}$$

and

$$\frac{\partial}{\partial z} = \cos\varphi\,\frac{\partial}{\partial s} - \sin\varphi\,\frac{\partial}{\partial t}$$

Now, apply this to the second partial of u to obtain

$$\frac{\partial^2 u}{\partial z^2} + \frac{\partial^2 u}{\partial r^2} = \frac{\partial^2 u}{\partial s^2} + \frac{\partial^2 u}{\partial t^2} + \frac{\partial u}{\partial s}\frac{\partial \varphi}{\partial t} - \frac{\partial u}{\partial t}\frac{\partial \varphi}{\partial s} \tag{B15}$$

In the program $\sin\varphi$ and $\cos\varphi$ are stored, so that it is more convenient to calculate the partials of φ by

$$\left.\begin{aligned} \frac{\partial \varphi}{\partial s} &= \frac{1}{\cos\varphi}\frac{\partial(\sin\varphi)}{\partial s} \\ \frac{\partial \varphi}{\partial t} &= \frac{1}{\cos\varphi}\frac{\partial(\sin\varphi)}{\partial t} \end{aligned}\right\} \tag{B16}$$

The s, t orthogonal coordinate system is in the same length units as z and r. In this case, the gradient can be expressed directly in s and t coordinates, that is,

$$\nabla B \cdot \nabla u = \frac{\partial B}{\partial s}\frac{\partial u}{\partial s} + \frac{\partial B}{\partial t}\frac{\partial u}{\partial t} \tag{B17}$$

Finally, putting all this together, we have

$$\begin{aligned} &\frac{\partial^2 u}{\partial s^2} + \frac{\partial^2 u}{\partial t^2} - \frac{\partial u}{\partial s}\left[\frac{\sin\varphi}{r} + \frac{1}{B}\frac{\partial B}{\partial s} + \frac{1}{\rho}\frac{\partial \rho}{\partial s} - \frac{1}{\cos\varphi}\frac{\partial(\sin\varphi)}{\partial t}\right] \\ &\quad - \frac{\partial u}{\partial t}\left[\frac{\cos\varphi}{r} + \frac{1}{B}\frac{\partial B}{\partial t} + \frac{1}{\rho}\frac{\partial \rho}{\partial t} + \frac{1}{\cos\varphi}\frac{\partial(\sin\varphi)}{\partial s}\right] \\ &\quad + \frac{rB\rho}{wW_z}\left\{\frac{W_\theta}{r}\left[\sin\varphi\,\frac{\partial(rV_\theta)}{\partial s} + \cos\varphi\,\frac{\partial(rV_\theta)}{\partial t}\right] + \xi W^2 + \zeta + F_r\right\} = 0 \end{aligned} \tag{B18}$$

where ξ, ζ, and F_r are as defined in equations (A2), (A3), and (A4)

CALCULATING F_r AND PARTIALS OF (rV_θ)

In equation (B18), F_r and the partials of rV_θ must be calculated differently outside the blade and within the blade. Within the blade, the partials of rV_θ are calculated

by a finite-difference approximation using the previous iteration. For the first iteration, the partials are assumed to be zero. Outside the blade, the partials are calculated from the input whirl distribution. From the input, the whirl is specified (or can be estimated) as a function of the stream function u. Hence, upstream of the blade,

$$\frac{\partial(rV_\theta)}{\partial r} = \frac{\partial\lambda}{\partial r} = \frac{d\lambda}{du}\frac{\partial u}{\partial r} = \frac{d\lambda}{du}\frac{rB\rho W_z}{w} \tag{B19}$$

Similarly, downstream of the blade,

$$\frac{\partial(rV_\theta)}{\partial r} = \frac{d\left(rV_\theta\right)_o}{du}\frac{rB\rho W_z}{w} \tag{B20}$$

The F_r is caused by the radial pressure gradient induced by the blade lean. We can calculate F_r from equation (B12). The blade-to-blade pressure gradient $\partial p/\partial\theta$ can be calculated from the blade loading by assuming constant entropy blade to blade, so that

$$dp = \rho C_p\, dT \tag{B21}$$

From equation (B13) we get

$$\frac{\partial p}{\partial\theta} = -\rho W\frac{\partial W}{\partial\theta} \tag{B22}$$

since T_i', λ, and r are all constant from blade to blade.

Now, substitute this in equation (B12) to get

$$F_r = -\frac{\partial\theta}{\partial r} W\frac{\partial W}{\partial\theta} \tag{B23}$$

The blade-to-blade velocity gradient is calculated from dW_θ/dm, as explained in appendix G, by using equation (G2). Outside the blade, there is no blade-to-blade pressure gradient. Hence,

$$F_r = 0 \tag{B24}$$

outside the blade.

APPENDIX C

DERIVATION OF VELOCITY-GRADIENT EQUATIONS

The general velocity-gradient equation is an expression for the value of the directional derivative of the relative velocity. The velocity-gradient equation is derived from Newton's three-dimensional force equation. In this program the velocity-gradient equation is used in two ways. One way is to obtain the flow distribution at the upstream and downstream boundaries to establish the boundary conditions for equation (A1). The second way is to determine the approximate velocity distribution when there is locally supersonic velocity on the meridional mid-channel stream surface.

VELOCITY-GRADIENT EQUATION FOR DETERMINING BOUNDARY CONDITIONS

The general velocity-gradient equation can be written

$$\frac{dW}{dq} = a\frac{dr}{dq} + b\frac{dz}{dq} + c\frac{d\theta}{dq} + \frac{1}{W}\left(C_p\frac{T_i'}{dq} - \omega\frac{d\lambda}{dq} + T\frac{ds}{dq}\right) \tag{C1}$$

where

$$\left.\begin{aligned} a &= \frac{W\cos\alpha\cos^2\beta}{r_c} - \frac{W\sin^2\beta}{r} + \sin\alpha\cos\beta\frac{dW_m}{dm} - 2\omega\sin\beta \\ b &= -\frac{W\cos^2\beta\sin\alpha}{r_c} + \cos\alpha\cos\beta\frac{dW_m}{dm} \\ c &= W\sin\alpha\sin\beta\cos\beta + r\cos\beta\left(\frac{dW_\theta}{dm} + 2\omega\sin\alpha\right) \end{aligned}\right\} \tag{C2}$$

This is the same as equation (B13) and (B14) of reference 2, but with the additional term, T(ds/dq), to allow for variation in entropy.

Outside the blade row, c = 0. This follows from the fact that $d(rV_\theta)/dm = 0$ in this region. Using this identity and the relation $W_\theta = V_\theta - \omega r$, we can derive the expression

$$\frac{dW_\theta}{dm} = -\frac{W_\theta + 2\omega r}{r}\sin\alpha$$

When this is substituted in the expression for c, we find that $c = 0$.

It is reasonable to assume that the boundary is normal to the flow along the upstream and downstream boundaries. Then $q = n$ and

$$\left.\begin{aligned} \frac{dr}{dn} &= \cos \alpha \\ \frac{dz}{dn} &= -\sin \alpha \end{aligned}\right\} \tag{C3}$$

When this is substituted in equations (C1) and (C2), we obtain

$$\frac{dW}{dn} = \frac{W \cos^2\beta}{r_c} - \frac{W \sin^2\beta \cos \alpha}{r} - 2\omega \cos \alpha \sin \beta + \frac{1}{W}\left(C_p \frac{dT_i'}{dn} - \omega \frac{d\lambda}{dn} + T \frac{ds}{dn}\right) \tag{C4}$$

This equation is the basic velocity-gradient equation along a meridional streamline normal. At the upstream boundary (or any place upstream of the blade) λ, T_i', and ρ_i' are specified as a function of the stream function. Also, along the boundary, α is assumed to be known, since it is assumed that the boundary is normal to the streamlines. The angle β, however, is not known directly. Therefore, in equation (C4), we desire to eliminate β in favor of λ, r, and W. This can easily be done since

$$W_\theta = \frac{\lambda}{r} - \omega r \tag{C5}$$

and

$$\sin \beta = \frac{W_\theta}{W} \tag{C6}$$

Then $\cos \beta$ is obtained from

$$\cos^2\beta = 1 - \sin^2\beta \tag{C7}$$

The entropy change, ds/dn, can be calculated from the differential form of the second law of thermodynamics:

$$\frac{ds}{dn} = \frac{C_p - R}{T}\frac{dT}{dn} - \frac{R}{\rho}\frac{d\rho}{dn}$$

Since the entropy of a particle at actual flow velocity is the same as the entropy at stagnation conditions, we can also use

$$\frac{ds}{dn} = \frac{(C_p - R)}{T_i'} \frac{dT_i'}{dn} - \frac{R}{\rho_i'} \frac{d\rho_i'}{dn} \tag{C8}$$

The meridional-plane streamline curvature $1/r_c$ is assumed to vary linearly from hub to tip.

By substituting equations (C5) to (C8) in equation (C4) we obtain the velocity-gradient equation in the form used in the computer program for the upstream boundary:

$$dW = \left(aW + \frac{b}{W}\right)dn + \frac{1}{W}\left(c_a + c_b \frac{T}{T_i'}\right) \tag{C9}$$

where

$$\left.\begin{aligned} a &= \frac{1}{r_c} \\ b &= -\left(\frac{\lambda - \omega r^2}{r^2}\right)\left[\frac{\lambda - \omega r^2}{r_c} + \frac{\cos \alpha}{r}(\lambda + \omega r^2)\right] \\ c_a &= C_p \, dT_i' - \omega \, d\lambda \\ c_b &= (C_p - R)dT_i' - \frac{RT_i'}{\rho_i'} d\rho_i' \end{aligned}\right\} \tag{C10}$$

Similarly, we can obtain a velocity-gradient equation for the downstream boundary. Here we use downstream conditions for temperature, density, and whirl, so that the downstream velocity-gradient equation is equation (C9) with coefficients given by

$$
\left.
\begin{aligned}
a &= \frac{1}{r_c} \\
b &= -\left[\frac{\left(rV_\theta\right)_o - \omega r^2}{r^2}\right]\left\{\frac{\left(rV_\theta\right)_o - \omega r^2}{r_c} + \frac{\cos\alpha}{r}\left[\left(rV_\theta\right)_o + \omega r^2\right]\right\} \\
c_a &= C_p\, dT'_o - \omega\, d\left(rV_\theta\right)_o \\
c_b &= (C_p - R)dT'_o - \frac{RT'_o}{\rho'_o}\, d\rho'_o
\end{aligned}
\right\} \qquad \text{(C11)}
$$

VELOCITY-GRADIENT EQUATION FOR CALCULATING APPROXIMATE TRANSONIC VELOCITIES

We start with the general velocity-gradient equations (C1) and (C2). These equations will be applied along vertical mesh lines in the t-direction, so that $q = t$. (See appendix B for a description of the orthogonal mesh.) Then

$$
\left.
\begin{aligned}
\frac{dr}{dq} &= \cos\varphi \\
\frac{dz}{dq} &= -\sin\varphi
\end{aligned}
\right\} \qquad \text{(C12)}
$$

Note that, by using equation (C12),

$$
\left.
\begin{aligned}
\sin(\alpha - \varphi) &= \sin\alpha\frac{dr}{dq} + \cos\alpha\frac{dz}{dq} \\
\cos(\alpha - \varphi) &= \cos\alpha\frac{dr}{dq} - \sin\alpha\frac{dz}{dq}
\end{aligned}
\right\} \qquad \text{(C13)}
$$

Using equations (C12) and (C13) in equations (C1) and (C2), we can get

$$\frac{dW}{dt} = \frac{W \cos^2\beta \cos(\alpha - \varphi)}{r_c} + \cos\beta \frac{dW_m}{dm} \sin(\alpha - \varphi) - \left(\frac{W \sin^2\beta}{r} + 2\omega \sin\beta\right)\cos\varphi + c\frac{d\theta}{dt}$$

$$+ \frac{1}{W}\left(C_p \frac{dT_i'}{dt} - \omega \frac{d\lambda}{dt} + T\frac{ds}{dt}\right) \qquad \text{(C14)}$$

We can express T ds in terms of the relative velocity W and relative stagnation conditions. We use

$$T = T'' - \frac{W^2}{2C_p} \qquad \text{(C15)}$$

By using equations (B8) and (C15), we get

$$T\,ds = C_p\,dT'' - \frac{RT''}{p''}\,dp'' + \frac{W^2}{C_p}\left(\frac{R\,dp''}{2p''} - C_p\frac{dT''}{2T''}\right) \qquad \text{(C16)}$$

Now we can write the velocity-gradient equation (C14) as

$$dW = (aW + b)\,dt + \frac{e}{W} + Wf \qquad \text{(C17)}$$

where

$$\left.\begin{aligned} a &= \frac{\cos^2\beta \cos(\alpha - \varphi)}{r_c} - \frac{\sin^2\beta \cos\varphi}{r} + \sin\alpha \sin\beta \cos\beta \frac{d\theta}{dt} \\ b &= \cos\beta \frac{dW_m}{dm}\sin(\alpha - \varphi) - 2\omega \sin\beta \cos\varphi + r\cos\beta\left(\frac{dW_\theta}{dm} + 2\omega \sin\alpha\right)\frac{d\theta}{dt} \\ e &= C_p\,dT_i' - \omega\,d\lambda + C_p\,dT'' - \frac{RT''}{p''}\,dp'' \\ f &= \frac{R\,dp''}{2C_p p''} - \frac{dT''}{2T''} \end{aligned}\right\} \qquad \text{(C18)}$$

Equations (C17) and (C18) can be used directly within the blade row. However, outside the blade row, the angle β is not known directly, so that we desire to eliminate

β in favor of λ, r, and W, as was done on the upstream boundary. For this, we use equations (C5) to (C7). Also, $c = 0$ in equation (C2) outside the blade as was shown previously. With these substitutions, equation (C14) becomes

$$dW = \left(aW + \frac{c}{W} + d\ \cos\beta\right)dt + \frac{e}{W} + Wf \tag{C19}$$

where

$$\left.\begin{aligned}
a &= \frac{\cos(\alpha - \varphi)}{r_c} \\
c &= -\left(\frac{\lambda - \omega r^2}{r^2}\right)\left[\frac{\lambda - \omega r^2}{r_c}\cos(\alpha - \varphi) + \frac{\lambda + \omega r^2}{r}\cos\varphi\right] \\
d &= \frac{dW_m}{dm}\sin(\alpha - \varphi) \\
e &= C_p\, dT_i' - \omega\, d\lambda + C_p\, dT'' - \frac{RT''}{p''}\, dp'' \\
f &= -\frac{dT''}{2T''} + \frac{R\, dp''}{2C_p p''} \\
\cos\beta &= \sqrt{1 - \left(\frac{\lambda - \omega r^2}{rW}\right)^2}
\end{aligned}\right\} \tag{C20}$$

Downstream of the blade, outlet whirl and absolute stagnation temperature and pressure should be used. Hence, in equation (C20), T_o' is used instead of T_i', ρ_o' is used instead of ρ_i', and $\left(rV_\theta\right)_o$ is used instead of λ. Equations (A7) to (A11) are obtained directly from equations (C17) to (C20).

APPENDIX D

LOSS CORRECTIONS

An approximate loss correction is made by reducing the relative stagnation pressure used in the program. This loss in stagnation pressure is specified by the input either directly or by specifying outlet stagnation pressure. These quantities may vary from hub to tip. If the outlet stagnation pressure is given as input, the fractional loss of stagnation pressure is calculated. So, in all cases, the fractional loss of stagnation pressure at the outlet is known from hub to tip. This loss is assumed to be zero upstream of the blade, then to vary linearly from leading edge to trailing edge within the blade, and to be constant downstream of the blade.

For the case where the downstream stagnation pressure is given as input, the fractional loss of stagnation pressure is calculated. First, the outlet total temperature T'_o is calculated from the change in whirl along a streamline,

$$T'_o = T'_i + \frac{\omega\left[\left(rV_\theta\right)_o - \lambda\right]}{C_p} \tag{D1}$$

Then the ratio of actual to ideal stagnation pressure is calculated from

$$\frac{p'_o}{\left(p'_o\right)_{ideal}} = \frac{p'_o}{p'_i}\left(\frac{T'_i}{T'_o}\right)^{\gamma/(\gamma-1)} \tag{D2}$$

Within the blade, the loss is distributed linearly from zero at the leading edge to the fraction given or calculated at the blade trailing edge. The loss fraction is the same whether it is expressed in terms of relative or absolute stagnation pressures. That is,

$$\frac{p''}{p''_{ideal}} = \frac{p'}{p'_{ideal}} \tag{D3}$$

When this ratio is known, the density can be calculated, since

$$\rho = \rho'_i\left(\frac{T}{T'_i}\right)^{1/(\gamma-1)} \frac{p''}{p''_{ideal}} \tag{D4}$$

Equation (D4) is derived as equation (B6) in reference 13. The value of p''/p''_{ideal} varies at each point of the region but does not change after the initial calculation. The value of ρ is used in checking continuity by means of equation (A12). Therefore, in the program, the loss correction is made by reducing the tangential blade space B at each mesh point.

APPENDIX E

DEFINING REDUCED-MASS-FLOW PROBLEM

When the mid-channel meridional-plane solution has locally supersonic flow, the solution cannot be obtained directly by solving the stream-function equation (eq. (A1)). However, an approximate solution can be obtained by getting a reduced-flow solution and extending this to the full-flow solution by the velocity-gradient method. This full-flow solution depends strongly on the reduced-flow solution, so that it is important to establish the conditions which will give the most suitable stream-function solution. With a reduced mass flow, if both the inlet and outlet whirl and the rotational speed are reduced in the same ratio as the mass flow, a similar flow will result. That is, the reduced-flow streamlines will have approximately the same angles and curvatures as the full-flow streamlines throughout the flow field.

Another consideration is the boundary conditions at the upstream and downstream boundaries. Again, the flow distribution will be similar to the reduced mass flow if the mass flow, inlet and outlet whirl, and rotational speed are all reduced by the same ratio.

In summary, then, for the reduced-mass-flow solution, the mass flow, inlet and outlet whirl, and rotational speed are all reduced in the same ratio. This reduction factor is specified in the input by REDFAC, as explained in the section INPUT.

APPENDIX F

INCIDENCE AND DEVIATION CORRECTIONS

The solution region is divided into three subregions: upstream, within the blade, and downstream. These three regions should match each other, that is, there should be no difference in the tangential momentum of a particle on either side of the lines at the leading and trailing edges. If there were no incidence or deviation, this condition would be satisfied automatically by using the actual blade shape in the blade region. Since there is almost always incidence and deviation, the mean flow will not follow the blade surface near the leading and trailing edges. Because of this, an empirical correction is made to the blade shape near the leading and trailing edges.

The blade shape correction is made for a distance from the leading or trailing edge. This distance varies between 1/6 and 1/2 of the blade chord, depending on solidity. The solidity is defined to be the ratio of the true blade chord along a streamline to the blade-to-blade distance. When there is a change in radius, the solidity differs at leading and trailing edges. For calculation purposes in the program the true blade chord along an s-coordinate line is used instead of that along a streamline. For a solidity of 2 or more, the distance is 1/6 of the chord; and for a solidity of 1/2 or less, the distance is 1/2 of the blade chord. The distance varies linearly with solidity between these limits. The correction is made to the blade angle so that tangential momentum is continuous at the blade leading or trailing edge, and then the angle correction is linearly decreased over the prescribed distance within the blade.

The free-stream flow angle is not known in advance at the blade leading edge. Therefore, an iterative procedure is used to make the blade shape correction. On the first iteration, no blade shape correction is made. After the first iteration, an approximate solution is obtained, and the flow angle β is calculated throughout the region. From the requirement of continuous tangential momentum,

$$\left(W_\theta\right)_{fs} = \left(W_\theta\right)_{bf}$$

From continuity,

$$\left(W_m\right)_{fs} \frac{2\pi}{NBL} = \left(W_m B\right)_{bf}$$

Hence, since $\tan \beta = W_\theta / W_m$

$$\tan \beta_{bf} = \tan \beta_{fs}\left(\frac{B \times NBL}{2\pi}\right) \tag{F1}$$

It is assumed that the s-coordinate is close to a streamline. Therefore, only $\partial\theta/\partial s$ will be changed, and $\partial\theta/\partial t$ will not be changed. We can express β in terms of the partials of θ by

$$\tan \beta_{bf} = r \frac{d\theta}{dm} = r\left[\left(\frac{\partial\theta}{\partial s}\right)_{bf} \cos(\alpha - \varphi) + \frac{\partial\theta}{\partial t} \sin(\alpha - \varphi)\right]$$

When this is solved for $(\partial\theta/\partial s)_{bf}$, we obtain

$$\left(\frac{\partial\theta}{\partial s}\right)_{bf} = \frac{\frac{\tan \beta_{bf}}{r} - \frac{\partial\theta}{\partial t} \sin(\alpha - \varphi)}{\cos(\alpha - \varphi)} \tag{F2}$$

Equations (F1) and (F2) are used to calculate $(\partial\theta/\partial s)_{bf}$ at the blade leading and trailing edges. The difference $(\partial\theta/\partial s)_{bf} - (\partial\theta/\partial s)_{b}$ is then varied linearly within the blade for the specified distance. The calculations for these blade shape corrections are done by subroutine INDEV.

APPENDIX G

BLADE SURFACE VELOCITIES AND BLADE-TO-BLADE AVERAGE DENSITIES

The blade surface velocities can be calculated once a meridional mid-surface solution is obtained. The blade-to-blade velocity gradient $\partial W/\partial\theta$ depends on dW_θ/dm. To obtain the desired relation, we use the velocity-gradient equations (C1) and (C2). In this case, $q = \theta$ and $dr/d\theta = dz/d\theta = 0$. Also, it is assumed that T_i', λ, and the entropy s are constant in the blade-to-blade direction. With this, equations (C1) and (C2) become

$$\frac{\partial W}{\partial \theta} = W \sin \alpha \sin \beta \cos \beta + r \cos \beta \left(\frac{dW_\theta}{dm} + 2\omega \sin \alpha \right) \tag{G1}$$

Using the fact that $V_\theta = W_\theta + \omega r$ and $W_\theta = W \sin \beta$, we can rewrite equation (G1) as

$$\frac{\partial W}{\partial \theta} = \cos \beta \frac{d(rV_\theta)}{dm} \tag{G2}$$

Since only a mid-channel solution is obtained, we assume that $\cos \beta$ and $d(rV_\theta)/dm$ are constant from blade to blade. This means that W varies linearly from blade to blade. (This may be in considerable error near the leading or trailing edge.) With this assumption, then

$$W_{mid} = \frac{W_l + W_{tr}}{2} \tag{G3}$$

Integrating (G2) from blade to blade (from $\theta = \theta_l$ to $\theta = \theta_{tr}$) and using (G3), we obtain

$$\left.\begin{aligned} W_{tr} &= W_{mid} + \frac{B \cos \beta}{2} \frac{d(rV_\theta)}{dm} \\ W_l &= W_{mid} - \frac{B \cos \beta}{2} \frac{d(rV_\theta)}{dm} \end{aligned}\right\} \tag{G4}$$

Note that equation (G4) is very close to that developed by Stanitz (eqs. (16) and (17), ref. 16).

Equation (G4) is used in subroutine BLDVEL to obtain blade surface velocities from the mid-channel meridional solution.

It is desirable to consider the blade-to-blade variation in density to satisfy continuity for the blade passage. Equation (G4) gives information we need to do this. Since the mid-channel solution is considered to be representative of all meridional-plane stream surfaces, we can consider the solution to be based on average blade-to-blade conditions. This means that in equation (B14) average blade-to-blade velocity and density should be used. Equation (B14) becomes

$$\left.\begin{aligned} \frac{\partial u}{\partial s} &= -\frac{rB}{w}\left(\rho W_t\right)_{av} \\ \frac{\partial u}{\partial t} &= \frac{rB}{w}\left(\rho W_s\right)_{av} \end{aligned}\right\} \qquad \text{(G5)}$$

If we use Simpson's rule to calculate the average value, we obtain

$$\left(\rho W_s\right)_{av} = \frac{\rho_l W_{s,l} + 4\rho_{mid} W_{s,mid} + \rho_{tr} W_{s,tr}}{6} \qquad \text{(G6)}$$

The velocity component W_s can be expressed in terms of the velocity and flow angles by

$$W_s = W \cos\beta \cos(\alpha - \varphi) \qquad \text{(G7)}$$

This relation holds also on the blade surfaces, since the flow angles are assumed to be constant in the blade-to-blade (θ) direction, so that

$$\left.\begin{aligned} W_{s,l} &= W_l \cos\beta \cos(\alpha - \varphi) \\ W_{s,tr} &= W_{tr} \cos\beta \cos(\alpha - \varphi) \end{aligned}\right\} \qquad \text{(G8)}$$

By using equations (G3), (G4), and (G8) in equation (G6), we can express $\left(\rho W_s\right)_{av}$ as

$$\left(\rho W_s\right)_{av} = \rho_{av} W_s + \frac{\rho_l - \rho_{tr}}{12} \cos\beta \cos(\alpha - \varphi)(W_l - W_{tr}) \qquad \text{(G9)}$$

where the subscript mid is omitted from W_s, and

$$\rho_{av} = \frac{\rho_l + 4\rho_{mid} + \rho_{tr}}{6}$$

When a solution of equation (A1) is obtained, all quantities in equation (G9) can be estimated from the previous iteration, except for W_s. So we solve for W_s in equation (G9) and use equation (G5) to obtain

$$W_s = \frac{w\,\frac{\partial u}{\partial t}}{rB\rho_{av}} - \frac{(\rho_l - \rho_{tr})\cos\beta\cos(\alpha - \varphi)(W_l - W_{tr})}{12\rho_{av}} \qquad \text{(G10)}$$

This is the equation used in subroutine NEWRHO to calculate W_s from $\partial u/\partial t$. On the first iteration, $\rho_{av} = \rho_i'$ is used, and the second term is omitted. After this, the values of ρ_{mid}, ρ_{tr}, ρ_l, W_l, W_{tr}, $\cos\beta$, and $\cos(\alpha - \varphi)$ from the previous iteration are used.

In a parallel manner, we can derive the equation for W_t:

$$W_t = -\frac{w\,\frac{\partial u}{\partial s}}{rB\rho_{av}} - \frac{(\rho_l - \rho_{tr})\cos\beta\sin(\alpha - \varphi)(W_l - W_{tr})}{12\rho_{av}} \qquad \text{(G11)}$$

APPENDIX H

SYMBOLS

a	coefficient in velocity-gradient equations (A7) and (C1)
B	tangential space between blades, rad
b	coefficient in velocity-gradient equations (A7) and (C1)
C_p	specific heat at constant pressure, J/(kg)(K)
c	coefficient in velocity-gradient equations (A7) and (C1)
d	coefficient in velocity-gradient equation (A7)
e	coefficient in velocity-gradient equation (A7)
F	vector normal to mid-channel stream surface and proportional to tangential pressure gradient, N/kg
f	coefficient in velocity-gradient equation (A7)
I	rothalpy, $C_p T_i' - \omega\lambda$, $meters^2/sec^2$
m	meridional streamline distance, meters
n	unit vector normal to mid-channel stream surface
p	pressure, $N/meters^2$
q	distance along an arbitrary space curve, meters
R	gas constant, J/(kg)(K)
r	radius from axis of rotation, meters
r_c	radius of curvature of meridional streamline, meters
S	entropy, J/(kg)(K)
s	distance along orthogonal mesh lines in throughflow direction, meters
T	temperature, K
t	distance along orthogonal mesh lines in direction across flow
u	normalized stream function
V	absolute fluid velocity, meters/sec
W	fluid velocity relative to blade, meters/sec
w	mass flow, kg/sec
z	axial coordinate, meters

α angle between meridional streamline and axis of rotation, rad; see fig. 2

β angle between relative velocity vector and meridional plane, rad; see fig. 2

γ specific-heat ratio

ζ coefficient in stream-function equation, defined in eq. (A3)

θ relative angular coordinate, rad; see fig. 2

λ prerotation, $\left(rV_\theta\right)_i$, meters^2/sec

ξ coefficient in stream-function equation, defined in eq. (A2)

ρ density, kg/meter^3

φ angle between s-coordinate line and axis of rotation, rad; see fig. 4

ψ stream function, kg/sec

ω rotational speed, rad/sec; see fig. 2

Subscripts:

av average blade-to-blade value

b blade

bf blade flow

cr critical

fs free stream

h hub

i inlet

l blade surface facing direction of positive rotation

m component in direction of meridional streamline

mid mid-channel blade to blade

o outlet

r component in radial direction

s component in the s-direction

t tip, or component in the t-direction

tr blade surface facing direction of negative rotation

z component in axial direction

θ component in tangential direction

Superscripts:

' absolute stagnation condition

'' relative stagnation condition

REFERENCES

1. Wu, Chung-Hua: A General Theory of Three-Dimensional Flow in Subsonic and Supersonic Turbomachines of Axial-, Radial-, and Mixed-Flow Types. NACA TN 2604, 1952.

2. Katsanis, Theodore: Use of Arbitrary Quasi-Orthogonals for Calculating Flow Distribution in the Meridional Plane of a Turbomachine. NASA TN D-2546, 1964.

3. Marsh, H.: A Digital Computer Program for the Through-Flow Fluid Mechanics in an Arbitrary Turbomachine Using a Matrix Method. R & M-3509, Aeronautical Research Council, Gt. Britain, 1968.

4. Davis, W. R.: A Matrix Method Applied to the Analysis of the Flow in Turbomachinery. Rep. ME/A 71-6, Carleton University, Ottawa, 1971.

5. Katsanis, Theodore: FORTRAN Program for Calculating Transonic Velocities on a Blade-to-Blade Stream Surface of a Turbomachine. NASA TN D-5427, 1969.

6. Katsanis, Theodore; and McNally, William D.: FORTRAN Program for Calculating Velocities and Streamlines on the Hub-Shroud Mid-Channel Flow Surface of an Axial- or Mixed-Flow Turbomachine. II - Programmer's Manual. NASA TN D-7344, 1973.

7. McNally, William D.: FORTRAN Program for Generating a Two-Dimensional Orthogonal Mesh Between Two Arbitrary Boundaries. NASA TN D-6766, 1972.

8. McCracken, Daniel D.; and Dorn, William S.: Numerical Methods and FORTRAN Programming. John Wiley & Sons, Inc., 1964.

9. Varga, Richard S.: Matrix Iterative Analysis. Prentice-Hall, Inc., 1962.

10. Shapiro, Ascher H.: The Dynamics and Thermodynamics of Compressible Fluid Flow. Vol. I. Ronald Press Co., 1953.

11. Crouse, James: Computer Program for the Definition of Transonic Axial-Flow Compressor Blade Rows. NASA TN D-7345, 1973.

12. Johnsen, Irving A.; and Bullock, Robert O., eds.: Aerodynamic Design of Axial-Flow Compressors. NASA SP-36, 1965.

13. Katsanis, Theodore: FORTRAN Program for Quasi-Three-Dimensional Calculation of Surface Velocities and Choking Flow for Turbomachine Blade Rows. NASA TN D-6177, 1971.

14. Mechtly, E. A.: The International System of Units: Physical Constants and Conversion Factors (Revised). NASA SP-7012, 1969.

15. Walsh, J. L.; Ahlberg, J. H.; and Nilson, E. N.: Best Approximation Properties of the Spline Fit. J. Math. Mech., vol. 11, no. 2, 1962, pp. 225-234.

16. Stanitz, John D.; and Prian, Vasily D.: A Rapid Approximate Method for Determining Velocity Distribution on Impeller Blades of Centrifugal Compressors. NACA TN 2421, 1951.

NASA-Langley, 1973 — 1 E-7154

"The aeronautical and space activities of the United States shall be conducted so as to contribute . . . to the expansion of human knowledge of phenomena in the atmosphere and space. The Administration shall provide for the widest practicable and appropriate dissemination of information concerning its activities and the results thereof."

—NATIONAL AERONAUTICS AND SPACE ACT OF 1958

NASA SCIENTIFIC AND TECHNICAL PUBLICATIONS

TECHNICAL REPORTS: Scientific and technical information considered important, complete, and a lasting contribution to existing knowledge.

TECHNICAL NOTES: Information less broad in scope but nevertheless of importance as a contribution to existing knowledge.

TECHNICAL MEMORANDUMS: Information receiving limited distribution because of preliminary data, security classification, or other reasons. Also includes conference proceedings with either limited or unlimited distribution.

CONTRACTOR REPORTS: Scientific and technical information generated under a NASA contract or grant and considered an important contribution to existing knowledge.

TECHNICAL TRANSLATIONS: Information published in a foreign language considered to merit NASA distribution in English.

SPECIAL PUBLICATIONS: Information derived from or of value to NASA activities. Publications include final reports of major projects, monographs, data compilations, handbooks, sourcebooks, and special bibliographies.

TECHNOLOGY UTILIZATION PUBLICATIONS: Information on technology used by NASA that may be of particular interest in commercial and other non-aerospace applications. Publications include Tech Briefs, Technology Utilization Reports and Technology Surveys.

Details on the availability of these publications may be obtained from:

SCIENTIFIC AND TECHNICAL INFORMATION OFFICE

NATIONAL AERONAUTICS AND SPACE ADMINISTRATION

Washington, D.C. 20546